SEISMIC LOSS ESTIMATION METHODOLOGY: A CASE STUDY IN ISTANBUL

by

Sarper Saygı

B.S., Civil Engineering, Middle East Technical University, 2012

Submitted to the Institute for Graduate Studies in
Science and Engineering in partial fulfillment of
the requirements for the degree of
Master of Science

Graduate Program in Civil Engineering

Boğaziçi University

2015

SEISMIC LOSS ESTIMATION METHODOLOGY: A CASE STUDY IN ISTANBUL

APPROVED BY:

Assoc. Prof. Serdar Soyöz .....
(Thesis Supervisor)

Assoc. Prof. Hilmi Lus .....

Assist. Prof. Ufuk Yazgan .....

DATE OF APPROVAL: 27.10.2015

To my family

ACKNOWLEDGEMENTS

I would like to pay special thankfulness, warmth and appreciation to the persons below who made my research successful and assisted me at every point to cherish my goal:

My supervisor, Assoc. Prof. Serdar Soyöz for his vital support and guidance and also whose reminders and constant motivation encouraged me to meet the deadlines. His encouragement and understanding made it possible to achieve the goal. I would like to acknowledge his patience, tolerance and positive approach during the intensive periods of my studies.

My colleagues, Selahattin Akalp, Burak Horoz, Mustafa Sekman and Simon Karabulut, Orçun Tokuç, Oguz Senkardesler and Korkut Kaynardag for their endless friendship, support, patience and amenity. Their academic skills and experience cannot be neglected. My friends, Dogu Deniz Demir, Ezgi Altinay and Tansu Ilyaz whose help and sympathetic attitude at every point during my research helped me to work in time and in peaceful environment.

All faculty members, whose support and guidance are very crucial for me. They encouraged and helped me during my study.

Most of all, my family, for their endless love, self-sacrifice and patience. I cannot compensate their invaluable support and encouragement to achieve my goal. Whatever success I have achieved, my family's role can never be paid.

ABSTRACT

SEISMIC LOSS ESTIMATION METHODOLOGY: A CASE STUDY IN ISTANBUL

Earthquakes have been considered as one of the most serious threats to human life in physical, social and financial manner. Throughout the years, earthquakes have resulted in millions of people death, injury, physical disability; having psychological disorder and billions of dollars economical loss. In order to reduce these negative effects, estimation of future earthquake occurrence and minimizing the potential risks have crucial importance. The main responsibility should be taken mainly by municipalities, the researchers and scientists dealing with earthquake and geophysics, urban and regional planners and insurance companies. After occurrence of last two destructive (Kocaeli - August, 17 1999 and Düzce - November, 12 1999) earthquakes that have affected Marmara Region seriously, urban renewal and rehabilitation of buildings has gained remarkable importance in the cities having seismic activities. Especially in İstanbul, which is the most crowded and popular city among these, urban renewal methodology has widely taken place. In addition, the submarine faults underneath the Marmara Sea at very close proximity to İstanbul has not reactivated since 1766 and these are considered having huge potential to create significant seismic activities. These are the main motivations of this thesis study. This study aims to propose deterministic and probabilistic methods to estimate the seismic risk using the three of these submarine faults at closest proximity to İstanbul and based on this corresponding risk with different return periods, to determine vulnerability of a fictitious residential building in Kadiköy, İstanbul.

ÖZET

SİSMİK KAYIP TAHMİNİ YÖNTEMİ İSTANBUL İÇİN ÖRNEK OLAY ÇALIŞMASI

Depremler, fiziksel, sosyal ve maddi açılardan insan hayatı için en ciddi tehditlerden biri olarak kabul edilir. Yıllar boyunca, milyonlarca insanın ölümüne, ciddi yaralanmalarına ve sakatlıklara; psikolojik rahatsızlıklara ve milyar dolarlık ekonomik kayıplara sebep olmuştur. Bu olumsuz etkilerin azaltılması amacıyla, ileride oluşacak depremlerin tahmini ve potansiyel risklerin minimuma indirilmesi büyük önem taşıyor. Bu konuda en büyük sorumluluk da belediyelere, deprem bilimi ve jeofizik konulariyla ilgilenen araştırmacılara ve bilim insanlarına, şehir ve bölge planlamacılarına ve sigorta firmalarına düşüyor. Marmara Bölgesi'ni ciddi bir biçimde etkileyen son iki yıkıcı depremin (Kocaeli - 17 Ağustos 1999 ve Düzce - 12 Kasım 1999) gerçekleşmesinden sonra sismik aktivite bulunan şehirlerde kentsel dönüşüm ve binaların iyileştirilmesi büyük önem kazandı. Özellikle, bu bölgedeki en kalabalık ve en popüler şehir olan İstanbul'da kentsel dönüşüm hızla yayginlastı. Ayrıca, Marmara Denizi'nin altında bulunan İstanbul'a yakın faylar 1776'dan bu yana harekete geçmemiş ve bu faylarin ciddi bir deprem yaratma potansiyelinin çok yüksek olduğu düşünülüyor. Bu hususlar, bu tezin yazılması için gerekli sebepler olmuştur. Bu çalışma nihai olarak, deterministik ve olasılıksal yöntemler sayesinde denizin altında bulunan İstanbul'a en yakın mesafedeki fayları kullanarak İstanbul'un deprem riskini değerlendirmeyi ve bu risklere bağli olarak, Kadiköy-İstanbul'da bulunan fiktif bir binanın hasar görebilirliğini hesaplamayı amaçlamıştır.

TABLE OF CONTENTS

ACKNOWLEDGEMENTS iv
ABSTRACT v
ÖZET vi
LIST OF FIGURES ix
LIST OF TABLES xix
LIST OF ACRONYMS/ABBREVIATIONS xxii
1. INTRODUCTION 1
1.1. Seismic Loss Estimation Methodology 1
1.2. Literature Review 3
1.3. Proposed Methodology and Scope of the Study 8
2. SEISMIC HAZARD ANALYSIS 11
2.1. General 11
2.2. Deterministic Seismic Hazard Analysis (DSHA) 12
2.3. Probabilistic Seismic Hazard Analysis (PSHA) 26
2.4. Kalkan-Gülkan 2004 (KG04) Attenuation Relationship 36
2.5. Campbell-Bozorgnia 2008 (CB08) Attenuation Relationship 40
2.6. Uniform Hazard Spectrum 51
3. STRUCTURAL PERFORMANCE ASSESSMENT 55
3.1. General 55
3.2. Properties of Structure 58
3.3. Structural Assessment using Non-Linear Time History Analysis 61
3.4. Development of Fragility Curve 64
3.5. Discussion of Results 65
4. SUMMARY AND CONCLUSION 68
4.1. Summary 68
4.2. Conclusion 70
4.3. Future Works and Recommendations 71
APPENDIX A: SEISMIC HAZARD MAPS OF MARMARA REGION 73
APPENDIX B: COLLABORATIVE STUDY OF ISTANBUL METROPOLITAN 85

APPENDIX C: SEISMIC HAZARD MAPS FOR MARMARA REGION . . . 87
APPENDIX D: TIME HISTORY AND RESPONSE SPECTRUM PLOTS . . 89
APPENDIX E: GROUND MOTION INTENSITY OF ISTANBUL DISTRICTS 95
APPENDIX F: PLASTIC ROTATION - TIME PLOTS FOR BEAMS 97
REFERENCES 101

LIST OF FIGURES

Figure 1.1. Map View of an Illustrative Site, with Two Nearby Sources Capable of Producing Earthquakes and Predicted Median Response Spectra from the Two Earthquake Events (Baker, 2008). 4

Figure 1.2. Quantification of the Possibility of Intense Ground Shaking at a Site (Baker, 2008). 5

Figure 1.3. Westward Propagated 10 Large Earthquakes (M¿6.7) on the North Anatolian Fault (Gülkan, 2012). 6

Figure 1.4. Fault Segmentation Model for the Marmara Region (Kalkan *et al.*, 2004). 6

Figure 1.5. Map of Sea of Marmara Region Showing a Proxy. 8

Figure 1.6. Seismic Loss Estimation Steps. 9

Figure 2.1. Earthquake Scenario for İstanbul Metropolitan Area Considering Multiple Rupturing of the Islands. 11

Figure 2.2. Peak Ground Acceleration Map for İstanbul Metropolitan Area. . 15

Figure 2.3. Spectral Acceleration at 0.2sec Map for İstanbul Metropolitan Area. 18

Figure 2.4. Spectral Acceleration at 0.3sec Map for İstanbul Metropolitan Area. 18

Figure 2.5. Spectral Acceleration at 0.5sec Map for İstanbul Metropolitan Area. 21

Figure 2.6. Spectral Acceleration at 1.0sec Map for İstanbul Metropolitan Area. 21

Figure 2.7. Spectral Acceleration at 1.5sec Map for İstanbul Metropolitan Area. 24

Figure 2.8. Spectral Acceleration at 2.0sec Map for İstanbul Metropolitan Area. 24

Figure 2.9. Seismic Hazard Analysis in Steps (FEMA, 2002). 28

Figure 2.10. The Relationship Between Annual Number of Earthquakes and Corresponding Magnitudes. 29

Figure 2.11. The Exponential Distribution of Magnitudes. 30

Figure 2.12. The Truncated Exponential Distribution of Magnitudes. 31

Figure 2.13. The Truncated Characteristic Exponential Distribution of Magnitudes. 32

Figure 2.14. Illustrative Seismic Hazard Curve with for Return Periods, 475 and 2475 Years. 35

Figure 2.15. Vs30 = 400m/sec and Using KG04 Attenuation Relationship PGA map with 475 Years Return Period. 36

Figure 2.16. Vs30 = 400m/sec and Using KG04 Attenuation Relationship PGA map with 2475 Years Return Period. 37

Figure 2.17. Vs30 = 400m/sec and Using KG04 Attenuation Relationship Seismic Hazard Curve for PGA at Kadiköy District Considering the Fault Effects. 37

Figure 2.18. Vs30 = 400m/sec and Using KG04 Attenuation Relationship SA at 0.2sec Map with 475 Years Return Period. 38

Figure 2.19. Vs30 = 400m/sec and Using KG04 Attenuation Relationship SA at 0.2sec Map with 2475 Years Return Period. 38

Figure 2.20. Vs30 = 400m/sec and Using KG04 Attenuation Relationship Seismic Hazard Curve for SA at 0.2sec at Kadiköy District Considering the Fault Effects. 39

Figure 2.21. Vs30 = 400m/sec and Using KG04 Attenuation Relationship SA at 1.0sec map with 475 Years Return Period. 39

Figure 2.22. Vs30 = 400m/sec and Using KG04 Attenuation Relationship SA at 1.0sec map with 2475 Years Return Period. 40

Figure 2.23. Vs30 = 400m/sec and Using KG04 Attenuation Relationship Seismic Hazard Curve for SA at 1.0sec at Kadiköy District Considering the Fault Effects. 40

Figure 2.24. Vs30 = 400m/sec and using CB08 Attenuation Relationship PGA Map with 475 Years Return Period. 46

Figure 2.25. Vs30 = 400m/sec and using CB08 Attenuation Relationship PGA map with 2475 Years Return Period. 46

Figure 2.26. Vs30 = 400m/sec and using CB08 Attenuation Relationship Seismic Hazard Curve for PGA at Kadiköy District Considering the Fault Effects. 47

Figure 2.27. Vs30 = 400m/sec and using CB08 Attenuation Relationship SA at 0.2sec map with 475 Years Return Period. 47

Figure 2.28. Vs30 = 400m/sec and using CB08 Attenuation Relationship SA at 0.2sec map with 2475 Years Return Period. 48

Figure 2.29. Vs30 = 400m/sec and using CB08 Attenuation Relationship Seismic Hazard Curve for SA at 0.2sec at Kadiköy District Considering the fault Effects. 48

Figure 2.30. Vs30 = 400m/sec and using CB08 Attenuation Relationship SA at 0.3sec map with 475 Years Return Period. 49

Figure 2.31. Vs30 = 400m/sec and using CB08 Attenuation Relationship SA at 0.3sec map with 2475 Years Return Period. 49

Figure 2.32. Vs30 = 400m/sec and using CB08 Attenuation Relationship Seismic Hazard Curve for SA at 0.3sec at Kadiköy District Considering the Fault Effects. 50

Figure 2.33. Vs30 = 400m/sec and using CB08 Attenuation Relationship SA at 1.0sec map with 475 Years Return Period. 50

Figure 2.34. Vs30 = 400m/sec and using CB08 Attenuation Relationship SA at 1.0sec map with 2475 Years Return Period 51

Figure 2.35. Vs30 = 400m/sec and using CB08 Attenuation Relationship Seismic Hazard Curve for SA at 1.0sec at Kadiköy District Considering the Fault Effects. 51

Figure 2.36. Uniform Hazard Spectrum of Kadiköy district for Vs30 = 200m/sec. 52

Figure 2.37. Uniform Hazard Spectrum of Kadiköy district with Vs30 = 400m/sec. 52

Figure 2.38. Uniform Hazard Spectrum of Kadiköy district with Vs30 = 600m/sec. 53

Figure 3.1. Limit States on Typical Force-Displacement Plot. 57

Figure 3.2. Information About the Region of Interest of the Building (Kadiköy Belediyesi, 2014). 59

Figure 3.3. Layout of the Typical Building (Units are in mm). 60

Figure 3.4. First three Modes of the Building. 61

Figure 3.5. Plastic Rotation-Time Plot for pga=0.604g. 62

Figure 3.6. Fragility Curve of the Building for pga and Spectral Acceleration at 1.0sec Values at Life Safety Limit State. 65

Figure A.1. Vs30 = 200m/sec and Using CB08 Attenuation Relationship PGA map with 475 Years Return Period. 73

Figure A.2. Vs30 = 200m/sec and Using CB08 Attenuation Relationship PGA map with 2475 Years Return Period. 73

Figure A.3. Vs30 = 200m/sec and Using CB08 Attenuation Relationship Seismic Hazard Curve for PGA at Kadiköy District Considering the Fault Effects. 74

Figure A.4. Vs30 = 200m/sec and Using CB08 Attenuation Relationship SA at 0.2sec map with 475 Years Return Period. 74

Figure A.5. Vs30 = 200m/sec and Using CB08 Attenuation Relationship SA at 0.2sec map with 2475 Years Return Period. 75

Figure A.6. Vs30 = 200m/sec and Using CB08 Attenuation Relationship Period Seismic Hazard Curve for SA at 0.2sec at Kadiköy District Considering the Fault Effects. 75

Figure A.7. Vs30 = 200m/sec and Using CB08 Attenuation Relationship SA at 0.3sec map with 475 Years Return Period. 76

Figure A.8. Vs30 = 200m/sec and Using CB08 Attenuation Relationship SA at 0.3sec map with 2475 Years Return Period. 76

Figure A.9. Vs30 = 200m/sec and Using CB08 Attenuation Relationship Seismic Hazard Curve for SA at 0.3sec at Kadiköy District Considering the Fault Effects. 77

Figure A.10. Vs30 = 200m/sec and Using CB08 Attenuation Relationship SA at 1.0sec map with 475 Years Return Period. 77

Figure A.11. Vs30 = 200m/sec and Using CB08 Attenuation Relationship SA at 1.0sec map with 2475 Years Return Period. 78

Figure A.12. Vs30 = 200m/sec and Using CB08 Attenuation Relationship Seismic Hazard Curve for SA at 1.0sec at Kadiköy District Considering the Fault Effects. 78

Figure A.13. Vs30 = 600m/sec and Using CB08 Attenuation Relationship PGA map with 475 Years Return Period. 79

Figure A.14. Vs30 = 600m/sec and Using CB08 Attenuation Relationship PGA map with 2475 Years Return Period. 79

Figure A.15. Vs30 = 600m/sec and Using CB08 Attenuation Relationship Seismic Hazard Curve for PGA at Kadiköy District Considering the Fault Effects. 80

Figure A.16. Vs30 = 600m/sec and Using CB08 Attenuation Relationship SA at 0.2sec map with 475 years Return Period. 80

Figure A.17. Vs30 = 600m/sec and Using CB08 Attenuation Relationship SA at 0.2sec map with 2475 Years Return Period. 81

Figure A.18. Vs30 = 600m/sec and Using CB08 Attenuation Relationship Seismic Hazard Curve for SA at 0.2sec at Kadiköy District Considering the Fault Effects. 81

Figure A.19. Vs30 = 600m/sec and Using CB08 Attenuation Relationship SA at 0.3sec map with 475 years Return Period. 82

Figure A.20. Vs30 = 600m/sec and Using CB08 Attenuation Relationship SA at 0.3sec map with 2475 Years Return Period. 82

Figure A.21. Vs30 = 600m/sec and Using CB08 Attenuation Relationship Seismic Hazard Curve for SA at 0.3sec at Kadiköy District Considering the Fault Effects. 83

Figure A.22. Vs30 = 600m/sec and Using CB08 Attenuation Relationship SA at 1.0sec map with 475 Years Return Period. 83

Figure A.23. Vs30 = 600m/sec and Using CB08 Attenuation Relationship SA at 1.0sec map with 2475 Years Return Period. 84

Figure A.24. Figure A.8. Vs30 = 600m/sec and Using CB08 Attenuation Relationship Seismic Hazard Curve for SA at 1.0sec at Kadiköy District Considering the Fault Effects. 84

Figure B.1. PGA map for 475 Years Return Period - İstanbul Metropolitan Municipality and OYO International Company Study. 85

Figure B.2. PGA map for 2475 Years Return Period - İstanbul Metropolitan Municipality and OYO International Company Study. 85

Figure B.3. Spectral Acceleration at 0.2sec map for 475 Years Return Period - İstanbul Metropolitan Municipality and OYO International Company Study. 85

Figure B.4. Spectral Acceleration at 0.2sec map for 2475 Years Return Period - İstanbul Metropolitan Municipality and OYO International Company Study. 86

Figure B.5. Spectral Acceleration at 1.0sec map for 475 Years Return Period - İstanbul Metropolitan Municipality and OYO International Company Study. 86

Figure B.6. Spectral Acceleration at 1.0sec map for 2475 Years Return Period - İstanbul Metropolitan Municipality and OYO International Company Study. 86

Figure C.1. PGA map for 475 Years Return Period - CRISIS2007. 87

Figure C.2. PGA map for 2475 Years Return Period - CRISIS2007. 87

Figure C.3. Spectral Acceleration at 0.2sec map for 475 Years Return Period - CRISIS 2007. 87

Figure C.4. Spectral Acceleration at 0.2sec map for 2475 Years Return Period - CRISIS 2007. 87

Figure C.5. Spectral Acceleration at 0.3sec map for 475 Years Return Period - CRISIS 2007. 88

Figure C.6. Spectral Acceleration at 0.3sec map for 2475 Years Return Period - CRISIS 2007. 88

Figure C.7. Spectral Acceleration at 1.0sec map for 475 Years Return Period - CRISIS 2007. 88

Figure C.8. Spectral Acceleration at 1.0sec map for 2475 Years Return Period - CRISIS 2007. 88

Figure D.1. PGA=0.013g (a)Acceleration-Time Graph (b)Spectral Acceleration-Time Graph. 89

Figure D.2. PGA=0.101g (a)Acceleration-Time Graph (b)Spectral Acceleration-Time Graph. 89

Figure D.3. PGA=0.201g (a)Acceleration-Time Graph (b)Spectral Acceleration-Time Graph. 90

Figure D.4. PGA=0.301g (a)Acceleration-Time Graph (b)Spectral Acceleration-Time Graph. 90

Figure D.5. PGA=0.401g (a)Acceleration-Time Graph (b)Spectral Acceleration-Time Graph. 91

Figure D.6. PGA=0.493g (a)Acceleration-Time Graph (b)Spectral Acceleration-Time Graph. 91

Figure D.7. PGA=0.604g (a)Acceleration-Time Graph (b)Spectral Acceleration-Time Graph. 92

Figure D.8. PGA=0.753g (a)Acceleration-Time Graph (b)Spectral Acceleration-Time Graph. 92

Figure D.9. PGA=0.828g (a)Acceleration-Time Graph (b)Spectral Acceleration-Time Graph. 93

Figure D.10. PGA=0.897g (a) Acceleration-Time Graph (b)Spectral Acceleration-Time Graph. 93

Figure D.11. PGA=1.000g (a) Acceleration-Time Graph (b)Spectral Acceleration-Time Graph. 94

Figure F.1. Plastic Rotation-Time Plot for pga=0.201g. 97

Figure F.2. Plastic Rotation-Time Plot for pga=0.301g. 97

Figure F.3. Plastic Rotation-Time Plot for pga=0.401g. 98

Figure F.4. Plastic Rotation-Time Plot for pga=0.493g. 98

Figure F.5. Plastic Rotation-Time Plot for pga=0.753g. 99

Figure F.6. Plastic Rotation-Time Plot for pga=0.828g. 99

Figure F.7. Plastic Rotation-Time Plot for pga=0.897g. 100

Figure F.8. Plastic Rotation-Time Plot for pga=1.000g. 100

LIST OF TABLES

Table 1.1. Characteristic Attributes of Fault Segmentation Model (Kalkan *et al.*, 2004). 7

Table 2.1. Coefficients for Attenuation Relation of Mean Horizontal PGA and 5-Percent-Damped Spectral Accelerations (Kalkan *et al.*, 2004). . . 14

Table 2.2. Peak Ground Acceleration Value Computed at Central Point of Districts in the İstanbul Metropolitan area Considering Multiple Rupturing of off-Tekirdag, Mid-Marmara and Islands Fault Segments. . 16

Table 2.3. Spectral Acceleration Value at 0.2 sec Computed at Central Point of Districts in the İstanbul Metropolitan Area Considering Multiple Rupturing of off-Tekirdag, Mid-Marmara and Islands Fault Segments. 17

Table 2.4. Spectral Acceleration Value at 0.3sec Computed at Central Point of Districts in the İstanbul Metropolitan Area Considering Multiple Rupturing of Off-Tekirdag, Mid-Marmara and Islands Fault Segments. 19

Table 2.5. Spectral Acceleration Value at 0.5sec Computed at Central Point of Districts in the İstanbul Metropolitan Area Considering Multiple Rupturing of Off-Tekirdag, Mid-Marmara and Islands Fault Segments. 20

Table 2.6. Spectral Acceleration Value at 1.0sec Computed at Central Point of Districts in the İstanbul Metropolitan Area Considering Multiple Rupturing of Off-Tekirdag, Mid-Marmara and Islands Fault Segments. 22

Table 2.7. Spectral Acceleration Value at 1.5sec Computed at Central Point of Districts in the İstanbul Metropolitan Area Considering Multiple Rupturing of Off-Tekirdag, Mid-Marmara and Islands Fault Segments. 23

Table 2.8. Spectral Acceleration Value t 2a.0sec Computed at Central Point of Districts in the İstanbul Metropolitan Area Considering Multiple Rupturing of Off-Tekirdag, Mid-Marmara and Islands Fault Segments. 25

Table 2.9. Rate of Exceedance Calculation and its Corresponding Return Period Values. 35

Table 2.10. Coefficients for the Geometric Mean and Arbitrary Horizontal Components of The Median Ground Motion Model (Campbell,2008). . 44

Table 2.11. Standard Deviations for Uncertainty Model (Campbell,2008). . . . 45

Table 2.12. Acceleration Values for Kadiköy District. 53

Table 3.1. Limits States for Reinforced Concrete Columns (ASCE, 2014). . . 57

Table 3.2. Limits States for Reinforced Concrete Beams. (ASCE, 2014). . . . 58

Table 3.3. Add caption 59

Table 3.4. Total Percentage of the Members with Limit State Range for Each Ground Motion Intensity. 62

Table 3.5. The Performance of the Building. 63

Table 3.6. The Behavior of the Building. 64

Table 3.7. Probability of Failure Chart for Kadiköy District at Different Return Periods and Shear Wave Velocities. 66

Table E.1. Ground Motion Intensities of İstanbul Districts with 475 Years Return Period. 95

Table E.2. Ground Motion Intensities of İstanbul Districts with 475 Years Return Period. 96

LIST OF ACRONYMS/ABBREVIATIONS

ASCE	American Society of Civil Engineers
CB08	Campbell - Bozorgnia 2008 Attenuation Relationship
CP	Collapse Prevention Limit State
DSHA	Deterministic Seismic Hazard Analysis
FAR	Floor Area Ratio
FEMA	Federal Emergency Management Agency
GMPE	Ground Motion Prediction Equation
IO	Immediate Occupancy Limit State
KG04	Kalkan - Gülkan 2004 Attenuation Relationship
LS	Life Safety Limit State
MCE	Maximum Credible Earthquake
NAFZ	North Anatolian Fault Zone
NGA	Next Generation of Attenuation Models
PGA	Peak ground Acceleration
PSHA	Probabilistic Seismic Hazard Analysis
SA	Spectral Acceleration
SAR	Story Area Ratio
SHA	Seismic Hazard Analysis
TEC2007	Turkish Earthquake Code - 2007
UHS	Uniform Hazard Spectrum
USGS	United States Geological Survey

1. INTRODUCTION

1.1. Seismic Loss Estimation Methodology

Earthquakes are one of the main aspects that affect both built environment and as well as human-being for thousands of years physically and socially. Fatalities, injuries, collapse of structures and change in landforms are the main physical effects; besides that economical causality and psychological disorders can be exemplified as social impacts of earthquakes. From 1900 to 2014, more than 8.200 number of M>6.0 earthquake has occurred worldwide, which caused about 6.2 million death. Turkey is also located on the seismically active fault segments and total number of earthquake occurred with the magnitude M>6.0 is 51 (0.6% compared to worldwide) that has resulted in more than 75,000 death. (1.2%). (USGS, 2015).

İstanbul, with a population more than 14 million people (TÜIK, 2014), is the most crowded city in Turkey. 20% of the people in Turkey are resident in İstanbul and every year millions of people visit İstanbul for different purposes. İstanbul has been considered as economical center of Turkey and one of the most popular cities around the world. All these positive features of İstanbul attract people to make investments in this city, ranging from small ones such as having a flat and office, getting a job here etc. to huge investments as constructing residences, infrastructure etc. with millions of dollars cost. However, this city is located close to one of the active fault system called as North Anatolian Fault (NAF). This 1500km-long fault has westward moving transform mechanism and causes almost 25mm/year of right lateral motion between Anatolia and Eurasian plate. (Straub *et al.*, 1997; McClusky *et al.*, 2000) NAF starts from Eastern Region of Turkey and extends to western regions, passing through southern Black sea region and then underneath the Marmara Sea. Since 1939, this fault system has produced ten destructive earthquakes with the magnitude, M>6.7 in westward progression. (Gülkan, 2012) The most recent ones on this faults has occurred three months apart, 17.08.1999 M7.4 Kocaeli and 12.11.2014 M7.2 Düzce earthquakes. The 17.08.2014 M7.4 Kocaeli Earthquake has caused 18,000 death, 15,400 building collapse

and $ 10 - 25 billion economic loss. (Parsons, 2004). The submarine faults underneath the Marmara Sea at very close proximity to İstanbul have not reactivated since 1766 and time-dependent probability of occurrence of M>7 until at these faults that directly affects İstanbul and the neighboring cities was computed as 44±18% (Parsons 2004). This dreadful numbers have shown that detailed risk reducing measurements should be taken.

The methodology for estimating the physical and social consequences of an earthquake is called as "Seismic Loss Estimation", which plays an important role in earthquake engineering for design and rehabilitation purposes, insurance sector and governance by municipalities. It consists of seismic hazard analysis, structural performance assessment and quantification of damage in terms of socio-economic aspects. Generally, deterministic approaches have been used for this purpose but it may yield very conservative results and can only give understanding and judgment about a predefined scenario. It does not take inherent uncertainty of earthquake itself into consideration. These uncertainties can be listed in uncertainty in size, location and shaking intensity. In this study, with incorporation the uncertainties, probabilistic approaches have also been introduced while quantifying the seismic hazard in specified regions. Having developed seismic hazard maps utilizing submarine faults for İstanbul, fragility curves have been created for a ten-story fictitious reinforced concrete beam-column framed typical building by means of simulating seismic response of the structure based on non-linear structural dynamic analysis. After determining the vulnerability of the structures based on specified return periods, decision-making methodology takes role about determination of the action on related structures.

In this study, "Seismic Physical Loss Estimation" for a typical ten-story building located in Kadiköy region in İstanbul has been discussed considering submarine fault segments underneath the Marmara Sea.

1.2. Literature Review

"Seismic Loss Estimation" methodology has first gained remarkable importance in the performance assessment of structures such as nuclear power plants, dams and bridges, which have significant effects in case of a damage during seismic event. The first studies on "Seismic Loss Estimation" was conducted by Freeman (1932) for insurance companies. Since 1930s, numerous remarkable studies and researches have been performed. It has been professionally used for more than 30 years worldwide, especially in highly developed countries such as United States and Japan. In Turkey, especially after Marmara earthquakes, this approach has been used by insurance companies, academicians, design companies and municipalities for different purposes.

Since loss estimation studies have gained remarkable importance, computer programs and software have been developed on this topic. One of the most popular ones is HAZUS, which is geographic information system-based natural hazard software developed by Federal Emergency Management Agency of United States (FEMA, 2003). The methodology estimates the potential losses from earthquake, flood and hurricanes. HAZUS is an integrated software that combines the estimation of physical, economic and social impact of disasters. Based on HAZUS software, HAZTURK has been developed for Turkey based on Mid-America Earthquake Center platform.

"Seismic Loss Estimation" procedure has 3 main components: development and quantification of the seismic hazard map, structural performance assessment and lastly quantification of damage in terms of failure probability.

The seismic hazard assessment is quantification of ground motion intensity in terms of different parameters such as peak ground acceleration (PGA), spectral acceleration (SA), peak ground velocity (PGV), and peak ground displacement (PGD). Ground motion demand can be estimated using two approaches, deterministic and probabilistic seismic hazard analyses. In the literature, majority of the seismic loss estimation studies utilizes deterministic approaches, however it does not include inherent uncertainties of earthquake itself, DSHA is mainly defined as the analysis for choosing

the ground motion parameter with maximum magnitude and minimum distance. This is very straightforward and user-friendly methodology but it may arise some problems. For illustration, a basic analysis (Baker, 2008) for any fictitious site can be can be conducted considering two faults, Fault A has 10km distance to site with a characteristic magnitude 6.5 and Fault B has 20 km distance with M= 7.5 characteristic magnitude. Acceleration response spectra from these two events are illustrated in Figure 1.1. As seen from the figure, effect of Fault A is critical at short periods and for Fault B, the situation is vice versa, it creates large spectral accelerations at longer periods (more than 1 second). In other words, there is not a single one worst-case event for all situations.

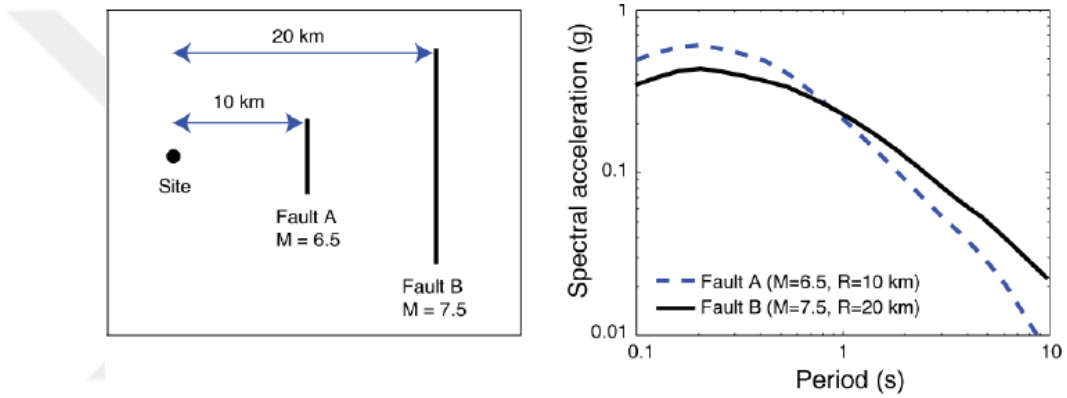

Figure 1.1. Map View of an Illustrative Site, with Two Nearby Sources Capable of Producing Earthquakes and Predicted Median Response Spectra from the Two Earthquake Events (Baker, 2008).

In order to include the inherent uncertainty of the earthquakes, "Probabilistic Seismic Hazard Analysis (PSHA)" can be used. With PSHA, rather than searching for the elusive worst-case ground motion demand, all possible uncertainties related with the earthquake generating source are taken into consideration for quantification of seismic hazard. Since probabilistic methods take these uncertainties into consideration, the resulting calculations are much more reliable and defensible for use in engineering decision-making for reducing risks. In order to quantify the risk due to earthquake shaking, annual probability or rate of exceeding some level of earthquake shaking at the region of interest should be determined (Baker, 2008). In Figure 1.2, an illustrative plot indicating that the exceedance probability is quite large at low level of intensities when compared to large levels is given.

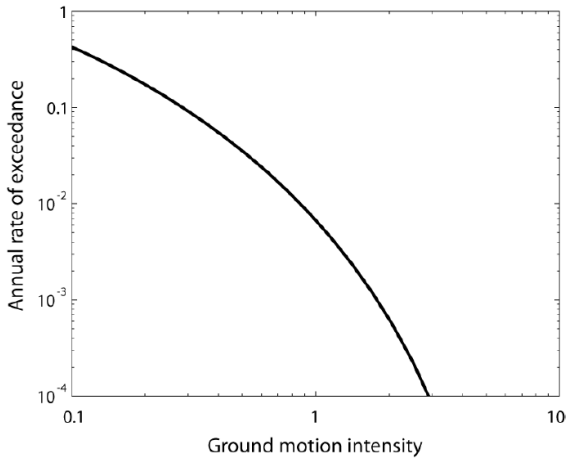

Figure 1.2. Quantification of the Possibility of Intense Ground Shaking at a Site (Baker, 2008).

The second and last components of seismic loss estimation are integrated with each other, assessment of structural response under earthquake effect and eventually development of structural fragility curves, which is mainly defined as seismic vulnerability of structures with various damage states. Having determined the structural responses considering earthquake loads, an analysis showing the vulnerability of the structure at certain damage states is conducted, which is defined as fragility curve assessment. This curve shows the behavior of the structure at a certain ground motion intensity, which is beneficial to see the probability of failure of the building under different ground motion levels.

The main motivation for this study is illustrated in Figure 1.3, which clearly indicates that there is a seismic gap in the Marmara Sea. Based on Coulomb stress calculations, there is significant shear stress increase after occurrence of earthquakes along North Anatolian Fault Zone in westward progression. Since 1939, this fault system has produced ten destructive M$\geq$6.7 earthquakes in westward progression as seen in Figure 1.3 (Gülkan, 2012). The most recent ones on this faults has occurred three months apart, 17.08.1999 M7.4 Kocaeli and 12.11.2014 M7.2 Düzce earthquakes. After occurrence of these two recent earthquakes, the submarine faults underneath the Marmara Sea has been considered to have huge potential to rupture (Parsons *et al.*, 2000; Hubert-Ferrari *et al.*, 2000) and time-dependent probability of occurrence

of M≥7 until 2034 in Marmara Sea that directly affects İstanbul and the neighboring cities was computed as 44±18

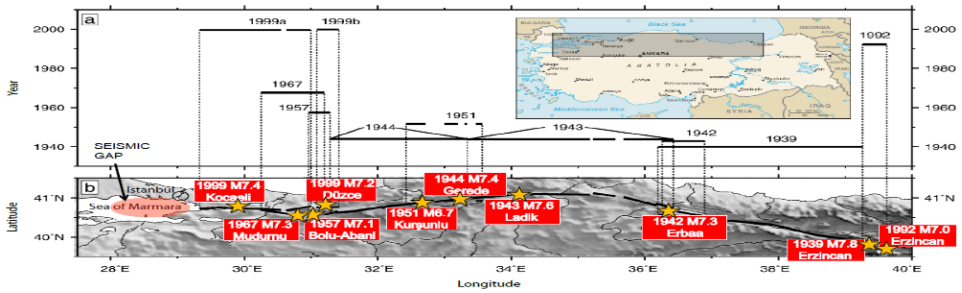

Figure 1.3. Westward Propagated 10 Large Earthquakes (M¿6.7) on the North Anatolian Fault (Gülkan, 2012).

Based on a survey in Marmara Region, the fault segments underneath and nearby the Marmara Sea are illustrated in Figure 1.4. The light-colored fault segments has shown the segments with high potential to create significant seismic activities. (Le Pichon *et al.*, 2001) The properties of fault segments are shown in Table 1.1. The main properties of the faults are length of fault, characteristic event which shows the maximum probable magnitude this fault can generate, slip rate and activity rate. While long-length faults generate larger magnitude earthquakes with more time interval, short-length faults generate more earthquakes with lesser magnitudes.

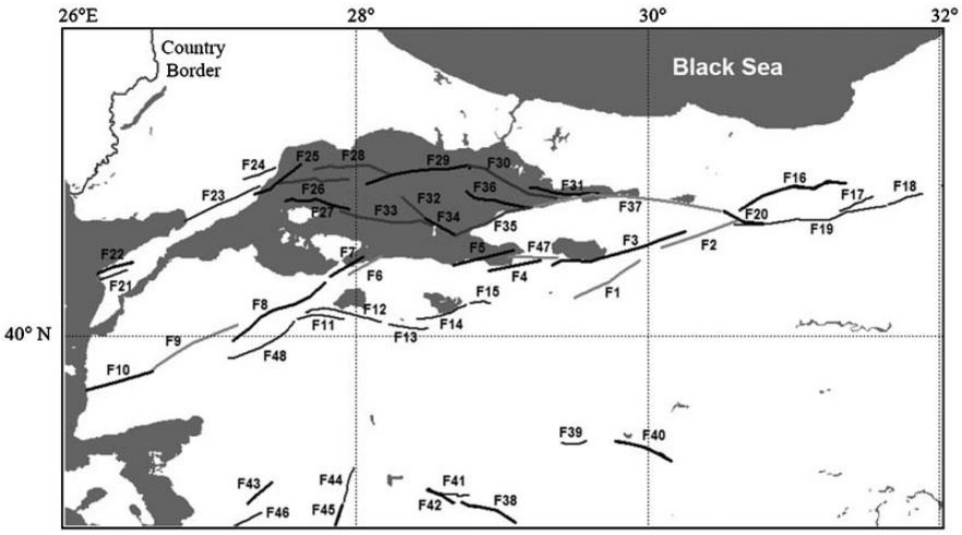

Figure 1.4. Fault Segmentation Model for the Marmara Region (Kalkan *et al.*, 2004).

Table 1.1. Characteristic Attributes of Fault Segmentation Model (Kalkan *et al.*, 2004).

Fault Segment	Length (km)	Characteristic Even (M)	Slip-Rate (mm-yr)	Activity Rate (Earthquake/yr)	Fault Segment	Length (km)	Characterstic Event (M)	Slip-Rate (mm-yr)	Activity Rate (Earthquake/yr)
F1	45	7.0	20	0.0073	F25	31	6.8	20	0.0095
F2	48	7.0	20	0.0070	F26	44	7.0	20	0.0074
F3	82	7.3	20	0.0049	F27	42	7.0	20	0.0077
F4	31	6.8	20	0.0094	F28	51	7.1	20	0.0077
F5	36	6.9	20	0.0085	F29	62	7.2	23	0.0068
F6	22	6.7	20	0.0119	F30	51	7.1	23	0.0077
F7	28	6.7	20	0.0101	F31	20	6.6	23	0.0148
F8	63	7.2	20	0.0058	F32	16	6.5	20	0.015
F9	58	7.1	20	0.0062	F33	57	7.1	20	0.0062
F10	40	7.0	20	0.0079	F34	20	6.6	20	0.0128
F11	28	6.8	20	0.0101	F35	41	7.0	20	0.0077
F12	46	7.0	20	0.0072	F36	36	6.9	20	0.0085
F13	21	6.6	20	0.0121	F37	112	7.5	23	0.0045
F14	29	6.8	20	0.0099	F38	36	6.9	18	0.0076
F15	21	6.7	20	0.0121	F39	15	6.5	18	0.0140
F16	66	7.2	20	0.0056	F40	37	6.9	18	0.0075
F17	21	6.6	20	0.0122	F41	30	6.8	18	0.0088
F18	21	6.6	20	0.0124	F42	10	6.3	18	0.0185
F19	90	7.3	20	0.0046	F43	20	6.6	15	0.0096
F20	26	6.6	20	0.0107	F44	22	6.7	15	0.0089
F21	19	6.6	20	0.0133	F45	15	6.5	15	0.0116
F22	23	6.7	20	0.0114	F46	20	6.6	15	0.0096
F23	49	7.1	10	0.0034	F47	30	6.8	20	0.0097
F24	33	6.9	10	0.0045	F48	46	7	20	0.0072

In order to incorporate site effects on ground motion estimates, the average shear-wave velocity between 0 and 30-meters depth, Vs30 is used shown in Figure 1.5. Dark color, light color and white color represent rock site, soft site and water, respectively. (Gülkan, 2011) It clearly indicates that for the entire Marmara Sea Region, surface soils generally have Vs30 values between 400 and 760 m/s in southern coastline of Marmara Sea Region. However, this value is between 200m/sec and 600m/s for İstanbul metropolitan area and most of the population in İstanbul resides on soft-soil deposits, where Vs30 value is around 300m/sec to 400m/sec. Within the scope of this thesis, three Vs30 values are used: 200m/s, 400m/s and 600m/s.

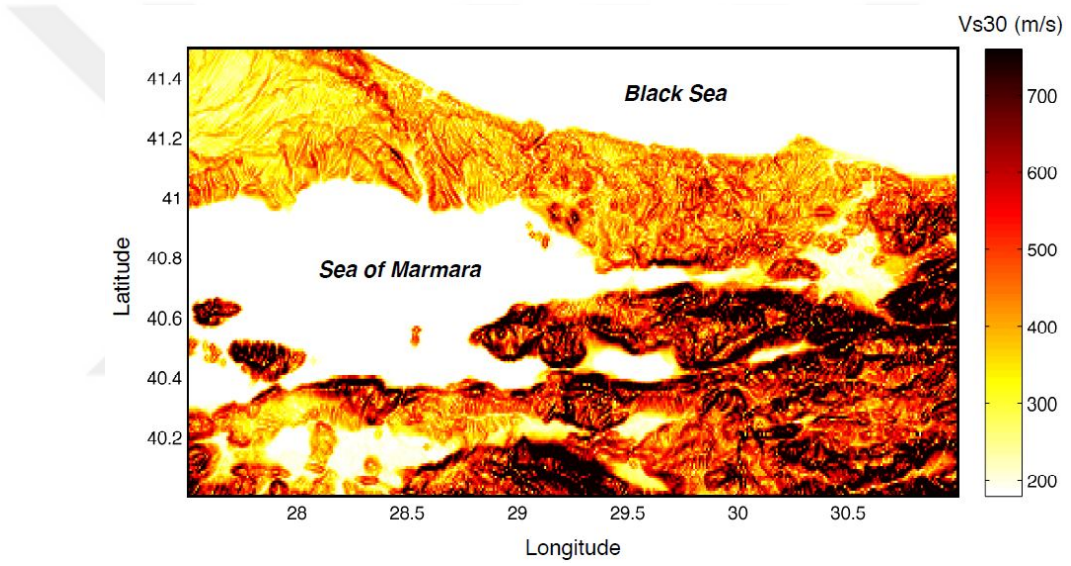

Figure 1.5. Map of Sea of Marmara Region Showing a Proxy for the Shear-Wave Velocity Averaged Over the Top 30m of the Ground (Vs30). Dark Color = Rock Site, Light Color = Soft Soil Site, white Color = Water (Gülkan, 2012).

1.3. Proposed Methodology and Scope of the Study

The flowchart in Figure 1.6 illustrates the general framework of this study.

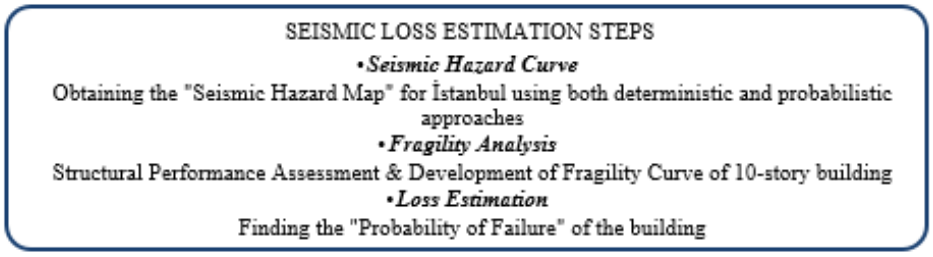

Figure 1.6. Seismic Loss Estimation Steps.

This study aims to evaluate the seismic loss estimation for a moment resisting frame building with ten-stories in İstanbul, considering submarine faults system underneath the Marmara Sea, F28-Island Fault, F29-Mid Marmara Fault, F30-Off Tekirdag Fault. These submarine faults has huge potential to rupture and time-dependent probability of occurrence of an earthquake with M≥7.0 until 2034 in Marmara Sea that directly affects İstanbul and the neighboring cities was computed as 44±18%. (Parsons *et al.*, 2000; Hubert-Ferrari *et al.*, 2000). Since İstanbul is highly populated and industrialized city, it is important to estimate the potential seismic effect. The outcome of this study can be utilized for insurance companies, municipalities and design companies for evaluation and retrofitting purposes. Loss estimation evaluates the probability of failure based on related ground motion intensity parameter (peak ground acceleration, peak ground velocity, peak ground displacement, spectral acceleration, and spectral displacement).

In Chapter 2, fundamentals of Seismic Hazard Analysis which is the first step of Loss Estimation Methodology has been discussed. Considering the submarine faults underneath the Marmara Sea, deterministic and probabilistic seismic hazard maps have been generated. Ground motion maps using deterministic approach are mainly based on the fact that the multiple rupture of these faults is certain. On the other hand, the maps generated using probabilistic approach are based on probability of exceedance in certain time period, namely return periods. 10% exceedance in 50 years gives 475 years return period, while 2% exceedance in 50 years represent 2475 years.

In Chapter 3, the second step of Seismic Loss Estimation, Structural Performance

Assessment, is introduced. Firstly, two dimensional nonlinear time history analysis for 10-story typical building has been executed using SAP2000 software considering 11 different acceleration values, from 0.01g to 1.00g. Based on ASCE 41-13 (American Society of Civil Engineers-Seismic Evaluation and Retrofit of Existing Buildings) limit states and its limitations, the overall structural performance with damage states has been determined for each acceleration value. Lastly, for each damage state, fragility curve have been generated to calculate the probability of failure and compared for deterministic and probabilistic approaches at different levels of ground motion demand values.

Chapter 4 summarizes and concludes the proposed study, and gives his recommendations for future works.

2. SEISMIC HAZARD ANALYSIS

2.1. General

Seismic Hazard Analysis, for brevity SHA, is the first step for Loss Estimation methodology. SHA provides ground motion demand for certain return periods of earthquake occurrence. Both probabilistic and deterministic methods have a role in seismic hazard and risk analyses for decision making purposes.

In this study, multiple rupturing of three faults that dominate the hazard in İstanbul has been considered. Three fault segments with closest distance to İstanbul have been chosen as illustrated in Figure 2.1; Off-Tekirdag (F28), Mid-Marmara (F29) and Islands (F30) faults. After occurrence of Kocaeli and Düzce Earthquakes on the same fault system, the energy has been transformed to western faults, which causes increase in stress concentration at these submarine faults (Gülkan *et al.*, 2010). These faults have been considered to rupture at the same time and the combined effect has been analyzed both by deterministic SHA and probabilistic SHA. In order to obtain reliable seismic hazard maps, İstanbul area is meshed on a fine grid of 0.05^o by 0.05^o, approximately 4km by 4km.

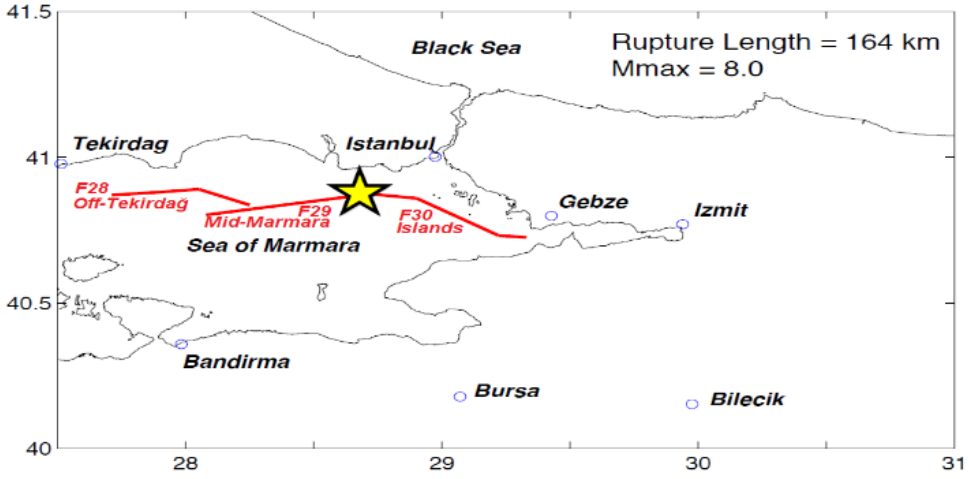

Figure 2.1. Earthquake Scenario for İstanbul Metropolitan Area Considering Multiple Rupturing of the Islands, Mid-Marmara and off-Tekirdag Fault Segments (Gülkan, 2012).

2.2. Deterministic Seismic Hazard Analysis (DSHA)

"Deterministic Seismic Hazard Analysis (DSHA)" is based on choosing the earthquake-generating sources with maximum magnitudes and closest source-to-site distances.

The DSHA is conducted for deterministic scenario and this scenario can be either a single event or numerous number of events where the faults are active and well-defined. The procedure for DSHA as follows:

- Identification and characterization of all earthquake sources
- Determination of shortest source-to-site
- Selection of controlling (critical) earthquake in terms of ground motion parameters (peak ground acceleration, peak ground velocity, peak ground displacement, spectral acceleration, spectral displacement)
- Expression of hazard in terms of related ground motion parameters

Input for DSHA, namely ground motion parameters, can be obtained by three main methods:

- Past Earthquakes
- Maximum Credible Earthquakes

When one have access to past earthquakes data, he/she uses the reasonable nearby earthquakes occurred in the history as input data.

If second option is to be used, the worst-case scenario earthquake with maximum magnitude and minimum distance to site is considered. Since it is going to create the greatest ground motion demand, this method is preferred to be used for special structures, such as nuclear power plants, shelters and very important public buildings.

As seen from the procedures above, it neglects the inherent uncertainty of main components that affects earthquake intensity, such as distance and magnitude uncer-

tainty. But, DSHA works well for "scenario" earthquake methods and provides a clear way about computing the seismic hazard. For this study, "Maximum Credible Earthquake (MCE)" method is used. The MCE value is referenced from Gülkan,2012. When these three faults have ruptured at the same time, an earthquake with magnitude 8.0 and rupture length 161km takes place (Gülkan, 2012).

In this thesis, deterministic SHA is based on single ground motion prediction equation, generated by Kalkan and Gülkan 2004 (Kalkan *et al.*,2004).The general form of the ground motion parameter estimation equation is as following.

$$\begin{aligned} lnY &= b_1 + b_2\,(M-6) + b_3(M-6)^2 + b_5 lnr + b_v ln\,(V_s/V_A) \\ r &= (r_{cl}^2 + h^2)^{1/2} \end{aligned} \tag{2.1}$$

where Y is the ground motion parameter (peak ground acceleration or spectral acceleration in terms of g), M is the moment magnitude, r_{cl} is the closest horizontal distance from the station to a site of interest in km, Vs is the characteristic shear-wave velocity for the station in m/sec; and b_1, b_2, b_3,b_5, h and V_A are the parameters to be determined h is the fictitious depth and V_A is a fictitious velocity that is determined by regression. σ is the standard deviation of the residuals. The coefficients for estimating the maximum horizontal peak ground acceleration and spectral acceleration responses are listed in Figure 2.2. Note that, the spectral ordinates are at 5-percent damping and are kept in the range of 0.1 sec to 1.5 sec. This table is available for magnitudes (M) 4.0 to 7.5 and distances (r_{cl}) up to 250km (Kalkan *et al.*,2004).

Table 2.1. Coefficients for Attenuation Relation of Mean Horizontal PGA and 5-Percent-Damped Spectral Accelerations (Kalkan *et al.*, 2004).

In (Y)=b1+b2(M-6)+b3(M-6)^2+b5In r+bv In(V_s/V_A with r=($r^2{}_{cl}$+h^2)$^{1/2}$								
period (sec)	b1	b2	b3	b5	b_v	V_A	h(km)	σ_{inY}
PGA	0.393	0.576	-0.107	-0.899	-0.200	1112	6.91	0.612
0.10	1.796	0.441	-0.087	-1,023	-0.054	1112	10.07	0.658
0.11	1.627	0.498	-0.086	-1,030	-0.051	1290	10.31	0.643
0.12	1.109	0.721	-0.233	-0.939	-0.215	1452	6.91	0.650
0.13	1.474	0.500	-0.127	-1.070	-0.300	1953	10.00	0.670
0.14	0.987	0.509	-0.114	-1.026	-0.500	1717	9.00	0.620
0.15	1.530	0.511	-0.127	-1.070	-0.300	1953	10.00	0.623
0.16	1.471	0.517	-0.125	-1.052	-298	1954	9.59	0.634
0.17	1.500	0.530	-0.115	-1.060	-0.297	1955	9.65	0.651
0.18	1.496	0.547	-0.115	-1.060	-0.301	1957	9.40	0.646
0.19	1.468	0.575	-0.108	-1.055	-0.302	1958	9.23	0.657
0.20	1.419	0.597	-0.097	-1.050	-0.303	1959	8.96	0.671
0.22	0.989	0.628	-0.118	-0.951	-0.301	1959	6.04	0.683
0.24	0.736	0.654	-0.113	-0.892	-0.302	1960	5.16	0.680
0.26	0.604	0.696	-0.109	-0.860	-0.305	1961	4.70	0.682
0.28	0.727	0.733	-0.127	-0.891	-0.303	1963	5.74	0.674
0.30	0.799	0.751	-0.148	-0.909	-0.297	1964	6.49	0.720
0.32	0.749	0.744	-0.161	-0.897	-0.300	1954	7.18	0.714
0.34	0.798	0.741	-0.154	-0.891	-0.266	1968	8.10	0.720
0.36	0.589	0.752	-0.143	-0.867	-0.300	2100	7.90	0.650
0.38	0.490	0.763	-0.138	-0.852	-0.300	2103	8.00	0.779
0.40	0.530	0.775	-0.147	-0.855	-0.264	2104	8.32	0.772
0.42	0.353	0.784	-0.150	-0.816	-0.267	2104	7.69	0.812
0.44	0.053	0.782	-0.132	-0.756	-0.268	2103	7.00	0.790
0.46	0.049	0.780	-0.157	-0.747	-0.290	2059	7.30	0.781
0.48	-0.170	0.796	-0.153	-0.704	-0.275	2060	6.32	0.789
0.50	-0.146	0.828	-0.161	-0.710	-0.274	2064	6.22	0.762
0.55	-0.306	0.866	-0.156	-0.702	-0.292	2071	5.81	0.808
0.60	-0.383	0.881	-0.179	-0.697	-0.303	2075	6.13	0.834
0.65	-0.491	0.896	-0.182	-0.696	-0.300	2100	5.80	0.845
0.70	-0.576	0.914	-0.190	-0.681	-0.301	2102	5.70	0.840
0.75	-0.648	0.933	-0.185	-0.676	-0.300	2104	5.90	0.828
0.80	-0.713	0.968	-0.183	-0.676	-0.301	2090	5.89	0.839
0.85	-0.567	0.786	-0.214	-0.695	-0.333	1432	6.27	0.825
0.90	-0.522	1.019	-0.225	-0.708	0.313	1431	6.69	0.826
0.95	-0.610	1.050	-0.229	-0.697	-0.303	1431	6.89	0.841
1.00	-0.662	1.070	-0.250	-0.696	-0.305	1405	6.89	0.874
1.10	-1.330	1.089	-0.255	-0.684	-0.500	2103	7.00	0.851
1.20	-1.370	1.120	-0.267	-0.690	-0.498	2103	6.64	0.841
1.30	-1.474	1.155	-0.269	-0.696	-0.496	2103	6.00	0.856
1.40	-1.665	1.170	-0.258	-0.674	-0.500	2104	5.44	0.845
1.50	-1.790	1.183	-0.262	-0.665	-0.501	2104	5.57	0.840
1.60	-1.889	1.189	-0.265	-0.662	-0.503	2102	5.50	0.834
1.70	-1.968	1.200	-0.272	-0.664	-0.502	2101	5.30	0.828
1.80	-2.037	1.210	-0.284	-0.666	-0.505	2098	5.10	0.849
1.90	-1.970	1.210	-0.295	-0.675	-0.501	1713	5.00	0.855
2.00	-2.110	1.200	-0.300	-0.663	-0.499	1794	4.86	0.878

Considering the parameters mentioned above, the hazard maps for peak ground horizontal acceleration (PGA) and spectral acceleration (SA) at 0.2s, 0.3s, 0.5s, 1.0s,

1.5s and 2.0s for 5% damping have been generated. In order to incorporate the site effects, shear-wave velocity at the upper 30m (Vs30) is used. For İstanbul region, Vs30 values varies between 200m/s and 600m/s. The DSHA analysis for İstanbul is conducted for average shear-wave velocity, 400m/s.

For the corresponding earthquake scenario (multiple rupturing of Off-Tekirdag, Mid-Marmara and Islands Fault) hazard maps for PGA and spectral acceleration values defined above have been generated. For verification, these results are compared with the values in Gülkan's study for İstanbul Metropolitan Area. (Gülkan, 2012) His study is mainly based on obtaining seismic hazard for İstanbul by utilizing 6 GMPEs; Abrahamson and Silva (2008), Boore and Atkinson (2008), Campbell and Bozorgnia (2008), Chiou and Young (2008), Grazier and Kalkan (2007 and 2009), and Kalkan and Gülkan (2004). These are abbreviated as AS08, BA08, CB08, CY08, GK07 and KG04, respectively. By using logic tree weighting, he has concluded that for peak ground acceleration and spectral accelerations up to 1.5sec, KG04 gives the best results. The results of his study and this thesis work have been compared at Table 2.1 to Table Table 2.7. The seismic hazard maps for peak ground acceleration and spectral acceleration using KG04 attenuation relationship are given in Figure 2.3 to Figure 2.9.

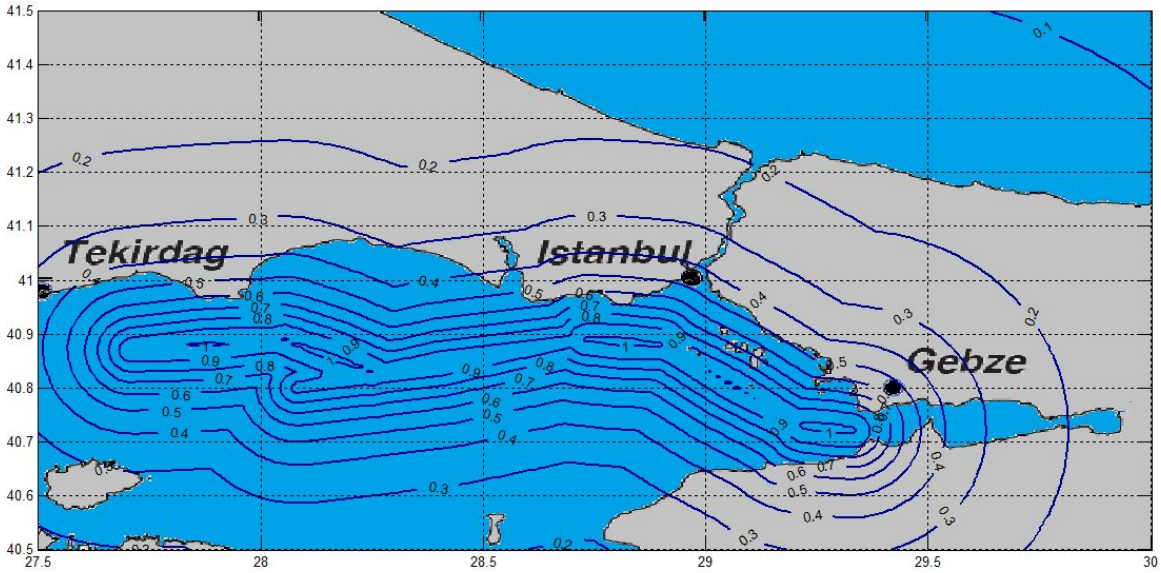

Figure 2.2. Peak Ground Acceleration Map for İstanbul Metropolitan Area.

Table 2.2. Peak Ground Acceleration Value Computed at Central Point of Districts in the İstanbul Metropolitan area Considering Multiple Rupturing of off-Tekirdag, Mid-Marmara and Islands Fault Segments.

DETERMINISTIC SEISMIC HAZARD ANALYSIS FOR ISTANBUL				Peak Ground Acceleration (g)			
District	Population (people)	Total Land Area (km^2)	Population Density (people km^2)	PGA	Article*	Difference	Absolute Difference
Adalar	16.166	11.05	1.463.00	0.69	0.65	6%	6%
Arnavutköy	215.531	506.5	425.5	0.23	0.27	-13%	13%
Atasehir	405.974	25.87	15.692.80	0.37	0.42	-12%	12%
Avcilar	407.240	41.92	9.714.70	0.47	0.55	-15%	15%
Bagcilar	752.250	22.4	33.582.60	0.41	0.38	8%	8%
Bahçelievler	602.931	16.57	36.386.90	0.51	0.56	-8%	8%
Bakirköy	220.974	29.65	7.452.70	0.57	0.65	-12%	12%
Basaksehir	333.047	104.5	3.187.10	0.34	0.37	-8%	8%
Bayrampasa	269.677	9.5	28.387.10	0.39	0.41	-5%	5%
Besiktas	186.570	18.04	10.342.00	0.32	0.34	-6%	6%
Beykoz	248.056	310.4	799.1	0.22	0.23	-3%	3%
Beylikdüzü	244.760	37.74	6.485.40	0.51	0.52	-1%	1%
Beyoglu	245.219	8.96	27.368.20	0.38	0.49	-21%	21%
Büyükçekmece	211.000	157.7	1.338.00	0.34	0.45	-23%	23%
Çatalca	65.811	1040	63.3	0.25	0.25	0%	0%
Çekmeköy	207.476	148	1.401.90	0.24	0.23	3%	3%
Esenler	462.621	18.51	24.993.00	0.36	0.37	-3%	3%
Esenyurt	624.733	43.12	14.488.20	0.4	0.49	-18%	18%
Eyüp	361.531	228.1	1.585.00	0.27	0.26	3%	3%
Fatih	425.875	15.93	26.734.10	0.45	0.5	-9%	9%
Gaziosmanpasa	495.006	11.67	42.417.00	0.35	0.34	3%	3%
Güngören	306.854	7.17	42.796.90	0.45	0.5	-9%	9%
Kadiköy	506.293	25.07	20.195.20	0.42	0.46	-9%	9%
Kagithane	428.755	14.83	28.911.30	0.32	0.31	4%	4%
Kartal	447.110	38.54	11.601.20	0.42	0.52	-19%	19%
Küçükçekmece	740.090	37.25	19.868.20	0.46	0.46	0%	0%
Maltepe	471.059	53.06	8.877.90	0.4	0.41	-3%	3%
Pendik	646.375	180.2	3.587.00	0.32	0.43	-26%	26%
Sancaktepe	304.406	61.87	4.920.10	0.27	0.26	3%	3%
Sariyer	335.598	151.3	2.218.10	0.24	0.23	3%	3%
Silivri	155.923	869.5	179.3	0.31	0.31	0%	0%
Sultanbeyli	309.347	28.86	10.718.90	0.31	0.33	-7%	7%
Sultangazi	505.190	36.24	13.940.10	0.3	0.34	-10%	10%
Sile	31.718	781.7	40.6	0.16	0.18	-13%	13%
Sisli	274.420	34.98	7.845.10	0.35	0.42	-16%	16%
Tuzla	208.807	123.9	1.685.30	0.44	0.57	-22%	22%
Ümraniye	660.125	45.3	14.572.30	0.33	0.4	-18%	18%
Üsküdar	534.636	35.34	15.128.40	0.34	0.34	0%	0%
Zeytinburnu	292.313	11.31	25.845.50	0.5	0.53	-6%	6%
				Average Absolute Difference			9%

Table 2.3. Spectral Acceleration Value at 0.2 sec Computed at Central Point of Districts in the İstanbul Metropolitan Area Considering Multiple Rupturing of off-Tekirdag, Mid-Marmara and Islands Fault Segments.

DETERMINISTIC SEISMIC HAZARD ANALYSIS FOR ISTANBUL				Spectral Acceleration at 0.2s (g)			
District	Population (people)	Area Land Area (km^2)	Population Density (people/km^2)	at 0.2s	Article*	Difference	Absolute Difference
Adalar	16.166	11.05	1.463.00	1.11	0.91	21%	21%
Arnavutköy	215.531	506.5	425.5	0.35	0.36	-2%	2%
Atasehir	405.974	25.87	15.692.80	0.58	0.57	1%	1%
Avcilar	407.240	41.92	9.714.70	0.75	0.77	-2%	2%
Bagcilar	752.250	22.4	33.582.60	0.66	0.53	24%	24%
Bahçelievler	602.931	16.57	36.386.90	0.82	0.74	11%	11%
Bakirköy	220.974	29.65	7.452.70	0.92	0.87	5%	5%
Basaksehir	333.047	104.5	3.187.10	0.53	0.5	5%	5%
Bayrampasa	269.677	9.5	28.387.10	0.61	0.56	9%	9%
Besiktas	186.570	18.04	10.342.00	0.49	0.47	4%	4%
Beykoz	248.056	310.4	799.1	0.33	0.32	2%	2%
Beylikdüzü	244.760	37.74	6.485.40	0.82	0.72	13%	13%
Beyoglu	245.219	8.96	27.368.20	0.61	0.68	-10%	10%
Büyükçekmece	211.000	157.7	1.338.00	0.54	0.62	-13%	13%
Çatalca	65.811	1040	63.3	0.37	0.35	6%	6%
Çekmeköy	207.476	148	1.401.90	0.36	0.31	14%	14%
Esenler	462.621	18.51	24.993.00	0.57	0.51	10%	10%
Esenyurt	624.733	43.12	14.488.20	0.64	0.65	-2%	2%
Eyüp	361.531	228.1	1.585.00	0.41	0.35	17%	17%
Fatih	425.875	15.93	26.734.10	0.73	0.67	8%	8%
Gaziosmanpasa	495.006	11.67	42.417.00	0.55	0.47	17%	17%
Güngören	306.854	7.17	42.796.90	0.72	0.68	6%	6%
Kadiköy	506.293	25.07	20.195.20	0.66	0.63	5%	5%
Kagithane	428.755	14.83	28.911.30	0.51	0.44	14%	14%
Kartal	447.110	38.54	11.601.20	0.67	0.7	-4%	4%
Küçükçekmece	740.090	37.25	19.868.20	0.75	0.65	14%	14%
Maltepe	471.059	53.06	8.877.90	0.63	0.56	12%	12%
Pendik	646.375	180.2	3.587.00	0.49	0.61	-19%	19%
Sancaktepe	304.406	61.87	4.920.10	0.41	0.36	13%	13%
Sariyer	335.598	151.3	2.218.10	0.36	0.32	11%	11%
Silivri	155.923	869.5	179.3	0.48	0.43	12%	12%
Sultanbeyli	309.347	28.86	10.718.90	0.47	0.46	2%	2%
Sultangazi	505.190	36.24	13.940.10	0.47	0.46	2%	2%
Sile	31.718	781.7	40.6	0.22	0.24	-8%	8%
Sisli	274.420	34.98	7.845.10	0.55	0.56	-1%	1%
Tuzla	208.807	123.9	1.685.30	0.71	0.78	-9%	9%
Ümraniye	660.125	45.3	14.572.30	0.51	0.54	-6%	6%
Üsküdar	534.636	35.34	15.128.40	0.54	0.48	12%	12%
Zeytinburnu	292.313	11.31	25.845.50	0.8	0.73	9%	9%
			Average Absolute Difference				9%

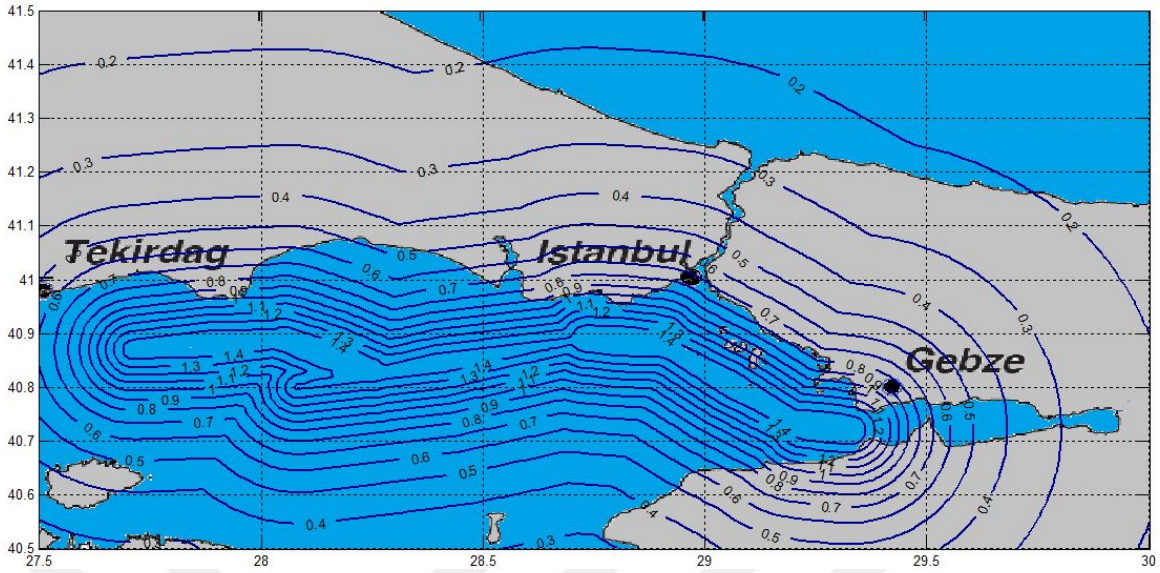

Figure 2.3. Spectral Acceleration at 0.2sec Map for İstanbul Metropolitan Area.

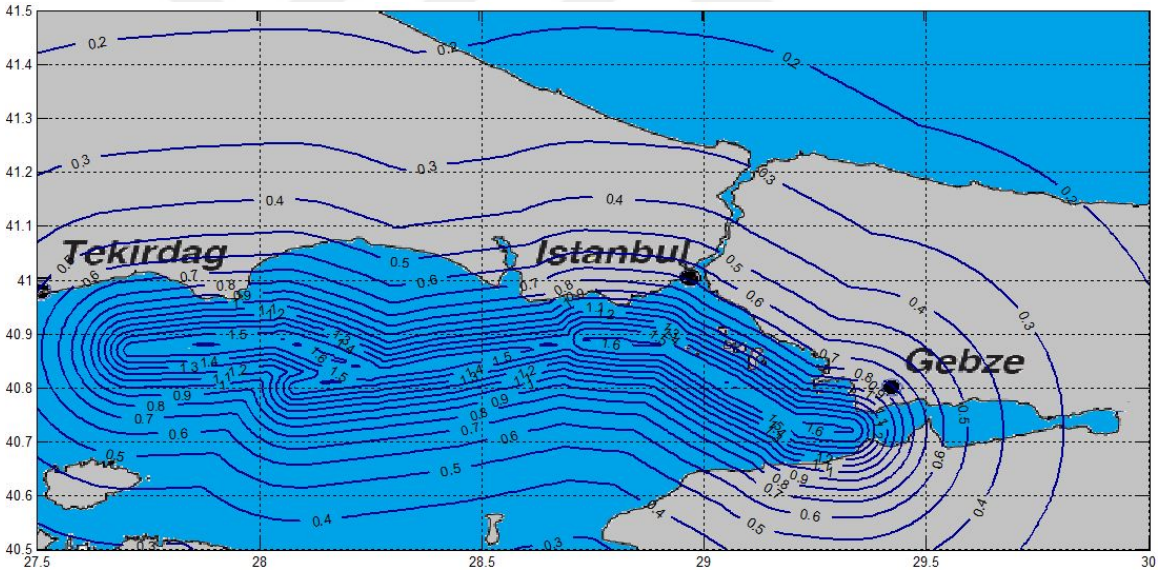

Figure 2.4. Spectral Acceleration at 0.3sec Map for İstanbul Metropolitan Area.

Table 2.4. Spectral Acceleration Value at 0.3sec Computed at Central Point of Districts in the İstanbul Metropolitan Area Considering Multiple Rupturing of Off-Tekirdag, Mid-Marmara and Islands Fault Segments.

DETERMINISTIC SEISMIC HAZARD ANALYSIS FOR ISTANBUL				Spectral Acceleration at 0.2s (g)			
District	Population (people)	Area Land Area (km^2)	Population Density (people/km^2)	at 0.2s	Article*	Difference	Absolute Difference
Adalar	16.166	11.05	1.463.00	1.07	0.95	12%	12%
Arnavutköy	215.531	506.5	425.5	0.35	0.37	-6%	6%
Atasehir	405.974	25.87	15.692.80	0.55	0.57	-3%	3%
Avcilar	407.240	41.92	9.714.70	0.7	0.78	-9%	9%
Bagcilar	752.250	22.4	33.582.60	0.62	0.53	17%	17%
Bahçelievler	602.931	16.57	36.386.90	0.77	0.77	0%	0%
Bakirköy	220.974	29.65	7.452.70	0.87	0.9	-3%	3%
Basaksehir	333.047	104.5	3.187.10	0.5	0.51	-1%	1%
Bayrampasa	269.677	9.5	28.387.10	0.58	0.56	3%	3%
Besiktas	186.570	18.04	10.342.00	0.47	0.48	-1%	1%
Beykoz	248.056	310.4	799.1	0.33	0.32	2%	2%
Beylikdüzü	244.760	37.74	6.485.40	0.77	0.73	5%	5%
Beyoglu	245.219	8.96	27.368.20	0.58	0.69	-16%	16%
Büyükçekmece	211.000	157.7	1.338.00	0.51	0.63	-18%	18%
Çatalca	65.811	1040	63.3	0.37	0.35	5%	5%
Çekmeköy	207.476	148	1.401.90	0.35	0.3	17%	17%
Esenler	462.621	18.51	24.993.00	0.54	0.52	3%	3%
Esenyurt	624.733	43.12	14.488.20	0.6	0.67	-10%	10%
Eyüp	361.531	228.1	1.585.00	0.4	0.35	14%	14%
Fatih	425.875	15.93	26.734.10	0.68	0.68	0%	0%
Gaziosmanpasa	495.006	11.67	42.417.00	0.53	0.48	9%	9%
Güngören	306.854	7.17	42.796.90	0.68	0.69	-1%	1%
Kadiköy	506.293	25.07	20.195.20	0.63	0.64	-2%	2%
Kagithane	428.755	14.83	28.911.30	0.48	0.44	10%	10%
Kartal	447.110	38.54	11.601.20	0.63	0.72	-12%	12%
Küçükçekmece	740.090	37.25	19.868.20	0.7	0.65	7%	7%
Maltepe	471.059	53.06	8.877.90	0.59	0.57	4%	4%
Pendik	646.375	180.2	3.587.00	0.47	0.61	-22%	22%
Sancaktepe	304.406	61.87	4.920.10	0.4	0.36	11%	11%
Sariyer	335.598	151.3	2.218.10	0.35	0.31	13%	13%
Silivri	155.923	869.5	179.3	0.46	0.43	8%	8%
Sultanbeyli	309.347	28.86	10.718.90	0.46	0.46	0%	0%
Sultangazi	505.190	36.24	13.940.10	0.45	0.47	-3%	3%
Sile	31.718	781.7	40.6	0.23	0.24	-4%	4%
Sisli	274.420	34.98	7.845.10	0.52	0.58	-9%	9%
Tuzla	208.807	123.9	1.685.30	0.67	0.8	-16%	16%
Ümraniye	660.125	45.3	14.572.30	0.49	0.55	-11%	11%
Üsküdar	534.636	35.34	15.128.40	0.51	0.48	7%	7%
Zeytinburnu	292.313	11.31	25.845.50	0.75	0.74	1%	1%
			Average Absolute Difference				8%

Table 2.5. Spectral Acceleration Value at 0.5sec Computed at Central Point of Districts in the İstanbul Metropolitan Area Considering Multiple Rupturing of Off-Tekirdag, Mid-Marmara and Islands Fault Segments.

DETERMINISTIC SEISMIC HAZARD ANALYSIS FOR ISTANBUL				Spectral Acceleration at 0.2s (g)			
District	Population (people)	Area Land Area (km^2)	Population Density (people/km^2)	at 0.2s	Article*	Difference	Absolute Difference
Adalar	16.166	11.05	1.463.00	0.68	0.71	-4%	4%
Arnavutköy	215.531	506.5	425.5	0.28	0.27	3%	3%
Atasehir	405.974	25.87	15.692.80	0.4	0.41	-2%	2%
Avcilar	407.240	41.92	9.714.70	0.49	0.57	-14%	14%
Bagcilar	752.250	22.4	33.582.60	0.44	0.39	13%	13%
Bahçelievler	602.931	16.57	36.386.90	0.53	0.55	-4%	4%
Bakirköy	220.974	29.65	7.452.70	0.58	0.65	-11%	11%
Basaksehir	333.047	104.5	3.187.10	0.37	0.37	0%	0%
Bayrampasa	269.677	9.5	28.387.10	0.42	0.41	1%	1%
Besiktas	186.570	18.04	10.342.00	0.36	0.35	1%	1%
Beykoz	248.056	310.4	799.1	0.27	0.24	11%	11%
Beylikdüzü	244.760	37.74	6.485.40	0.52	0.53	-1%	1%
Beyoglu	245.219	8.96	27.368.20	0.42	0.5	-16%	16%
Büyükçekmece	211.000	157.7	1.338.00	0.38	0.46	-17%	17%
Çatalca	65.811	1040	63.3	0.29	0.26	12%	12%
Çekmeköy	207.476	148	1.401.90	0.28	0.22	28%	28%
Esenler	462.621	18.51	24.993.00	0.39	0.38	3%	3%
Esenyurt	624.733	43.12	14.488.20	0.43	0.48	-10%	10%
Eyüp	361.531	228.1	1.585.00	0.31	0.26	20%	20%
Fatih	425.875	15.93	26.734.10	0.48	0.49	-2%	2%
Gaziosmanpasa	495.006	11.67	42.417.00	0.39	0.35	10%	10%
Güngören	306.854	7.17	42.796.90	0.47	0.5	-5%	5%
Kadiköy	506.293	25.07	20.195.20	0.44	0.46	-3%	3%
Kagithane	428.755	14.83	28.911.30	0.36	0.32	13%	13%
Kartal	447.110	38.54	11.601.20	0.45	0.52	-13%	13%
Küçükçekmece	740.090	37.25	19.868.20	0.49	0.47	3%	3%
Maltepe	471.059	53.06	8.877.90	0.43	0.42	1%	1%
Pendik	646.375	180.2	3.587.00	0.36	0.44	-18%	18%
Sancaktepe	304.406	61.87	4.920.10	0.31	0.27	15%	15%
Sariyer	335.598	151.3	2.218.10	0.28	0.24	17%	17%
Silivri	155.923	869.5	179.3	0.35	0.32	9%	9%
Sultanbeyli	309.347	28.86	10.718.90	0.35	0.34	1%	1%
Sultangazi	5.190	36.24	13.940.10	0.34	0.34	0%	0%
Sile	31.718	781.7	40.6	0.2	0.18	12%	12%
Sisli	274.420	34.98	7.845.10	0.39	0.42	-8%	8%
Tuzla	208.807	123.9	1.685.30	0.47	0.58	%-19 %19	
Ümraniye	660.125	45.3	14.572.30	0.36	0.4	-8%	8%
Üsküdar	534.636	35.34	15.128.40	0.38	0.35	8%	8%
Zeytinburnu	292.313	11.31	25.845.50	0.51	0.54	-5%	5%
			Average Absolute Difference				9%

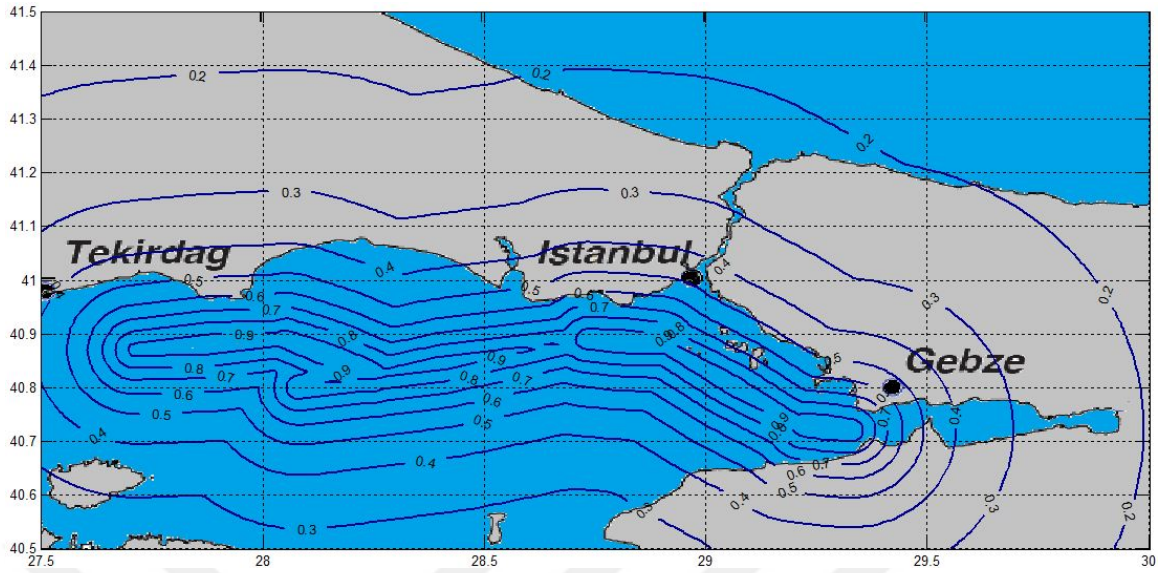

Figure 2.5. Spectral Acceleration at 0.5sec Map for İstanbul Metropolitan Area.

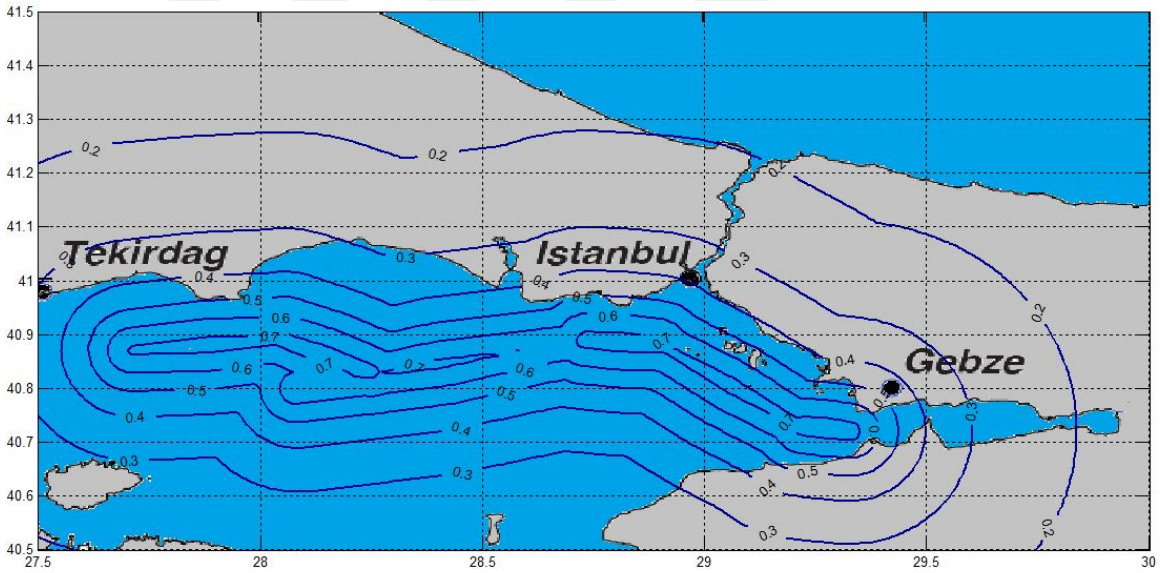

Figure 2.6. Spectral Acceleration at 1.0sec Map for İstanbul Metropolitan Area.

Table 2.6. Spectral Acceleration Value at 1.0sec Computed at Central Point of Districts in the İstanbul Metropolitan Area Considering Multiple Rupturing of Off-Tekirdag, Mid-Marmara and Islands Fault Segments.

DETERMINISTIC SEISMIC HAZARD ANALYSIS FOR ISTANBUL				Spectral Acceleration at 0.2s (g)			
District	Population (people)	Area Land Area (km^2)	Population Density (people/km^2)	at 0.2s	Article*	Difference	Absolute Difference
Adalar	16.166	11.05	1.463.00	0.54	0.59	-8%	8%
Arnavutköy	215.531	506.5	425.5	0.23	0.24	-3%	3%
Atasehir	405.974	25.87	15.692.80	0.33	0.36	-8%	8%
Avcilar	407.240	41.92	9.714.70	0.4	0.48	-17%	17%
Bagcilar	752.250	22.4	33.582.60	0.36	0.33	9%	9%
Bahçelievler	602.931	16.57	36.386.90	0.43	0.48	-10%	10%
Bakirköy	220.974	29.65	7.452.70	0.46	0.56	-17%	17%
Basaksehir	333.047	104.5	3.187.10	0.31	0.32	-3%	3%
Bayrampasa	269.677	9.5	28.387.10	0.34	0.36	-4%	4%
Besiktas	186.570	18.04	10.342.00	0.29	0.3	-1%	1%
Beykoz	248.056	310.4	799.1	0.22	0.21	6%	6%
Beylikdüzü	244.760	37.74	6.485.40	0.43	0.45	-5%	5%
Beyoglu	245.219	8.96	27.368.20	0.34	0.42	-18%	18%
Büyükçekmece	211.000	157.7	1.338.00	0.31	0.4	-21%	21%
Çatalca	65.811	1040	63.3	0.24	0.22	10%	10%
Çekmeköy	207.476	148	1.401.90	0.24	0.19	23%	23%
Esenler	462.621	18.51	24.993.00	0.32	0.33	-1%	1%
Esenyurt	624.733	43.12	14.488.20	0.35	0.43	-17%	17%
Eyüp	361.531	228.1	1.585.00	0.26	0.22	17%	17%
Fatih	425.875	15.93	26.734.10	0.39	0.44	-11%	11%
Gaziosmanpasa	495.006	11.67	42.417.00	0.32	0.3	6%	6%
Güngören	306.854	7.17	42.796.90	0.39	0.44	-12%	12%
Kadiköy	506.293	25.07	20.195.20	0.36	0.41	-11%	11%
Kagithane	428.755	14.83	28.911.30	0.3	0.27	10%	10%
Kartal	447.110	38.54	11.601.20	0.37	0.45	-18%	18%
Küçükçekmece	740.090	37.25	19.868.20	0.4	0.4	0%	0%
Maltepe	471.059	53.06	8.877.90	0.35	0.36	-2%	2%
Pendik	646.375	180.2	3.587.00	0.29	0.37	-20%	20%
Sancaktepe	304.406	61.87	4.920.10	0.26	0.23	12%	12%
Sariyer	335.598	151.3	2.218.10	0.24	0.2	17%	17%
Silivri	155.923	869.5	179.3	0.29	0.27	7%	7%
Sultanbeyli	309.347	28.86	10.718.90	0.29	0.29	0%	0%
Sultangazi	505.190	36.24	13.940.10	0.29	0.3	-4%	4%
Sile	31.718	781.7	40.6	0.17	0.16	6%	6%
Sisli	274.420	34.98	7.845.10	0.32	0.37	-14%	14%
Tuzla	208.807	123.9	1.685.30	0.38	0.5	-23%	23%
Ümraniye	660.125	45.3	14.572.30	0.3	0.36	-16%	16%
Üsküdar	534.636	35.34	15.128.40	0.31	0.3	4%	4%
Zeytinburnu	292.313	11.31	25.845.50	0.42	0.46	-9%	9%
			Average Absolute Difference				10%

Table 2.7. Spectral Acceleration Value at 1.5sec Computed at Central Point of Districts in the İstanbul Metropolitan Area Considering Multiple Rupturing of Off-Tekirdag, Mid-Marmara and Islands Fault Segments.

DETERMINISTIC SEISMIC HAZARD ANALYSIS FOR ISTANBUL				Spectral Acceleration at 0.2s (g)			
District	Population (people)	Area Land Area (km^2)	Population Density (people/km^2)	at 0.2s	Article*	Difference	Absolute Difference
Adalar	16.166	11.05	1.463.00	0.37	0.37	0%	0%
Arnavutköy	215.531	506.5	425.5	0.16	0.16	0%	0%
Atasehir	405.974	25.87	15.692.80	0.22	0.23	-4%	4%
Avcilar	407.240	41.92	9.714.70	0.26	0.29	-9%	9%
Bagcilar	752.250	22.4	33.582.60	0.24	0.21	14%	14%
Bahçelievler	602.931	16.57	36.386.90	0.28	0.32	-11%	11%
Bakirköy	220.974	29.65	7.452.70	0.31	0.37	-16%	16%
Basaksehir	333.047	104.5	3.187.10	0.2	0.21	-2%	2%
Bayrampasa	269.677	9.5	28.387.10	0.23	0.23	0%	0%
Besiktas	186.570	18.04	10.342.00	0.2	0.2	-2%	2%
Beykoz	248.056	310.4	799.1	0.15	0.13	14%	14%
Beylikdüzü	244.760	37.74	6.485.40	0.28	0.28	0%	0%
Beyoglu	245.219	8.96	27.368.20	0.23	0.26	-12%	12%
Büyükçekmece	211.000	157.7	1.338.00	0.21	0.26	-20%	20%
Çatalca	65.811	1040	63.3	0.16	0.14	16%	16%
Çekmeköy	207.476	148	1.401.90	0.16	0.12	30%	30%
Esenler	462.621	18.51	24.993.00	0.21	0.21	0%	0%
Esenyurt	624.733	43.12	14.488.20	0.23	0.28	-16%	16%
Eyüp	361.531	228.1	1.585.00	0.17	0.15	15%	15%
Fatih	425.875	15.93	26.734.10	0.26	0.29	-11%	11%
Gaziosmanpasa	495.006	11.67	42.417.00	0.21	0.19	11%	11%
Güngören	306.854	7.17	42.796.90	0.26	0.29	-11%	11%
Kadiköy	506.293	25.07	20.195.20	0.24	0.27	-10%	10%
Kagithane	428.755	14.83	28.911.30	0.2	0.17	16%	16%
Kartal	447.110	38.54	11.601.20	0.24	0.29	-16%	16%
Küçükçekmece	740.090	37.25	19.868.20	0.26	0.25	4%	4%
Maltepe	471.059	53.06	8.877.90	0.23	0.23	0%	0%
Pendik	646.375	180.2	3.587.00	0.2	0.23	-15%	15%
Sancaktepe	304.406	61.87	4.920.10	0.17	0.15	15%	15%
Sariyer	335.598	151.3	2.218.10	0.16	0.13	20%	20%
Silivri	155.923	869.5	179.3	0.19	0.17	13%	13%
Sultanbeyli	309.347	28.86	10.718.90	0.19	0.18	5%	5%
Sultangazi	505.190	36.24	13.940.10	0.19	0.2	-5%	5%
Sile	31.718	781.7	40.6	0.11	0.11	0%	0%
Sisli	274.420	34.98	7.845.10	0.21	0.25	-15%	15%
Tuzla	208.807	123.9	1.685.30	0.25	0.31	-18%	18%
Ümraniye	660.125	45.3	14.572.30	0.2	0.24	-16%	16%
Üsküdar	534.636	35.34	15.128.40	0.21	0.19	9%	9%
Zeytinburnu	292.313	11.31	25.845.50	0.28	0.3	-7%	7%
			Average Absolute Difference				10%

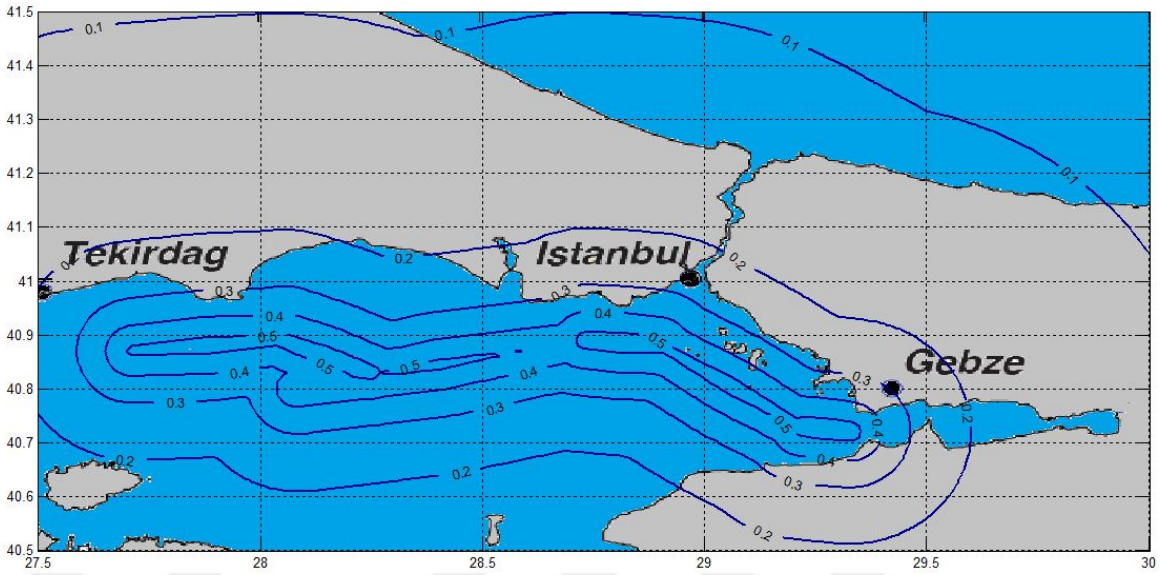

Figure 2.7. Spectral Acceleration at 1.5sec Map for İstanbul Metropolitan Area.

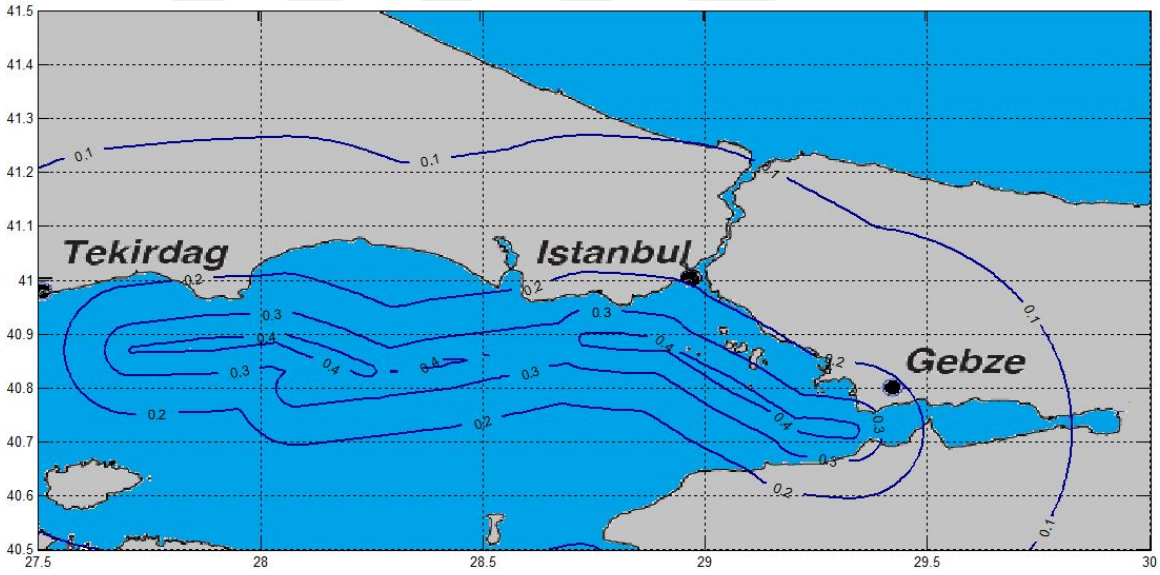

Figure 2.8. Spectral Acceleration at 2.0sec Map for İstanbul Metropolitan Area.

Table 2.8. Spectral Acceleration Value t 2a.0sec Computed at Central Point of Districts in the İstanbul Metropolitan Area Considering Multiple Rupturing of Off-Tekirdag, Mid-Marmara and Islands Fault Segments.

DETERMINISTIC SEISMIC HAZARD ANALYSIS FOR ISTANBUL				Spectral Acceleration at 0.2s (g)			
District	Population (people)	Area Land Area (km^2)	Population Density (people/km^2)	at 0.2s	Article*	Difference	Absolute Difference
Adalar	16.166	11.05	1.463.00	0.27	0.28	-2%	2%
Arnavutköy	215.531	506.5	425.5	0.11	0.12	-5%	5%
Atasehir	405.974	25.87	15.692.80	0.16	0.17	-5%	5%
Avcilar	407.240	41.92	9.714.70	0.19	0.22	-11%	11%
Bagcilar	752.250	22.4	33.582.60	0.18	0.15	17%	17%
Bahçelievler	602.931	16.57	36.386.90	0.21	0.24	-12%	12%
Bakirköy	220.974	29.65	7.452.70	0.23	0.28	-17%	17%
Basaksehir	333.047	104.5	3.187.10	0.15	0.15	0%	0%
Bayrampasa	269.677	9.5	28.387.10	0.17	0.17	0%	0%
Besiktas	186.570	18.04	10.342.00	0.14	0.15	-4%	4%
Beykoz	248.056	310.4	799.1	0.11	0.1	9%	9%
Beylikdüzü	244.760	37.74	6.485.40	0.21	0.2	4%	4%
Beyoglu	245.219	8.96	27.368.20	0.17	0.19	-12%	12%
Büyükçekmece	211.000	157.7	1.338.00	0.15	0.19	-19%	19%
Çatalca	65.811	1040	63.3	0.12	0.1	19%	19%
Çekmeköy	207.476	148	1.401.90	0.12	0.09	27%	27%
Esenler	462.621	18.51	24.993.00	0.16	0.16	0%	0%
Esenyurt	624.733	43.12	14.488.20	0.17	0.22	-21%	21%
Eyüp	361.531	228.1	1.585.00	0.13	0.11	15%	15%
Fatih	425.875	15.93	26.734.10	0.19	0.22	-13%	13%
Gaziosmanpasa	495.006	11.67	42.417.00	0.16	0.14	11%	11%
Güngören	306.854	7.17	42.796.90	0.19	0.22	-14%	14%
Kadiköy	506.293	25.07	20.195.20	0.18	0.2	-11%	11%
Kagithane	428.755	14.83	28.911.30	0.15	0.12	21%	21%
Kartal	447.110	38.54	11.601.20	0.18	0.22	-18%	18%
Küçükçekmece	740.090	37.25	19.868.20	0.19	0.18	5%	5%
Maltepe	471.059	53.06	8.877.90	0.17	0.17	0%	0%
Pendik	646.375	180.2	3.587.00	0.14	0.17	-15%	15%
Sancaktepe	304.406	61.87	4.920.10	0.13	0.11	15%	15%
Sariyer	335.598	151.3	2.218.10	0.12	0.09	27%	27%
Silivri	155.923	869.5	179.3	0.14	0.12	17%	17%
Sultanbeyli	309.347	28.86	10.718.90	0.14	0.13	7%	7%
Sultangazi	505.190	36.24	13.940.10	0.14	0.16	-13%	13%
Sile	31.718	781.7	40.6	0.08	0.08	5%	5%
Sisli	274.420	34.98	7.845.10	0.15	0.19	-18%	18%
Tuzla	208.807	123.9	1.685.30	0.19	0.24	-22%	22%
Ümraniye	660.125	45.3	14.572.30	0.15	0.19	-22%	22%
Üsküdar	534.636	35.34	15.128.40	0.15	0.14	9%	9%
Zeytinburnu	292.313	11.31	25.845.50	0.2	0.22	-7%	7%
			Average Absolute Difference				12%

The results of Gülkan's and this thesis study differ at most 10% in absolute average for peak ground acceleration and spectral accelerations up to 1.5sec. For larger spectral periods, this difference increases up to 12% when the results of spectral acceleration at 2.0sec. The main reasons of differences are use of different grid size and

use of exact shear wave velocity for each grid. Gülkan has used 0.002^o to 0.002^o (250m by 250m) grid size and corresponding shear wave velocity. This study utilizes rougher grid size 0.05^o to 0.05^o (4km by 4km) with average shear wave velocity for İstanbul, 400m/s. In general, it can be concluded that these results comply with Gülkan's paper and it can be considered as proper.

The tables and figures have indicated that multiple rupturing of these submarine faults seems to have catastrophic outcomes, especially along the coastline of İstanbul, where Off-Tekirdag, Mid-Marmara and Islands faults are at most 20km offshore and almost half of the population of İstanbul lives. European coastal district (Avcilar, Bahçelievler, Bakirköy, Beylikdüzü, Küçükçekmece) are expected to shake with a median PGA range of 0.5 g to 0.7 g. This values are in the range of 0.4 g to 0.6 g at coastal districts of the city in the Asian side (Kadiköy, Maltepe, Kartal, Pendik). The estimated PGA reaches up to around 0.7g level in Adalar district. Tables and figures above lists the PGA and spectral acceleration (SA) values at 0.2s, 0.3s, 0.5s, 1.0s, 1.5s and 2.0sec computed at central point each districts. These indicate that expected spectral acceleration at short periods (0.2s and 0.3s) which is very close to fundamental vibration periods of 3 to 5 story buildings is around 1.0 g. Considering that the majority of building stock along the coastline of İstanbul are lower than 5 storys, these buildings turn out to be the most vulnerable ones. The scenario earthquake seems to have less effect on high-rise building, since spectral acceleration at 1.0 s, 1.5s and 2.0 sec are not large values. Especially the financial districts of İstanbul, Sisli and Sariyer, are expected to be shaken at quite low acceleration levels, at most around 0.3 g.

Considering that computation of these peak ground and acceleration values includes empirical values such as standard deviation, these values is called as "median". These values can be less or more depending on the standard deviation values.

2.3. Probabilistic Seismic Hazard Analysis (PSHA)

Rather than ignoring the uncertainties present in the nature of earthquake occurrence, probabilistic methods incorporates the uncertainties into calculations of ground

motion intensity. By adding some complexity to the procedure, the resulting calculations and outcomes become much more defensible and applicable for use in decision-making process.

"Probabilistic Seismic Hazard Analysis (PSHA)" was first proposed by Cornell (1968). Using this former methodology, many studies have been performed and developed. For regional utilization, various computer software programs have been generated. In chronological order, EQRisk (McGuire, 1976), FRISK (McGuire, 1978), SEISRISK II (Bender and Perkins 1982), STASHA (Chiang et al., 1984), SEISRISK III (Bender and Perkins, 1987), Crisis (Ordaz, 2001), EZ-FRISK (Risk Engineering Inc., 2004) and EXPEL (Benito et al., 2004). These software mainly serves to facilitate PSHA calculations, main differences between those are source characterization methods and integration methods.

PSHA considers all possible earthquake events and resulting ground motions with their associated probabilities of occurrence, in order to find the level of ground motion parameter exceeded with some tolerance rate (Baker, 2008). The main procedure of PSHA can be illustrated in Figure 2.9. Probabilistic Seismic Hazard Analysis can be categorized into four main steps which are definition of sources and their characterization of distribution of source-to-site distance, characterization of distribution of earthquake magnitude, determination of ground motion parameter and finally determination of temporal occurrence relationships and combination of all these uncertainties.

(i) Identification and characterization of all potential earthquake sources with their probability distribution and Characterization of distribution of source-to-site distance: Unlike deterministic approach mentioned above, PSHA considers all possible earthquake sources capable of producing damage. The earthquake sources can be classified in three main categories according to their amount of information available. This information provides to define these earthquake sources in geometrical manner as point source, line source and area source.
   - Point Sources: Point source model is a former methodology when PSHA was first proposed. (Cornell, 1968). Nowadays, if faults cannot be identified

properly or if the fault is too short compared to its distance to site, the fault can be modeled as point source. For point faults, the source-to-site distance is always constant. Otherwise, the line fault and area fault models take place.

- Line Source: Line sources can be modeled where the location of active faults are known and epicenters of past events are concentrated around these faults. For a given earthquake source, earthquakes are considered equally likely to occur at any location (Baker, 2008). For brevity, line sources can be used for representations of active faults. The parameters for line sources are magnitude and source-to-site distance.
- Area Source: If epicenters of earthquakes are not concentrated along a line, but it is spread, area source model can be utilized. Actually it can be considered as the combination of point and line sources. Area source can be modeled by finite number of point sources and like line source the random variables are magnitude and source-to-site distance. Also, earthquakes are considered equally likely to occur at any location.

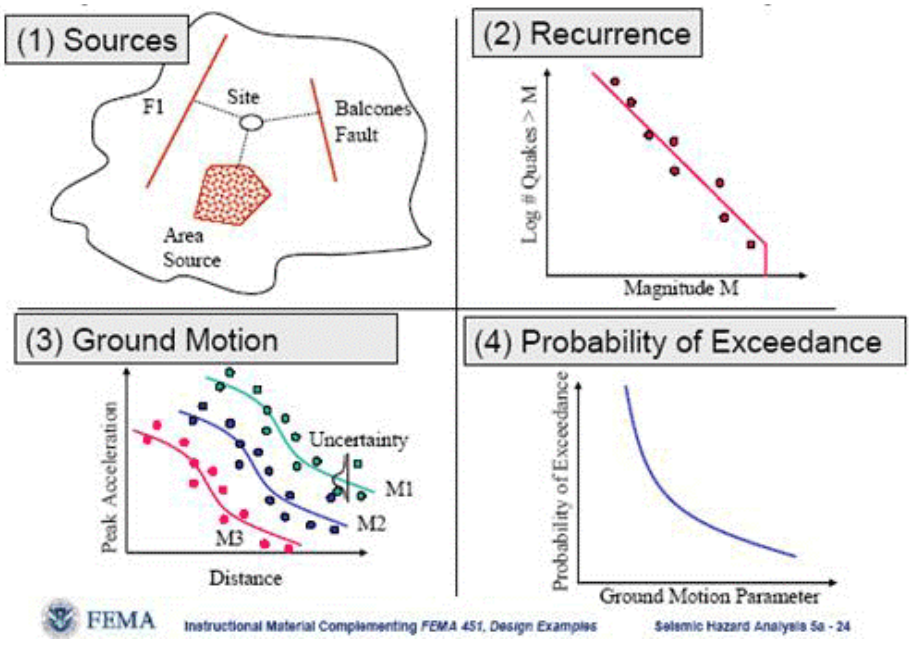

Figure 2.9. Seismic Hazard Analysis in Steps (FEMA, 2002).

In this study, since the geometry in two-dimension is known, line source model is

better to be used considering submarine fault system underneath the Marmara Sea.

(ii) Characterization of distribution of earthquake magnitudes: The second step is magnitude recurrence relationship of potential seismic sources which is defined as probability density function of occurring an earthquake at a given magnitude. (Reiter, 1990). There are several models for the development of magnitude recurrence relationships: exponential, truncated exponential, characteristic models.

- Exponential Model (Gutenberg-Richter, 1956): This model assumes that there is a linear relationship between natural logarithm of annual rate of exceedance and magnitude. The equations for this model is as follows.

The Number of Earthquakes

$$\log(N) = a - b \cdot M_w \tag{2.2}$$

where N is annual number of earthquake of magnitude equal or greater than certain magnitude, M_w. The "10^a" is mean yearly number of earthquakes of magnitude greater than or equal to zero. The term "b" is likelihood of large and small earthquakes. "b" is inversely proportional with number of larger earthquakes. The illsutrative plot is given in Figure 2.10.

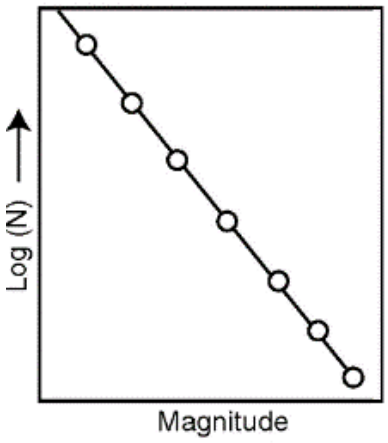

Figure 2.10. The Relationship Between Annual Number of Earthquakes and Corresponding Magnitudes.

The probability density function of exponential distribution of magnitude is given as following equation and in Figure 2.11.

$$f_M(M) = \beta \cdot e^{-\beta \cdot (M_w - M_0)} \tag{2.3}$$

where β= ln?(10)*b, and M_0 is the minimum magnitude which is zero for this model.

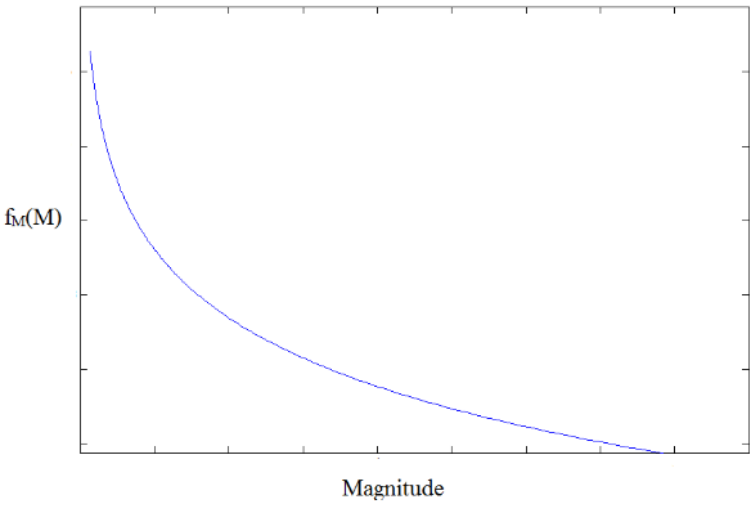

Figure 2.11. The Exponential Distribution of Magnitudes.

- Truncated Exponential Model: The only difference between Truncated Exponential Model and Gutenberg-Richter Model is the boundaries, where the magnitude range is from zero to infinity. In truncated exponential model, the boundaries are more reasonable. Lower bound is in the vicinity of M_0= 4.0 because of the engineering judgment. It is considered that M<4.0 does not contribute significant effect. Upper bound, M_{max} can be determined by two ways; first one is by relying on past earthquakes, second one is calculating the characteristic magnitude using the parameters of rupture length and width. The probability density function of truncated distribution of magnitude is given as in the following equation and in Figure 2.12.

$$f_M(M) = \frac{\beta \cdot e^{-\beta \cdot (M_w - M_0)}}{1 - e^{[-\beta (M_{max} -)]}} \tag{2.4}$$

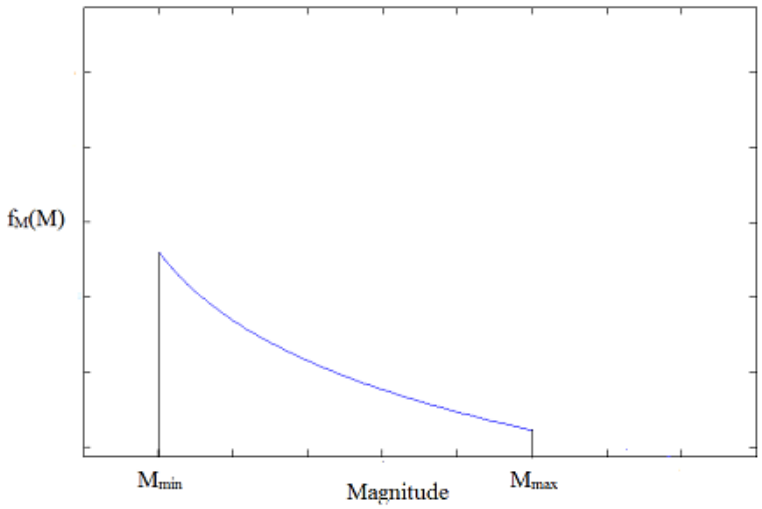

Figure 2.12. The Truncated Exponential Distribution of Magnitudes.

- Characteristic Model (Youngs and Coppersmith, 1985): According to Youngs and Coppersmith, 1985, characteristic earthquake model may be more appropriate for individual faults, which tend to generate same-size and characteristic earthquakes. This model is based on both geological and seismicity data.

The probability density function of truncated characteristic exponential model is given in the following equations.

$$f_M(M_w) = \left\{ \begin{array}{l} \frac{\beta \cdot exp[-\beta \cdot (M_w - M_{min})]}{1 - exp[-\beta \cdot (M_{max} - \Delta M_2 - M_{min})]} \times \frac{1}{1+c}, where M_w \leq M_{max} - 0.5 \cdot \Delta M_2 \\ \frac{\beta \cdot exp[-\beta \cdot (M_{max} - \Delta M_1 - \Delta M_2 - M_{min})]}{1 - exp[-\beta \cdot (M_{max} - \Delta M_2 - M_{min})]}, where M_w > M_{max} - 0.5 \cdot \Delta M_2 \end{array} \right\} \quad (2.5)$$

$$where \Delta M_1 = 1.0, \Delta M_2 = 0.5 \quad (2.6)$$

and c is defined by;

$$c = \frac{\beta \cdot exp\left[-\beta \cdot (M_{max} - \Delta M_1 - \Delta M_2 - M_{min})\right]}{1 - exp\left[-\beta \cdot (M_{max} - \Delta M_2 - M_{min})\right]} \cdot \Delta M_2 \quad (2.7)$$

The illustrates the probability distribution function of magnitude for this model.

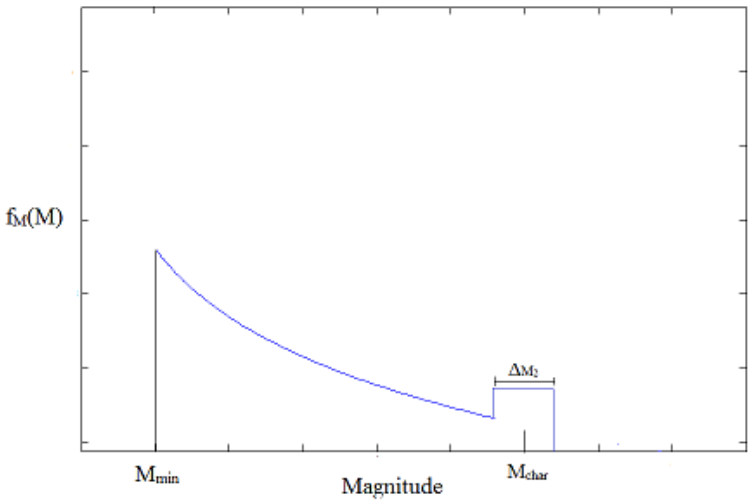

Figure 2.13. The Truncated Characteristic Exponential Distribution of Magnitudes.

(iii) Determination of ground motion parameter by earthquakes of any magnitude and any distance: After quantifying the distribution of source-to-site distance and magnitude, the probability distribution of ground motion parameter is necessary. This distribution mainly depends on distance and magnitude, however shear-wave velocity, faulting mechanism, near-fault effects, directivity effects etc. are also important parameters. The ground motion intensity parameter may be peak ground acceleration (PGA), peak ground velocity (PGV), peak ground displacement (PGD), spectral acceleration (Sa) or spectral displacement (Sd). Ground Motion Prediction Equations (GMPE) have been derived using regression analysis on past event datasets, and they have potential to be developed with further information and data. Numerous GMPEs have been developed in the last decades globally. Nowadays, Next Generation of Attenuation (NGA) models that are widely used in the recent years listed below. (OpenSHA http://www.opensha.org/glossary-ngaModels)
   - Abrahamson and Silva (2008)
   - Boore and Atkinson (2008)
   - Campbell and Bozorgnia (2008)
   - Chiou and Youngs (2008)

These GMPEs have been considered compatible to use for Europe and Middle East

(Stafford *et al.*, 2008). Besides that, numerous GMPEs have been developed especially for Turkey. The most popular ones are listed below.

- Grazier and Kalkan (2007)
- Kalkan and Gülkan (2004)
- Akkar and Bommer (2010)

These attenuation relationships have the following general form:

$$ln\left(IM\right) = \mu\left(M, R, \theta\right) + \sigma\left(M, R, \theta\right) \cdot \varepsilon \tag{2.8}$$

In which $\ln(IM)$ is the natural logarithm of the ground motion Intensity Measure (PGA, PGV, PGD, S_a, S_d). μ (M, R, θ) and σ (M, R, θ) are mean and standard deviation of $\ln(IM)$, respectively. (M, R, θ) terms are magnitude, distance and other parameters, respectively. ε is the standard normal random variable that represents the variability of $\ln(IM)$ (Baker, 2008).

Since natural logarithm of Intensity Measure (Ground Motion Parameter) is normally distributed, after obtaining the required parameters at GMPE, one can compute the probability of exceeding any ground motion parameters, namely x by using following equation:

$$P\left(IM > (x|M, R, \theta)\right) = 1 - \Phi\left(\frac{\ln\left(x\right) - \mu\left(M, R, \theta\right)}{\sigma\left(M, R, \theta\right)}\right) \tag{2.9}$$

where (Φ) is standard normal cumulative distribution function. By using z-table (standard normal table), this value can be obtained.

(iv) Combination of uncertainties in earthquake source-to-site distance, size, other parameters and obtaining seismic hazard using total probability theorem: When all uncertainties mentioned above are combined, seismic hazard curve can be obtained using total probability theorem. Considering all related potential earthquake-

generating sources, rate of occurrence of any Ground Motion Parameter, x, can be computed using the following equation:

$$\lambda\left(IM > x\right) = \sum_{i=1}^{n_{sources}} \lambda(M_i > m_{\min}) \int_{m_{\min}}^{m_{\max}} \int_{0}^{r_{\max}} P\left(IM > (x|M,R,\theta)\right) f_{m_i}\left(m\right) f_{r_i}\left(r\right) f_{\theta_i}\left(\theta\right) dmdrd\theta \tag{2.10}$$

In which $n_{sources}$ is number of sources, $\lambda(IM > x)$ is rate of exceedance of having any ground motion parameter, $\lambda(M)_i > m_{min})$ is seismicity of earthquake source, in other words rate of occurrence of earthquakes greater than m_{min}. P(IM >(x, M, R, θ)) represents the probability of exceeding any ground motion parameter computed by GMPEs, $f(_{mi}$) (m),f_{ri} (r),$f_{?i}$ (θ) are probability density functions for magnitude, distance and other parameters, respectively.

- Temporal Occurrence: The main motivation for Seismic Hazard Analysis is to calculate total annual rate of exceedance of a certain ground motion parameter. For this purpose, temporal occurrence models are used which provides to compute this exceedance in a certain period of time as defined in . The most commonly used model is Poisson's Model, which assumes earthquakes occurs randomly with no memory of time, size or location of the preceding event. This model is not only simple to use, but also it gives very reliable and successful results. (Cornell, 1988). The probability of observing at least one event in a period of time, t, is equal to

$$P\left(N \geq 1\right) = 1 - e^{-\lambda t} \tag{2.11}$$

The following figure shows a typical seismic hazard curve for two different return periods.

Table 2.9. Rate of Exceedance Calculation and its Corresponding Return Period Values.

Period of Time (t) in years	Probability of Exceedance (%)	Rate of Exceedance (λ)	Return Period (T=1/λ) in years
50	10%	0.00211	475
50	2%	0.00040	2475

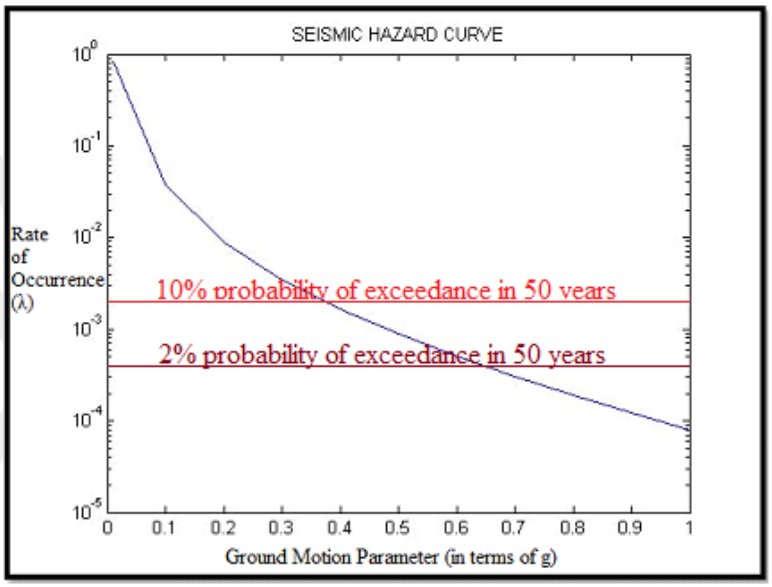

Figure 2.14. Illustrative Seismic Hazard Curve with for Return Periods, 475 and 2475 Years.

In this study, PSHA is conducted for two different attenuation relationship, Kalkan-Gülkan 2004 (abbreviated as KG04) and Campbell-Bozorgnia 2008 (CB08) using truncated characteristic exponential distribution of magnitudes. The resulting acceleration values are inconsistent, there is almost 100% difference between the acceleration values obtained for two GMPEs. For consistency of the results are checked with the collaborative study of İstanbul Metropolitan Municipality-Earthquake Risk Assessment Department and OYO International Company. Although that study has used different attenuation relationship, it has given an understanding and measure about the results. The seismic hazard maps can be found in Appendix B.

2.4. Kalkan-Gülkan 2004 (KG04) Attenuation Relationship

The detailed methodology for Kalkan-Gülkan 2004 attenuation relationship has given in "Deterministic Seismic Hazard Analysis" chapter. For two return periods, 475 and 2475 years, and average shear wave velocity, 400m/sec, as seen from Figure 2.15 to Figure 2.17, it has given too conservative results when compared to study of İstanbul Metropolitan Municipality-Earthquake Risk Assessment Department and OYO International Company in Appendix B. For Kadiköy region, seismic hazard curves are also given considering the faults separately and combined for better illustration.

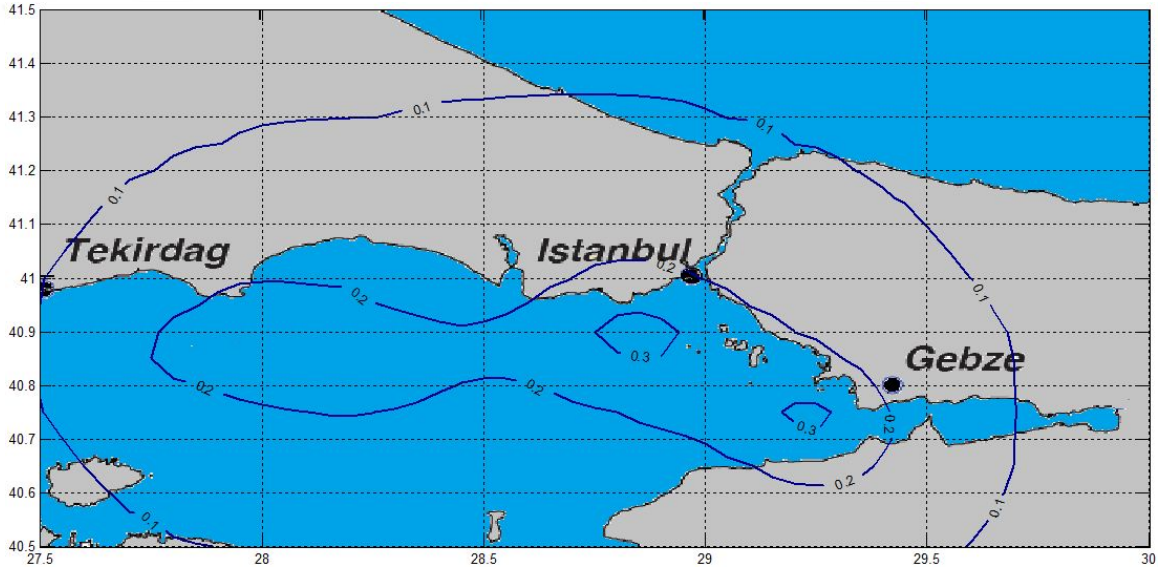

Figure 2.15. Vs30 = 400m/sec and Using KG04 Attenuation Relationship PGA map with 475 Years Return Period.

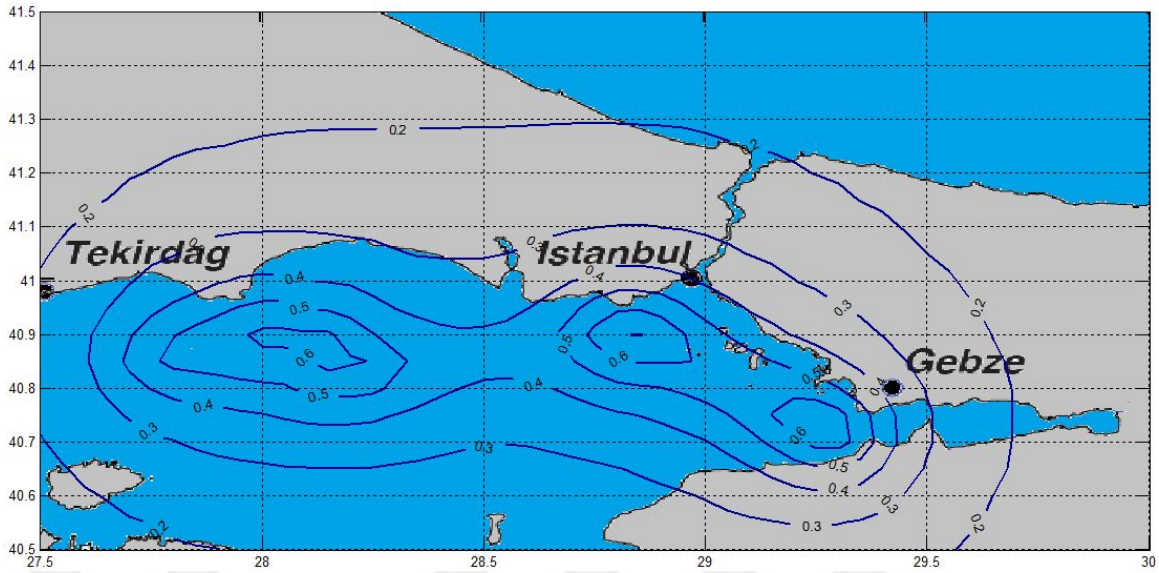

Figure 2.16. Vs30 = 400m/sec and Using KG04 Attenuation Relationship PGA map with 2475 Years Return Period.

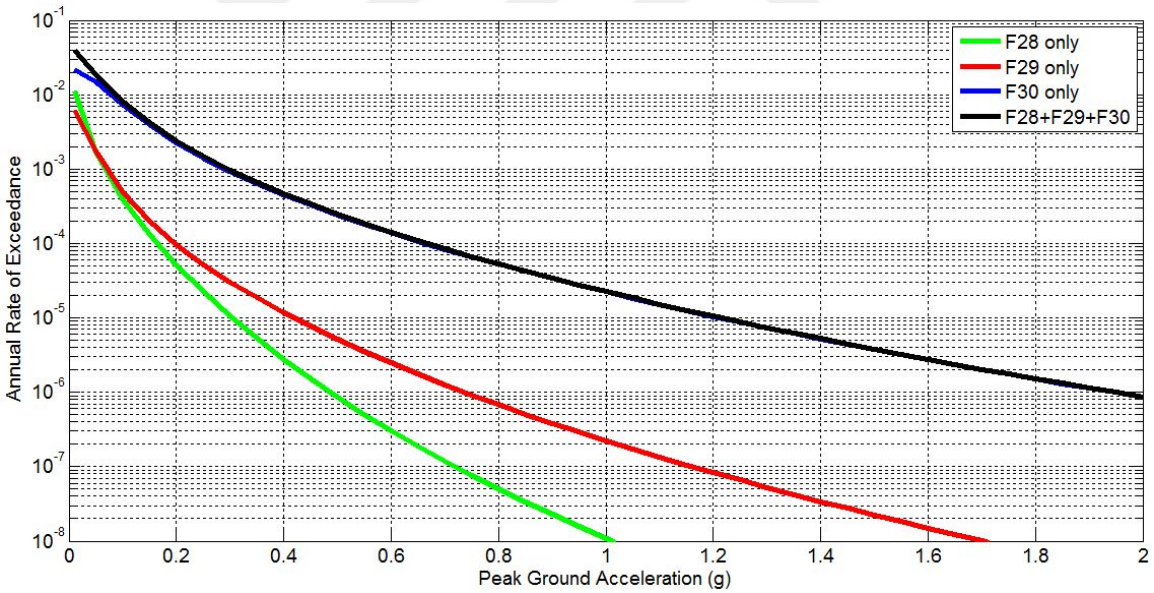

Figure 2.17. Vs30 = 400m/sec and Using KG04 Attenuation Relationship Seismic Hazard Curve for PGA at Kadiköy District Considering the Fault Effects.

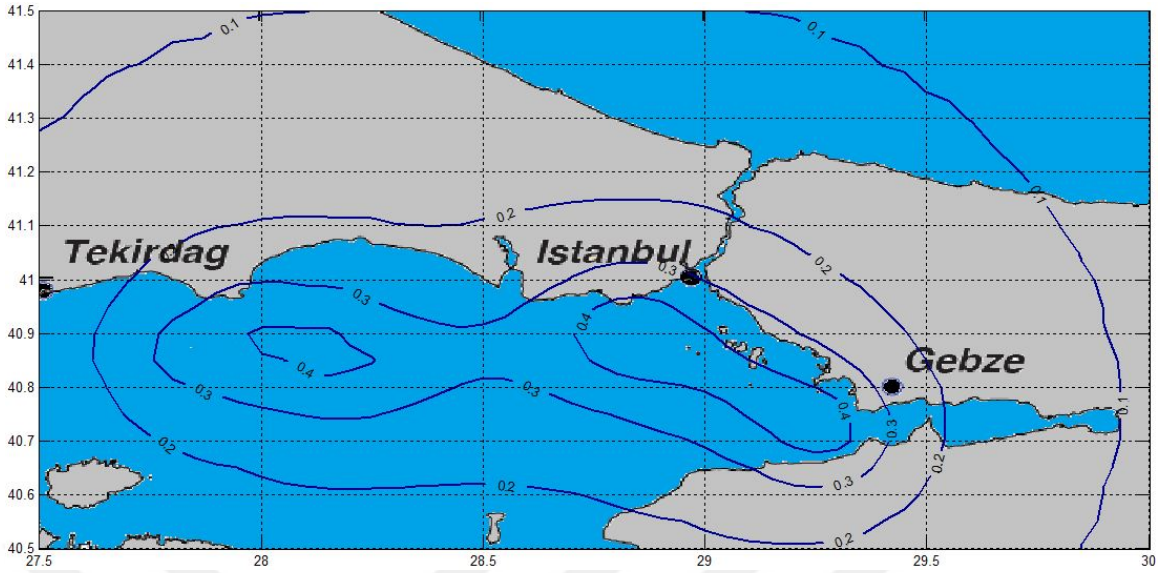

Figure 2.18. Vs30 = 400m/sec and Using KG04 Attenuation Relationship SA at 0.2sec Map with 475 Years Return Period.

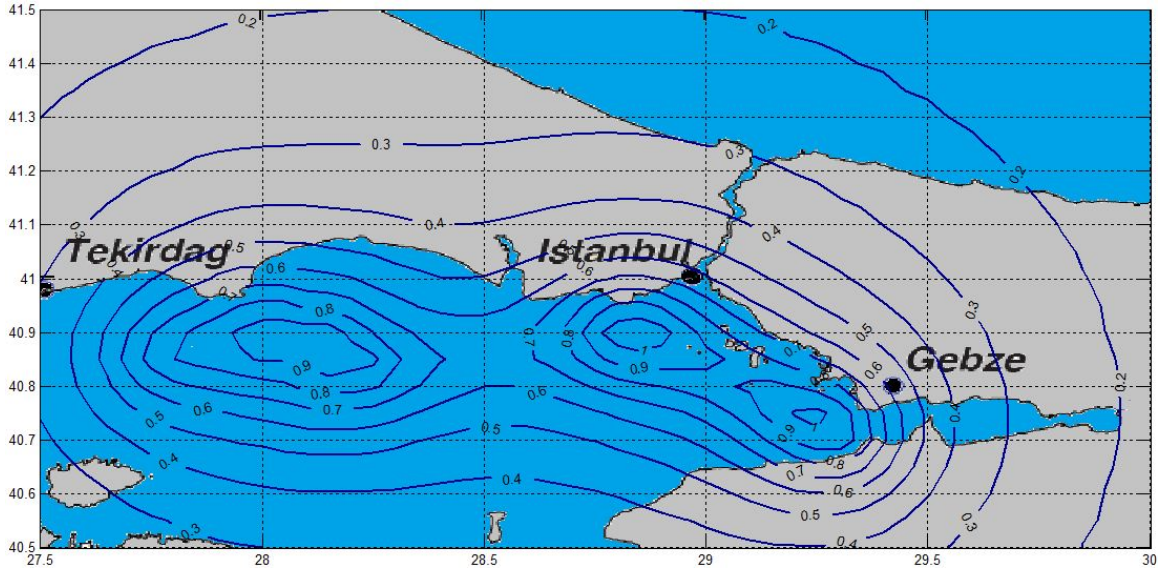

Figure 2.19. Vs30 = 400m/sec and Using KG04 Attenuation Relationship SA at 0.2sec Map with 2475 Years Return Period.

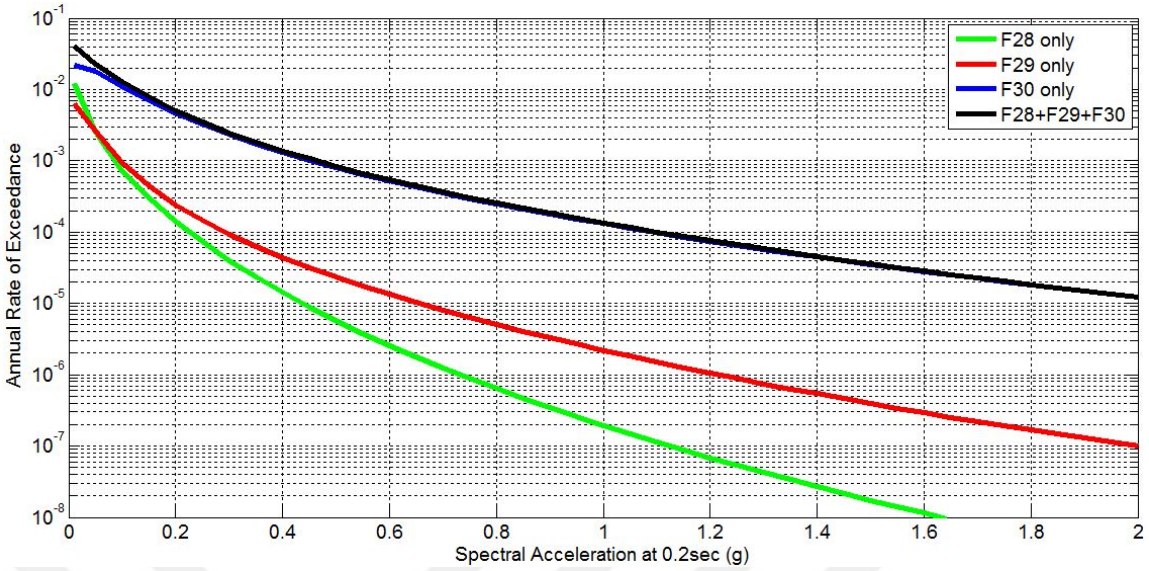

Figure 2.20. Vs30 = 400m/sec and Using KG04 Attenuation Relationship Seismic Hazard Curve for SA at 0.2sec at Kadiköy District Considering the Fault Effects.

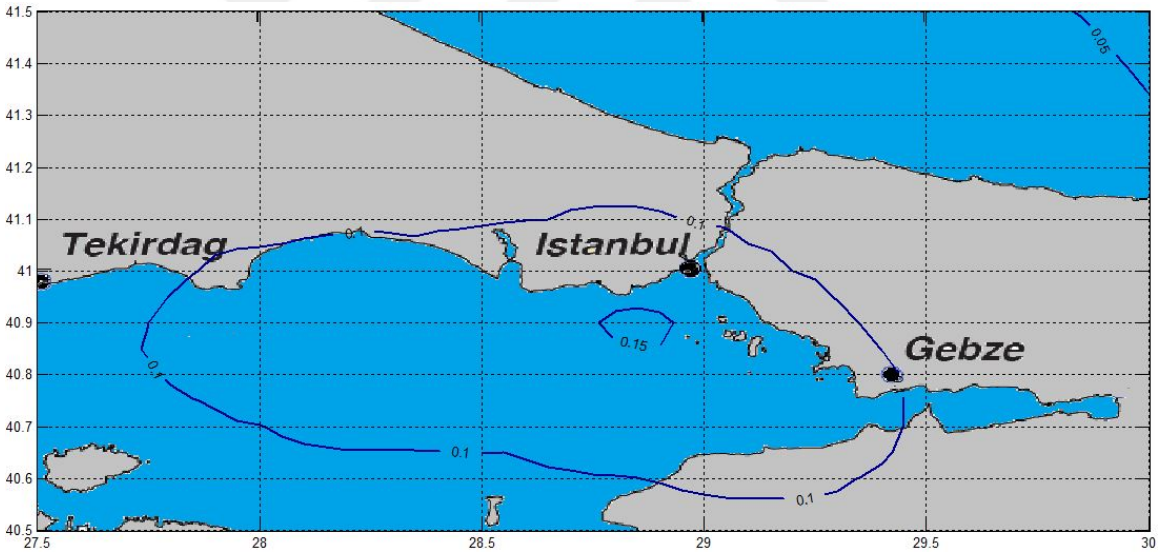

Figure 2.21. Vs30 = 400m/sec and Using KG04 Attenuation Relationship SA at 1.0sec map with 475 Years Return Period.

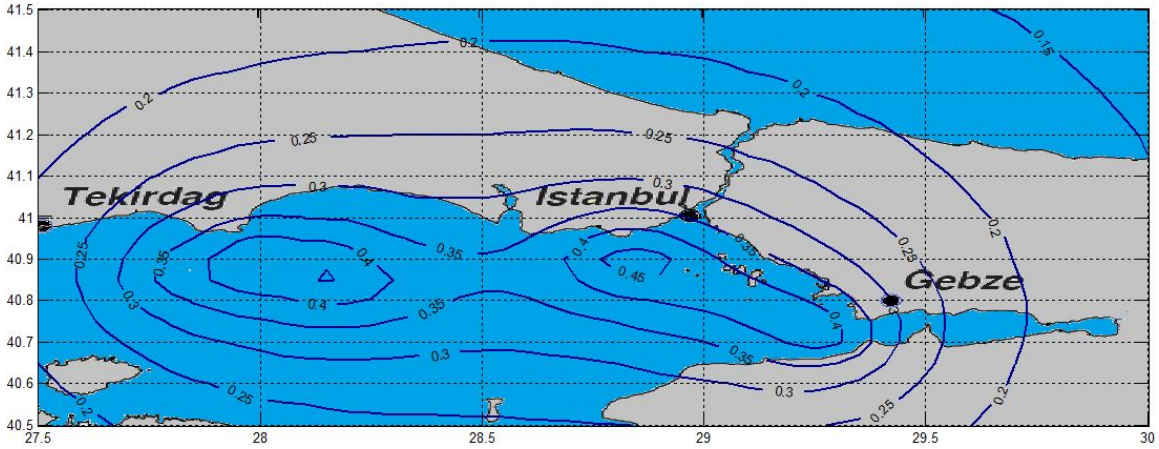

Figure 2.22. Vs30 = 400m/sec and Using KG04 Attenuation Relationship SA at 1.0sec map with 2475 Years Return Period.

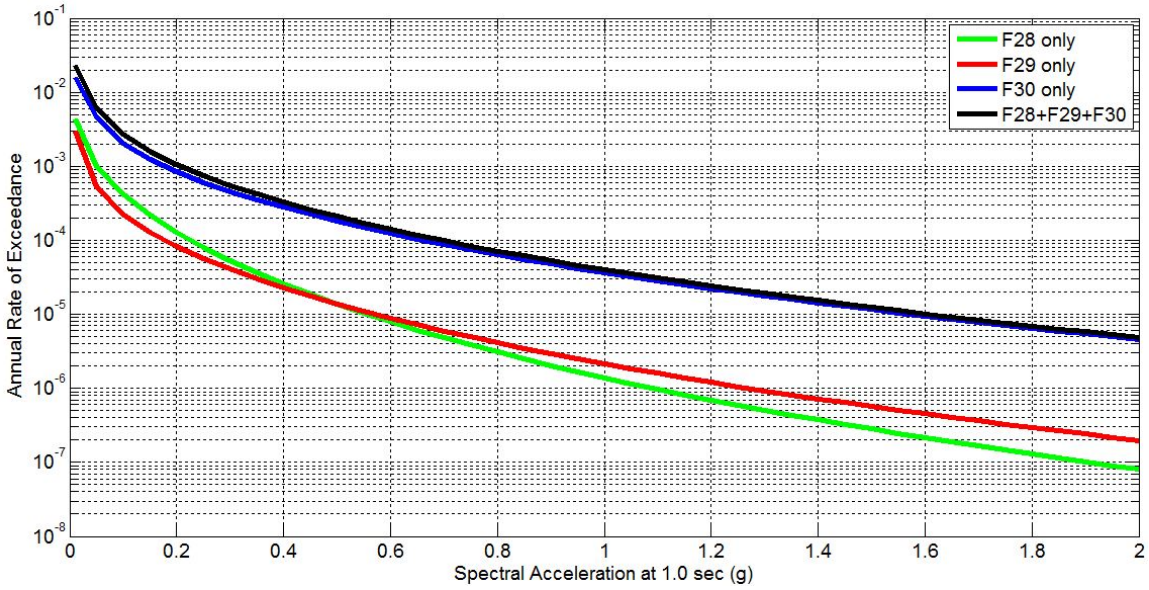

Figure 2.23. Vs30 = 400m/sec and Using KG04 Attenuation Relationship Seismic Hazard Curve for SA at 1.0sec at Kadiköy District Considering the Fault Effects.

2.5. Campbell-Bozorgnia 2008 (CB08) Attenuation Relationship

The general form for estimating the ground motion intensity is as follows (Campbell, 2008):

$$lnY = f_{mag} + f_{dis} + f_{flt} + f_{hng} + f_{site} + f_{sed} \tag{2.12}$$

Magnitude Term

$$f_{mag} = \left\{ \begin{array}{c} c_0 + c_1 M; \quad M \leq 5.5 \\ c_0 + c_1 M + c_2 \left(M - 5.5\right); \quad 5.5 < M \leq 6.5 \\ c_0 + c_1 M + c_2 \left(M - 5.5\right) + c_3 \left(M - 6.5\right); \quad M > 6.5 \end{array} \right\} \tag{2.13}$$

Distance Term

$$f_{dis} = \left(c_4 + c_5 M\right) ln \left(\sqrt{{R_{rup}}^2 + {c_6}^2}\right) \tag{2.14}$$

Style of Faulting Term

$$f_{flt} = c_7 F_{RV} f_{flt,Z} + c_8 F_{NM} \tag{2.15}$$

$$f_{flt,Z} = \left\{ \begin{array}{c} Z_{TOR}; Z_{TOR} < 1 \\ 1; Z_{TOR} \geq 1 \end{array} \right\} \tag{2.16}$$

Hanging-Wall Term

$$f_{hng} = c_9 f_{hng,R} f_{hng,M} f_{hng,Z} f_{hng,\delta} \tag{2.17}$$

$$f_{hng,R} = \left\{ \begin{array}{c} 1; \\ \left[max\left(R_{RUP}, \sqrt{{R_{JB}}^2 + 1}\right) - R_{JB}\right] / \\ \left(R_{RUP} - R_{JB}\right) / R_{RUP}; \\ R_{JB} = 0; \\ max\left(R_{RUP}, \sqrt{{R_{JB}}^2 + 1}\right); R_{JB} > 0, Z_{TOR} < 1; \\ R_{JB} > 0, Z_{TOR} \geq 1; \end{array} \right\} \tag{2.18}$$

$$f_{hng,M} = \left\{ \begin{array}{cc} 0; & M \leq 6.0 \\ 2\left(M - 6.0\right); & 6.0 < M < 6.5; \\ 1; & M \geq 6.5; \end{array} \right\} \tag{2.19}$$

$$f_{hng,Z} = \left\{ \begin{array}{cc} 0; & Z_{TOR} \geq 20 \\ \left(20 - Z_{TOR}\right)/20; & 0 \leq Z_{TOR} < 20 \end{array} \right\} \tag{2.20}$$

$$f_{hng,\delta} = \left\{ \begin{array}{cc} 1; & \delta \leq 70 \\ \left(90 - \delta\right)/20; & \delta > 70 \end{array} \right\} \tag{2.21}$$

Shallow Response Term

$$f_{site} = \left\{ \begin{array}{c} c_{10} ln\left(\frac{V_{s,30}}{k_1}\right) + k_2 \left\{ ln\left[A_{1100} + c\left(\frac{V_{s,30}}{k_1}\right)^n\right] - ln\left[A_{1100} + c\right]\right\}; \\ \left(c_{10} + k_2 n\right) ln\left(\frac{V_{s,30}}{k_1}\right); \\ \left(c_{10} + k_2 n\right) ln\left(\frac{1100}{k_1}\right); \end{array} \right. \tag{2.22}$$

$$\left. \begin{array}{l} V_{s,30} < k_1 \\ k_1 \leq V_{s,30} < 1100 \\ V_{s,30} \geq 1100 \end{array} \right\}$$

Basin Response Term

$$f_{sed} = \left\{ \begin{array}{cc} c_{11}\left(Z_{2.5} - 1\right); & Z_{2.5} < 1 \\ 0; & 1 \leq Z_{2.5} \leq 3 \\ c_{12} k_3 e^{-0.75}\left[1 - e^{-0.25\left(Z_{2.5} - 3\right)}\right]; & Z_{2.5} > 3 \end{array} \right\} \tag{2.23}$$

where Y is the median estimate of the ground motion component of peak ground acceleration (g), peak ground velocity (cm/s), peak ground displacement (cm) or spectral acceleration (g); M is the moment magnitude; RRUP is the closest distance to the coseismic rupture plane (km), R_{JB} is the closest distance to the surface projection to the surface projection of the coseismic rupture plane (km); F_{RV} and F_{NM} are indicator vari-

ables representing reverse and reverse-oblique faulting and normal and normal-oblique faulting, respectively. It depends on the λ defined as the average angle of slip measured in the plane of the rupture between the strike direction and the slip vector. FRV=1 for $30^o < \lambda < 150^o$, otherwise 0, and FNM=1 for -$150^o < \lambda <$-30° and otherwise 0. Z_{TOR} is the depth to the coseismic rupture plane (km), δ is the dip of the rupture plane (^{o}), $V_{s,30}$ is the shear wave velocity in the top 30m of the site profile (m/sec), A_{1100} is the median estimate of PGA on a reference rock profile ($V_{s,30}$=1100m/sec), $Z_{2.5}$ is the depth to the 2.5km/sec shear wave velocity, also defined as basin or sediment depth. σ is the standard deviation of the residuals. The coefficients c_i, c, n, k_i and standard deviation, σ are listed in Figure 2.18 and Table 2.10.

Table 2.10. Coefficients for the Geometric Mean and Arbitrary Horizontal Components of The Median Ground Motion Model (Campbell,2008).

T(s)	c_0	c_1	c_2	c_3	c_4	c_5	c_6	c_7	c_8	c_9	c_{10}	c_{11}	c_{12}	k_1	k_2	k_3
0.010	-1.715	0.500	-0.530	-0.262	-2.118	0.170	5.60	0.280	-0.120	0.490	1.058	0.040	0.610	865	-1.186	1.839
0.020	-1.680	0.500	-0.530	-0.262	-2.123	0.170	5.60	0.280	-0.120	0.490	1.102	0.040	0.610	865	-1.219	1.840
0.030	-1.552	0.500	-0.530	-0.262	-2.145	0.170	5.60	0.280	-0.120	0.490	1.174	0.040	0.610	908	-1.273	1.841
0.050	-1.209	0.500	-0.530	-0.267	-2.199	0.170	5.74	0.280	-0.120	0.490	1.272	0.040	0.610	1054	-1.346	1.843
0.075	-0.657	0.500	-0.530	-0.302	-2.277	0.170	7.09	0.280	-0.120	0.490	1.438	0.040	0.610	1086	-1.471	1.845
0.10	-0.314	0.500	-0.530	-0.324	-2.318	0.170	8.05	0.280	-0.099	0.490	1.604	0.040	0.610	1032	-1.624	1.847
0.15	-0.133	0.500	-0.530	-0.339	-2.309	0.170	8.79	0.280	-0.048	0.490	1.928	0.040	0.610	878	-1.931	1.852
0.20	-0.486	0.500	-0.446	-0.398	-2.220	0.170	7.60	0.280	-0.012	0.490	2.194	0.040	0.610	748	-2.188	1.856
0.25	-0.890	0.500	-0.362	-0.458	-2.146	0.170	6.58	0.280	0.000	0.490	2.351	0.040	0.700	654	-2.381	1.861
0.30	-1.171	0.500	-0.294	-0.511	-2.095	0.170	6.04	0.280	0.000	0.490	2.460	0.040	0.750	587	-2.518	1.865
0.40	-1.466	0.500	-0.186	-0.592	-2.066	0.170	5.30	0.280	0.000	0.490	2.587	0.040	0.850	503	-2.657	1.874
0.50	-2.569	0.656	-0.304	-0.536	-2.041	0.170	4.73	0.280	0.000	0.490	2.544	0.040	0.883	457	-2.669	1.883
0.75	-4.844	0.972	-0.578	-0.406	-2.000	0.170	4.00	0.280	0.000	0.490	2.133	0.077	1.000	410	-2.401	1.906
1.0	-6.406	1.196	-0.772	-0.314	-2.000	0.170	4.00	0.255	0.000	0.490	1.571	0.150	1.000	400	-1.955	1.929
1.5	-8.692	1.513	-1.046	-0.185	-2.000	0.170	4.00	0.161	0.000	0.490	0.406	0.253	1.000	400	-1.025	1.974
2.0	-9.701	1.600	-0.978	-0.236	-2.000	0.170	4.00	0.094	0.000	0.371	-0.456	0.300	1.000	400	-0.299	2.019
3.0	-10.556	1.600	-0.638	-0.491	-2.000	0.170	4.00	0.000	0.000	0.154	-0.820	0.300	1.000	400	0.000	2.110
4.0	-11.212	1.600	-0.316	-0.770	-2.000	0.170	4.00	0.000	0.000	0.000	-0.820	0.300	1.000	400	0.000	2.200
5.0	-11.684	1.600	-0.070	-0.986	-2.000	0.170	4.00	0.000	0.000	0.000	-0.820	0.300	1.000	400	0.000	2.291
7.5	-12.505	1.600	-0.070	-0.656	-2.000	0.170	4.00	0.000	0.000	0.000	-0.820	0.300	1.000	400	0.000	2.517
10.0	-13.087	1.600	-0.070	-0.422	-2.000	0.170	4.00	0.000	0.000	0.000	-0.820	0.300	1.000	400	0.000	2.744
PGA	-1.715	0.500	-0.530	-0.262	-2.118	0.170	5.60	0.280	-0.120	0.490	1.058	0.040	0.610	865	-1.186	1.839
PGV	0.954	0.696	-0.309	-0.019	-2.016	0.170	4.00	0.245	0.000	0.358	1.694	0.092	1.000	400	-1.955	1.929
PGD	-5.270	1.600	-0.070	0.000	-2.000	0.170	4.00	0.000	0.000	0.000	-0.820	0.300	1.000	400	0.000	2.744

Note: c=1.88 and n= 1.18 for all periods (T); PGA and PSA have units of g: PGV and PGD have uits of cm/s and cm, respectively

Table 2.11. Standard Deviations for Uncertainty Model (Campbell,2008).

T (sec)	0.01	0.02	0.03	0.05	0.075	0.1	0.15	0.2
σ_{InY}	0.478	0.48	0.489	0.51	0.52	0.531	0.532	0.534
T (sec)	0.25	0.3	0.4	0.5	0.75	1	1.5	2
σ_{InY}	0.534	0.544	0.541	0.55	0.568	0.568	0.564	0.571
T (sec)	3	4	5	7.5	10	PGA	PGV	PGD
σ_{InY}	0.558	0.576	0.601	0.628	0.667	0.478	0.484	0.667

In this study, hanging-wall and sediment terms are not included in calculating the seismic demand.

The results for Campbell-Bozorgnia 2008 at 400m/s shear wave velocity at different spectral periods, PGA, 0.2sec, 0.3sec and 1.0sec are listed from Figure 2.20 to Figure 2.23. For Kadiköy region, seismic hazard curves are also given considering the faults separately and combined for better illustration. The results for 200m/s and 600m/s shear-wave velocities can be found in Appendix A. The acceleration values for all the districts in İstanbul can also be found in Appendix E considering different acceleration values (peak ground acceleration, spectral acceleration at 0.2 sec, 0.3 sec and 1.0sec) and two return periods (475 years and 2475 years).

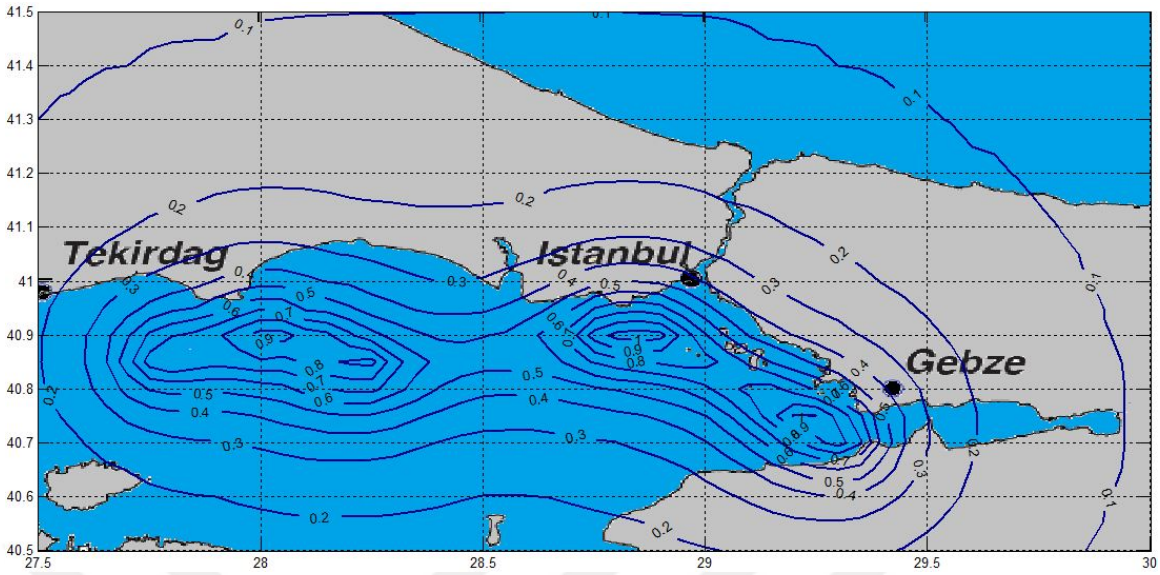

Figure 2.24. Vs30 = 400m/sec and using CB08 Attenuation Relationship PGA Map with 475 Years Return Period.

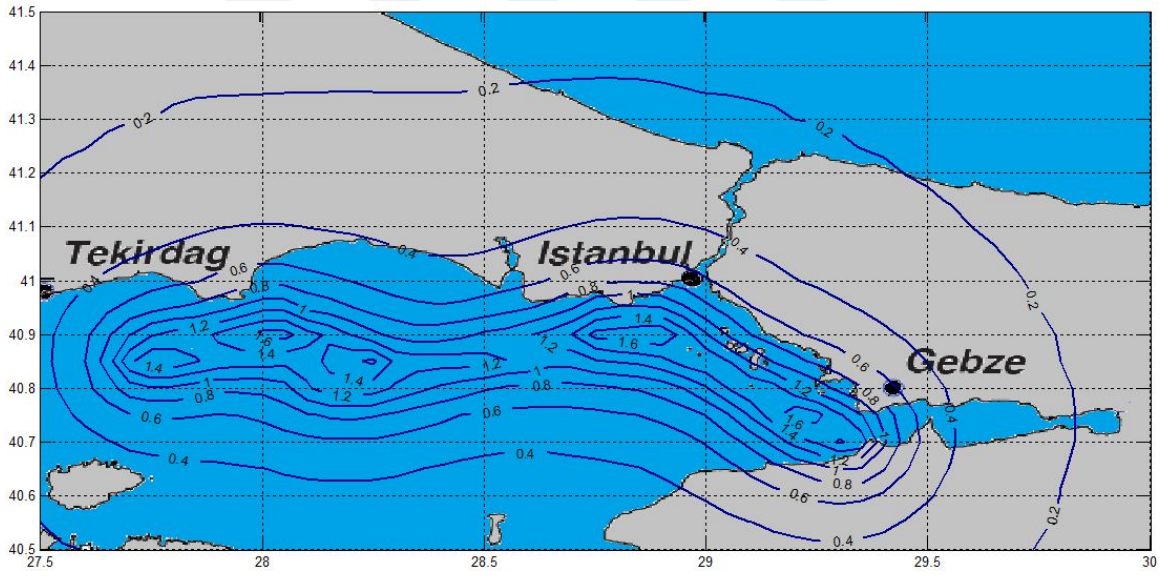

Figure 2.25. Vs30 = 400m/sec and using CB08 Attenuation Relationship PGA map with 2475 Years Return Period.

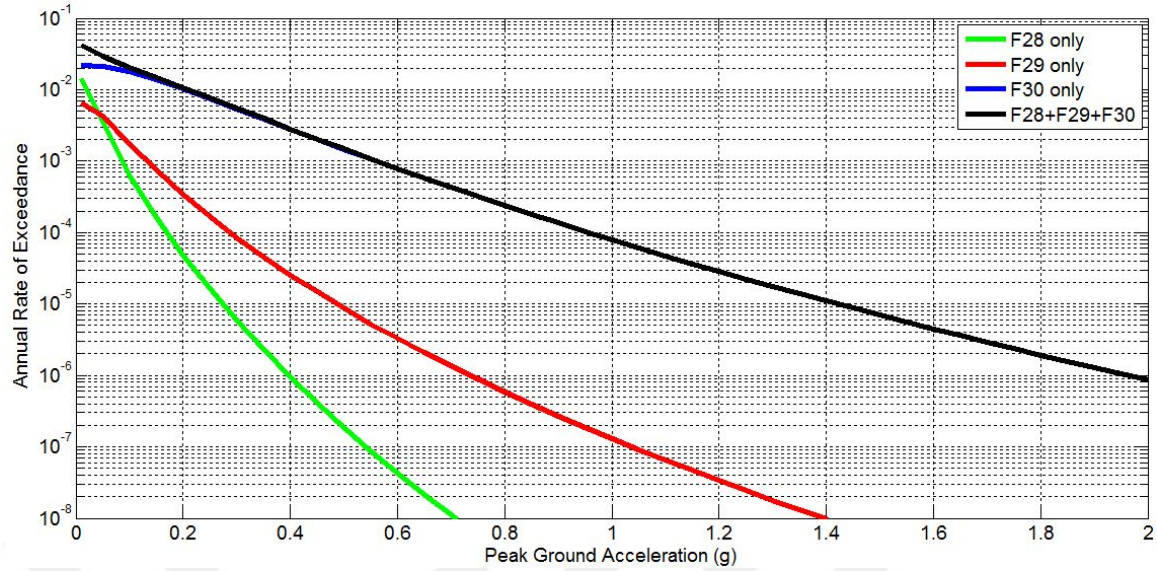

Figure 2.26. Vs30 = 400m/sec and using CB08 Attenuation Relationship Seismic Hazard Curve for PGA at Kadiköy District Considering the Fault Effects.

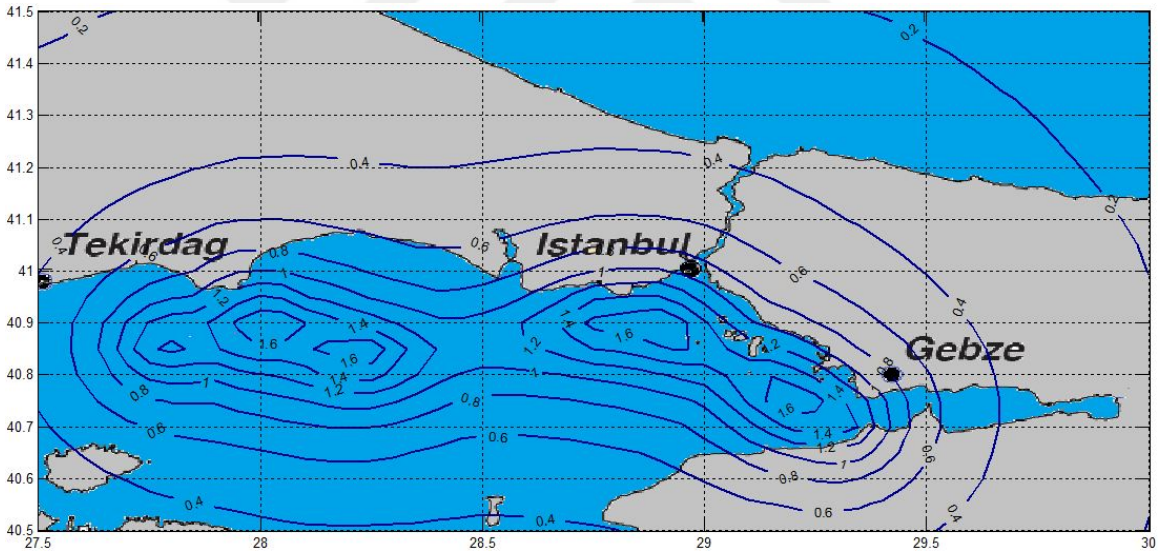

Figure 2.27. Vs30 = 400m/sec and using CB08 Attenuation Relationship SA at 0.2sec map with 475 Years Return Period.

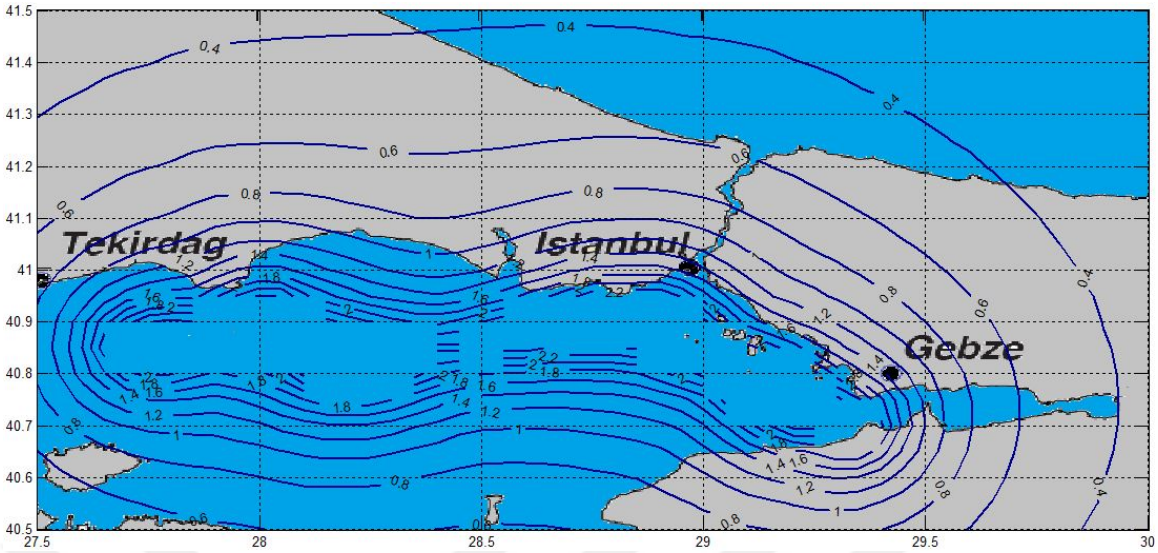

Figure 2.28. Vs30 = 400m/sec and using CB08 Attenuation Relationship SA at 0.2sec map with 2475 Years Return Period.

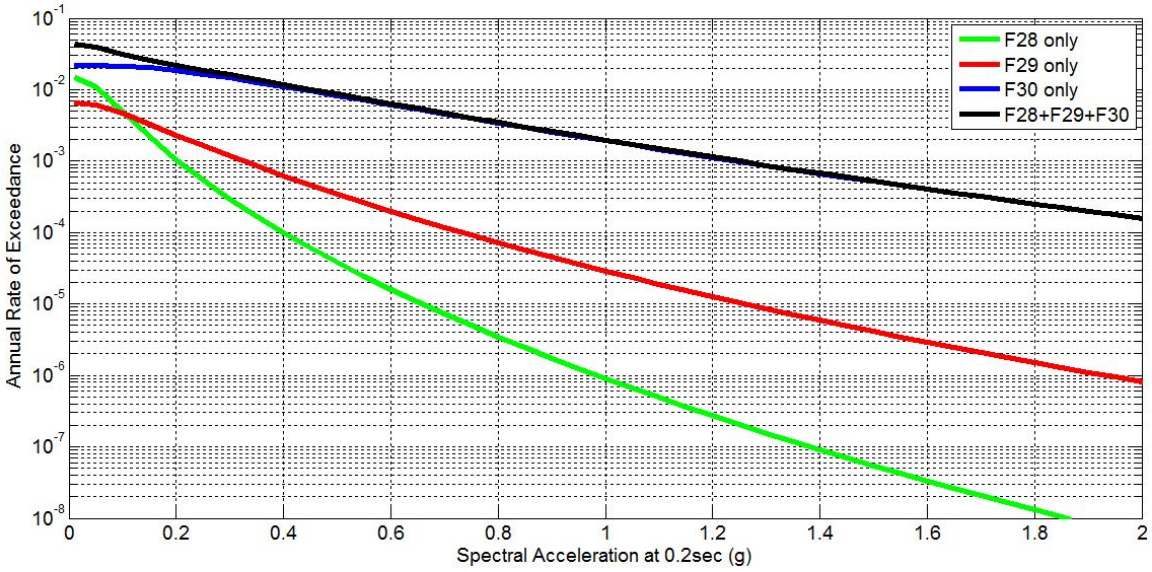

Figure 2.29. Vs30 = 400m/sec and using CB08 Attenuation Relationship Seismic Hazard Curve for SA at 0.2sec at Kadiköy District Considering the fault Effects.

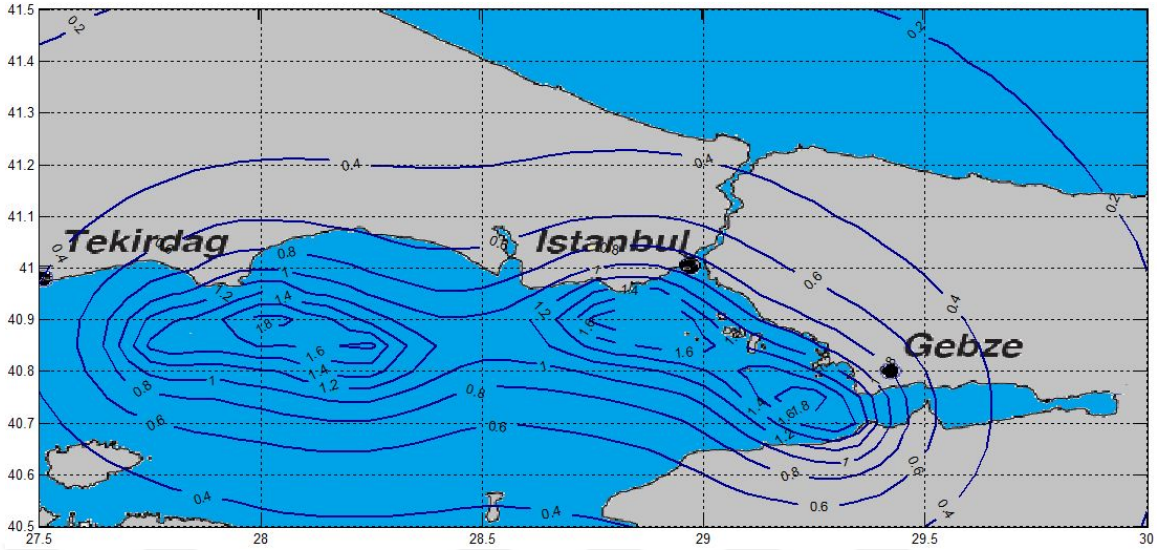

Figure 2.30. Vs30 = 400m/sec and using CB08 Attenuation Relationship SA at 0.3sec map with 475 Years Return Period.

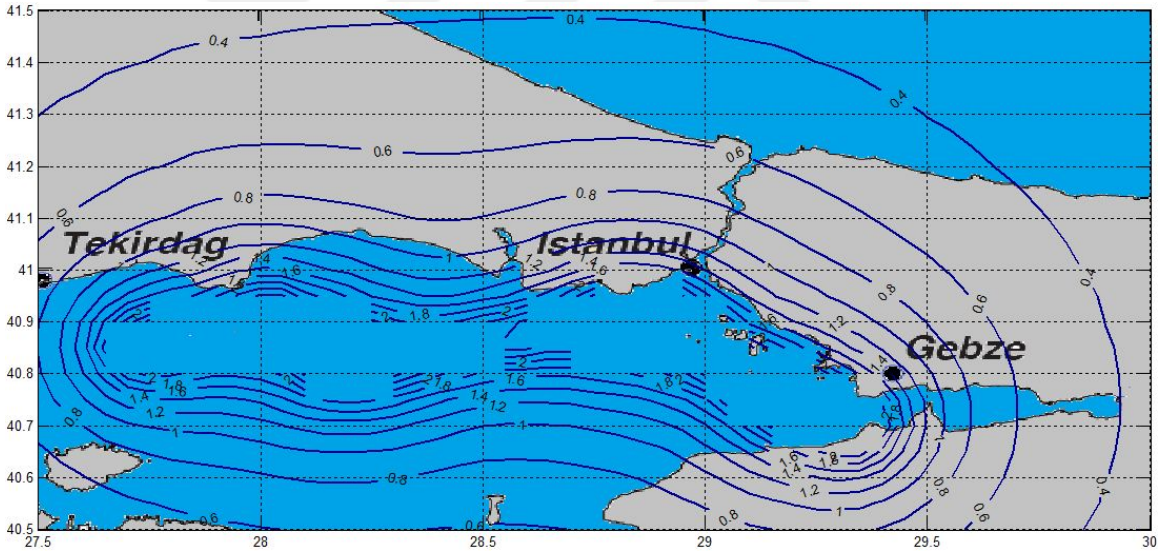

Figure 2.31. Vs30 = 400m/sec and using CB08 Attenuation Relationship SA at 0.3sec map with 2475 Years Return Period.

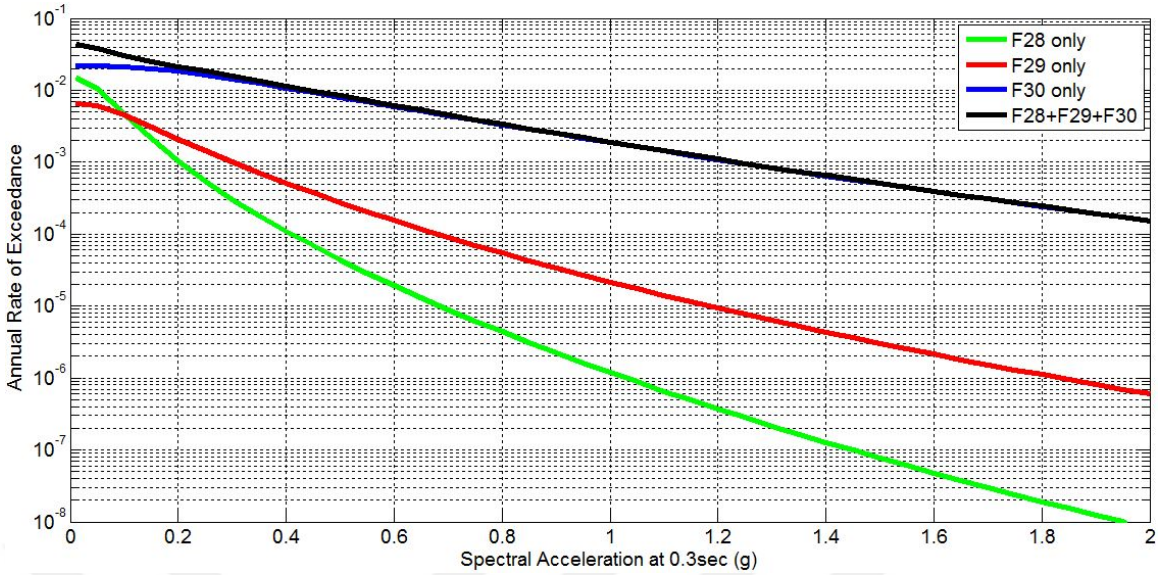

Figure 2.32. Vs30 = 400m/sec and using CB08 Attenuation Relationship Seismic Hazard Curve for SA at 0.3sec at Kadiköy District Considering the Fault Effects.

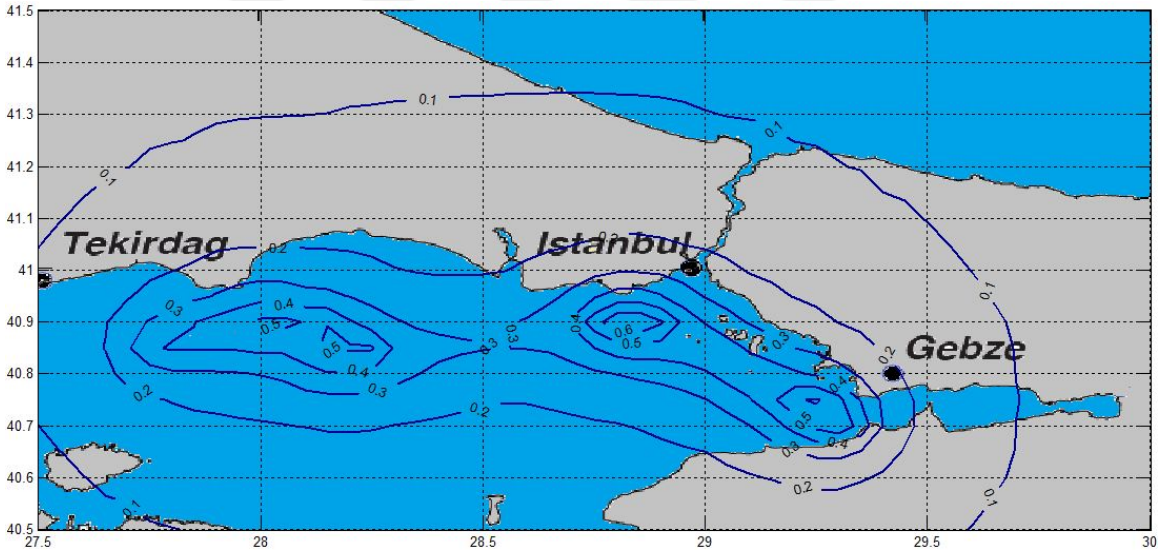

Figure 2.33. Vs30 = 400m/sec and using CB08 Attenuation Relationship SA at 1.0sec map with 475 Years Return Period.

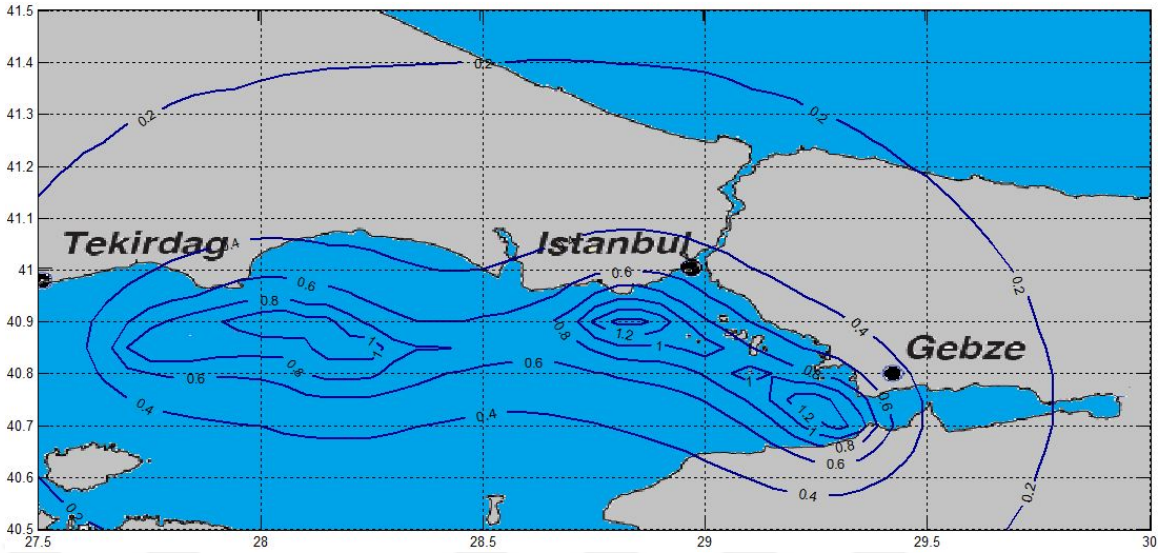

Figure 2.34. Vs30 = 400m/sec and using CB08 Attenuation Relationship SA at 1.0sec map with 2475 Years Return Period .

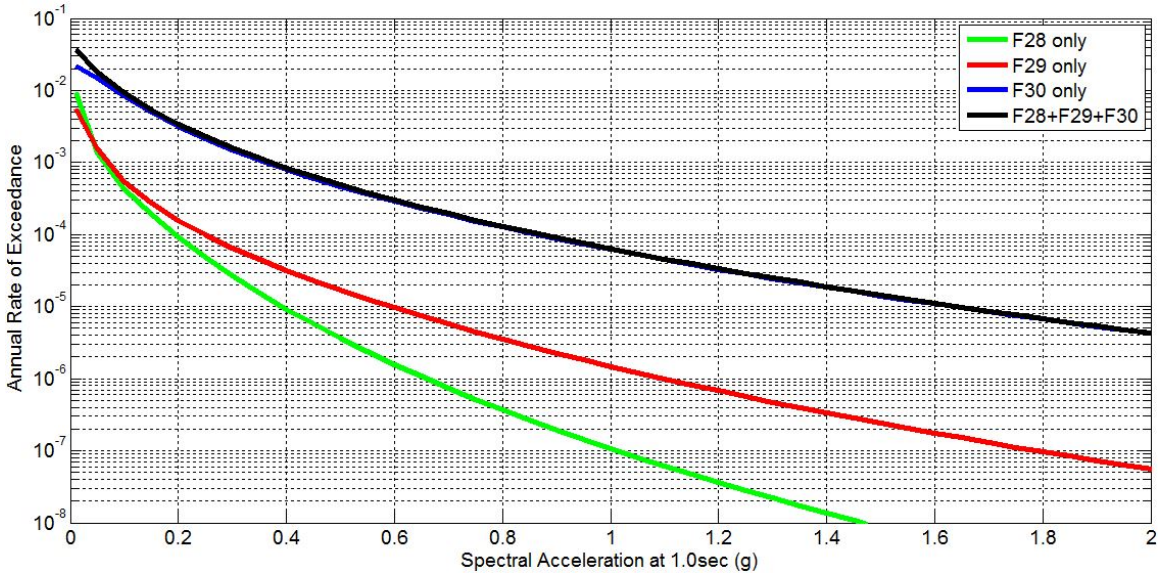

Figure 2.35. Vs30 = 400m/sec and using CB08 Attenuation Relationship Seismic Hazard Curve for SA at 1.0sec at Kadiköy District Considering the Fault Effects.

2.6. Uniform Hazard Spectrum

The Uniform Hazard Spectrum is defined as a spectrum with equal probability of exceedance of a certain hazard in all structural periods. In the context of PSHA, uniform hazard spectra (UHS) can provide very essential probabilistic information required

for performance based seismic design. In brevity, it can be defined as a ground hazard spectrum including probabilistic information based on earthquake hazard (Datta *et al.*, 2007). Since the performance based and probabilistic methods became more popular compared to deterministic approaches, the concept of UHS became more common in earthquake engineering. These spectra provide an effective means of probabilistic seismic hazard estimation.

In this study, after obtaining the probabilistic ground motion demands, the corresponding uniform hazard spectra have been generated for Kadiköy region for two return periods and three Vs30 values in Figure 2.36 to Figure 2.38.

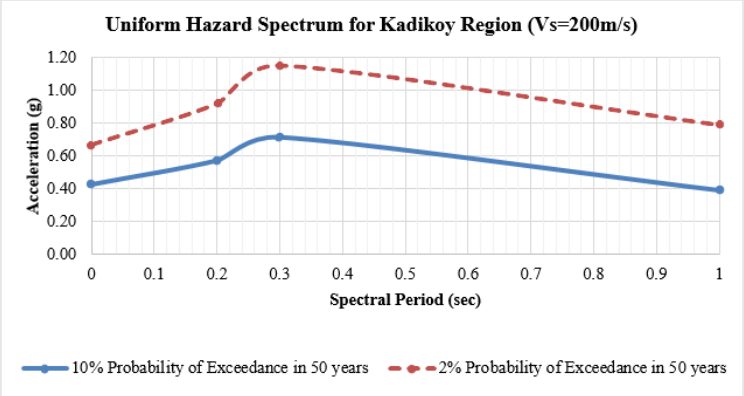

Figure 2.36. Uniform Hazard Spectrum of Kadiköy district for Vs30 = 200m/sec.

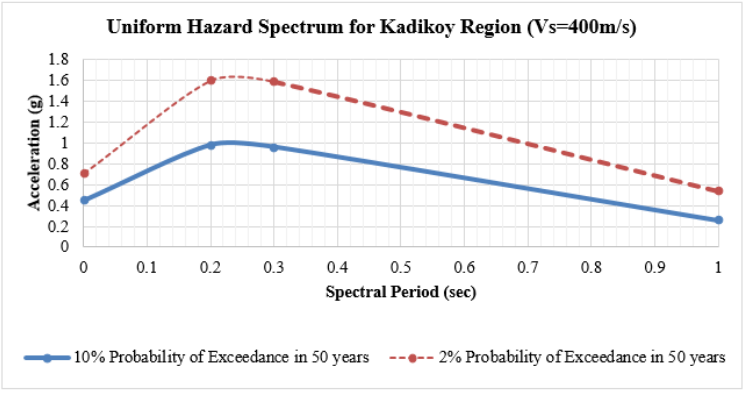

Figure 2.37. Uniform Hazard Spectrum of Kadiköy district with Vs30 = 400m/sec.

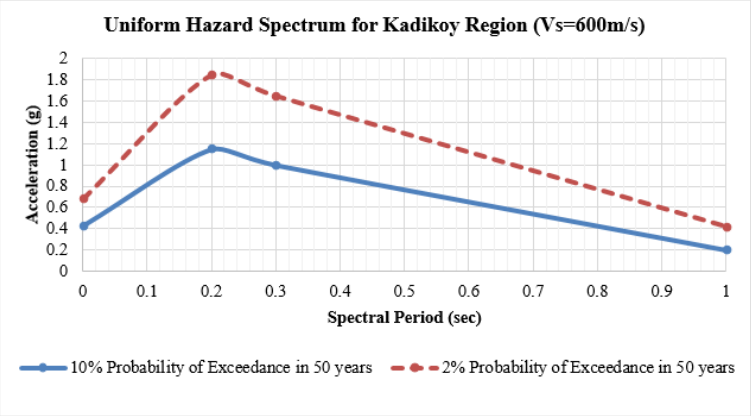

Figure 2.38. Uniform Hazard Spectrum of Kadiköy district with Vs30 = 600m/sec.

Table 2.12. Acceleration Values for Kadiköy District.

Acceleration Values for Kadiköy Region				
Return Period (years)	Peak Ground Acceleration (g)	Spectral Acceleration at 0.2sec (g)	Spectral Acceleration at 0.3sec (g)	Spectral Acceleration at 1.0sec (g)
200 m/sec Shear Wave Velocity				
475	0.42	0.57	0.71	0.39
2475	0.67	0.92	1.15	0.79
400 m/sec Shear Wave Velocity				
475	0.45	0.98	0.96	0.26
2475	0.71	1.6	1.59	0.54
600 m/sec Shear Wave Velocity				
475	0.43	1.15	1.00	0.20
2475	0.68	1.85	165	0.42

Utilizing the shear wave velocity map in Figure 1.6, the Vs30 value for Kadiköy region is around 400m/s. Based on uniform hazard spectra, Figure 2.24 and Table 2.12 show that the acceleration values for 475 years return (10% probability of exceedance in 50 years) period reveals good performance when compared to design spectrum defined in Turkish Earthquake Code. Moreover, for 2475 years return period (2% probability of exceedance in 50 years), the design code states the peak ground acceleration and

spectral acceleration values of the earthquakes for which the possibility to be exceeded in 50 years is 2% (2475 years return period) are decided to be taken as approximately 1.5 times of the corresponding values of the earthquakes for which the possibility to be exceeded in 50 years is 10% (475 years). As seen from Table 2.12, the acceleration values comply with this regulation, in other words, acceleration values with 2475 years return periods are around 1.5 times of values with 475 years return period.

3. STRUCTURAL PERFORMANCE ASSESSMENT

3.1. General

Second major component of "Seismic Loss Estimation" is assessment of structural performance. Damage states of structures can be obtained by fragility analysis. Fragility is defined as probability of having damage to a given element or sets of element at risk resulting from a given level of hazard (Coburn and Spence, 2002). Fragility curves have shown the probability of failure at predefined damage state. In principle, fragility curves can be developed using the following methods: (1) Professional judgment; (2) quasi-static and design code consistent analysis; (3) utilization of damage data associated with past earthquakes; and (4) numerical simulation of the seismic response of structures based on dynamic analysis (Shinozuka *et al.*, 2000). In general, Method (3) and (4) are mostly used ones.

Fragility curves can be generated for an individual building or for a group of structures. It is mainly based on the scope and aim of the study. If one wants to assess the performance of a special structure such as nuclear power plant, shelter etc. or only wants to see the trend of the building, individual building assessment is enough. If extended study is needed for insurance companies or municipality for regional assessment, a group of structures could also be assessed.

In order to develop the fragility curve, the ground motion demand at area of interest should be determined. This demand can be obtained by two main ways, either by using past earthquake data or synthetically generated ground motions. Different ground motion parameters can be used in developing fragility curve; intensity, peak ground acceleration (pga), peak ground displacement (pgd), spectral acceleration (S_a), spectral velocity (S_d).

The curves can be expressed in the form of two-parameter (median and log-standard deviation) is performed by means of maximum likelihood method. (Shi-

nozuka, 2000). The likelihood function for this purpose is expressed as follows.

$$L = \prod_{i=1}^{N} \left[F\left(a_i\right)\right]^{x_i} \cdot \left[1 - F\left(a_i\right)\right]^{1-x_i} \tag{3.1}$$

where N is total number of structure, $F(a_i)$ represent the fragility curve for a specific state of damage of corresponding structure, (a_i) is the ground motion parameter, x_i= 1 or x_i=0 shows that the structure withstands under ground motion parameter (a_i). Under the log-normal assumption, F(a) takes this analytical form:

$$F\left(a\right) = \phi\left[\frac{ln\left(\frac{a}{c}\right)}{\xi}\right] \tag{3.2}$$

In which (a) represents the ground motion parameter, $\phi[.]$ represents the standardized normal distribution function. c and ξ are log-normal median and standard deviation parameters. These parameters are obtained by optimization of likelihood function, L.

$$\frac{\partial \ln\left(L\right)}{\partial c} = \frac{\partial \ln\left(L\right)}{\partial \xi} = 0 \tag{3.3}$$

Behavior of a structure can be divided into 3 main categories according to ASCE/SEI 41-13, American Society of Civil Engineers-Seismic Evaluation and Retrofit of Existing Buildings; (ASCE,2014) immediate occupancy (IO), life safety (LS) and collapse prevention (CP), overall they can be called as "Limit States" shown in Figure 3.1. This limitations of these states are mainly based on structural response parameters and some ratios between these as illustrated in Figure 3.2 and Figure 3.3. In this study, nonlinear time history analysis has been conducted for calculations of structural responses using SAP2000 software. The input motions and corresponding spectral acceleration plots are given in Appendix D.

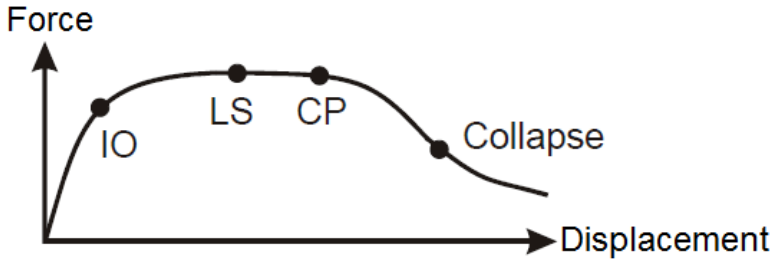

Figure 3.1. Limit States on Typical Force-Displacement Plot.

Table 3.1. Limits States for Reinforced Concrete Columns (ASCE, 2014).

Acceptance Criteria					
Plastic Rotations Angle (radians)					
Performance Level					
Conditions			IO	LS	CP
$\frac{P^c}{A_g f'_c}$	$\rho \frac{A_v}{b_w S}$	$\frac{V^d}{b_w d \sqrt{f'_c}}$			
≤ 0.1	≥ 0.006	≤ 3 (0.25)	0.005	0.045	0.060
≤ 0.1	≥ 0.006	≥ 6 (0.5)	0.005	0.045	0.060
≥ 0.6	≥ 0.006	≤ 3 (0.25)	0.003	0.009	0.001
≥ 0.6	≥ 0.006	≥ 6 (0.5)	0.003	0.007	0.008
≤ 0.1	≤ 0.0005	≤ 3 (0.25)	0.005	0.010	0.012
≤ 0.1	≤ 0.0005	≥ 6 (0.5)	0.004	0.005	0.006
≥ 0.6	≤ 0.0005	≤ 3 (0.25)	0.002	0.003	0.004
≥ 0.6	≤ 0.0005	≥ 6 (0.5)	0.0	0.0	0.0

Table 3.2. Limits States for Reinforced Concrete Beams. (ASCE, 2014).

Acceptance Criteria					
Plastic Rotations Angle (radians)					
Performance Level					
Conditions			IO	LS	CP
$\frac{\rho-\rho'}{\rho_{bal}}$	Transverse reinforcement	$\frac{V^d}{b_w d\sqrt{f'_c}}$			
≤ 0.0	C	≤ 3 (0.25)	0.010	0.025	0.05
≤ 0.0	C	≥ 6 (0.5)	0.005	0.02	0.04
≥ 0.5	C	≥ 3 (0.25)	0.005	0.02	0.03
≥ 0.5	C	≥ 6 (0.5)	0.005	0.015	0.02
≤ 0.0	NC	≤ 3 (0.25)	0.005	0.02	0.03
≤ 0.0	NC	≥ 6 (0.5)	0.0015	0.01	0.015
≥ 0.5	NC	≤ 3 (0.25)	0.005	0.01	0.015
≥ 0.5	NC	≥ 6 (0.5)	0.0015	0.005	0.01

3.2. Properties of Structure

This typical building is assumed to be located on 1000 m^2 base area in Caddebostan Kadikoy, İstanbul. The reason of choosing this area is that urban projects have widely taken place. The number of story is based on the regulations of Municipality, in which the story level calculation is given clearly in Figure 3.2. (Kadiköy Belediyesi, 2014)

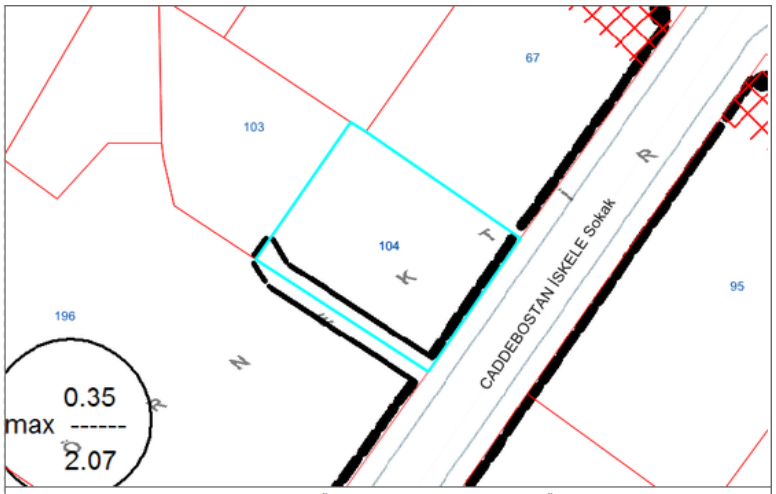

Not	- Parselde tescilli eski eser bina/ tescilli ağaç bulunması veya tescilli bina parseli komşuluğunda kalması halinde K.T.V.K. Kurulu' ndan görüş alınmadan uygulama yapılamaz.				
Mer'i İmar Planı	KADIKÖY MERKEZ E-5 (D100) OTOYOLU ARA BÖLGESİ UYGULAMA İMAR PLANI VE PLAN NOTLARI İLE LEJAND TADİLLERİ--1/1000(11.5.2006)				
Ölçeği	1/1000	Bina Yüksekliği	h:serbest	KAKS %	max KAKS:2.07
İlçesi	KADIKÖY	Kat Adedi	-	TAKS %	max TAKS:0.35
Mahallesi	CADDEBOSTAN	Ön Bahçe Mesafesi	min.5m	Arka Bahçe Mesafesi	min.4m
İnşaat Nizamı	AYRIK	Yan Bahçe Mesafesi	min.4m	Kot Alınacak Nokta	Plan Notu
Genişlik	min.6m	Derinlik	YÖNETMELİK		
Kadastro	Pafta: P.106/4	Ada: 368	Parsel: 104	Parselin Plan Fonksiyon Bilgisi : KONUT ALANI	

Figure 3.2. Information About the Region of Interest of the Building (Kadiköy Belediyesi, 2014).

where KAKS and TAKS are Story Area Ratio and Floor Area ratio, respectively. The detailed calculation for story level is given in Table 3.3.

Table 3.3. Add caption

(A)	Base Area (BA)	-	1000	m^2
(B)	Floor Area Ratio (FAR)	max	0,35	
(C)=(A)(B)*	Floor Area (FA)	max	350	m^2
(D)	Story Area Ratio (SAR)	max	2,07	
(E)=(A)(D)*	Total Story Area (SA)	max	2070	m^2
(F) = (E)/(C)	Number of Story	min	5	

The minimum number of story is calculated as five stories. In practice, the number of story is usually changing from ten to twelve stories around this region. So, without any restriction, the story level for this typical building can be chosen as

10-story providing that the material and frame properties are designed to meet the minimum criteria complying with the regulations, TS500 and TEC2007. The layout of the building is given in Figure 3.3.

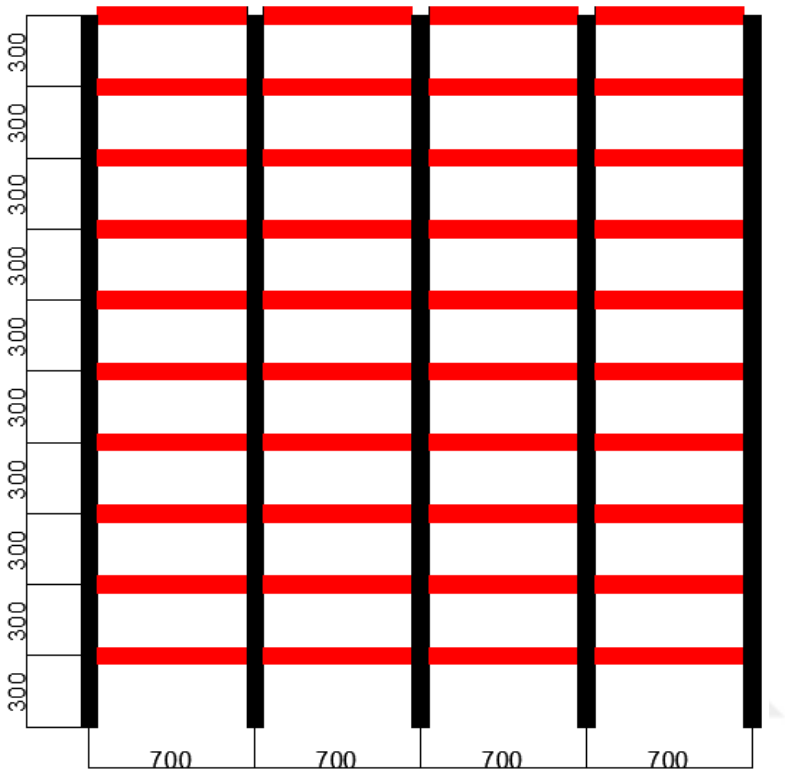

Figure 3.3. Layout of the Typical Building (Units are in mm).

Fixed end restraint are assigned at the bottom. Frame

- Material: C25/30 Concrete Modulus of Elasticity = 30000 MPa S420 Steel (Reinforcement)
- Column: 700 mm x 700 mm with 20F18 reinforcement No Transverse Reinforcement
- Beams: 400 mm x 700 mm with 3F18 top and 3F18 bottom reinforcement No Transverse Reinforcement
- Beam-Column Joints: First Story Columns End I = 0.35 (0 for first story), End J = 0.35m Rigid Zone Factor = 1 Beams End I = 0.35m, End J = 0.35m Rigid Zone Factor = 1
- Loads: Dead Load + Self Weight, G = 20kN/m Live Load, Q = 10kN/m (Dis-

tributed Load on Beams) Since our building is residential building, in accordance with Turkish Earthquake Code 2007, 0.30 live load reduction factor has been used in analyses.

Noting that, for beams and columns, cracked section stiffness with 0.40 multiplier has been used After all these parameters have been defined properly, the modal analysis has been conducted and the first three natural periods of the building are found as 0.96sec, 0.31sec and 0.18sec as shown in Figure 3.4. Their corresponding mass participation ratios are found to be 81.8%, 91.5% and 95.1%, respectively.

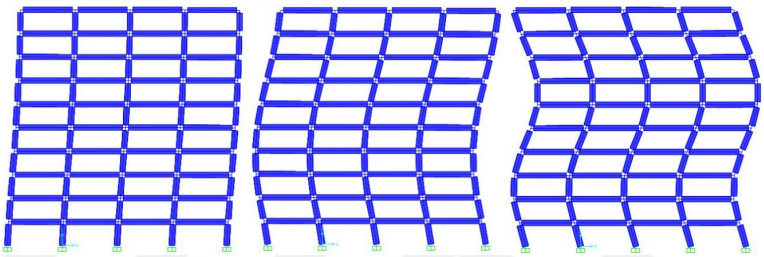

Figure 3.4. First three Modes of the Building.

3.3. Structural Assessment using Non-Linear Time History Analysis

Two dimensional non-linear time history analysis has been conducted in order to determine the structural performance level. The input motions are chosen from 1994 Northridge, California earthquake data, of which the input motions can be found at Appendix D. For each acceleration value, the structural response of the building has been assessed based on the limitations of regulations of ASCE/SEI 41-13, American Society of Civil Engineers-Seismic Evaluation and Retrofit of Existing Buildings. (ASCE,2014) For each column and beam, the total percentage of the members with damage state range has been determined in Table 3.4.

Table 3.4. Total Percentage of the Members with Limit State Range for Each Ground Motion Intensity.

	Column Elements				Beam Elements			
Acceleration Value (g)	%Elastic Range	%Immediate Occopancy Range	% Life Safety Range	%Collapse Prevention Range	%Elastic Range	%Immediate Occopancy Range	% Life Safety Range	%Collapse Prevention Range
0.013	100%	0%	0%	0%	100%	0%	0%	0%
0.101	100%	0%	0%	0%	100%	0%	0%	0%
0.201	100%	0%	0%	0%	28%	73%	0%	0%
0.301	100%	0%	0%	0%	15%	85%	0%	0%
0.401	100%	0%	0%	0%	10%	90%	0%	0%
0.493	100%	0%	0%	0%	10%	90%	0%	0%
0.604	100%	0%	0%	0%	10%	20%	70%	0%
0.758	96%	4%	0%	0%	0%	20%	60%	20%
0.828	90%	8%	2%	0%	3%	25%	43%	30%
0.897	90%	10%	0%	0%	0%	15%	60%	25%
1.000	98%	2%	0%	0%	0%	20%	60%	20%

For each acceleration value, the plastic rotation-time history plots for beams are also plotted. For better illustration, one plot for beam showing the limit states and hinge results is given in Figure 3.5. The plots for other acceleration values can be found in Appendix F.

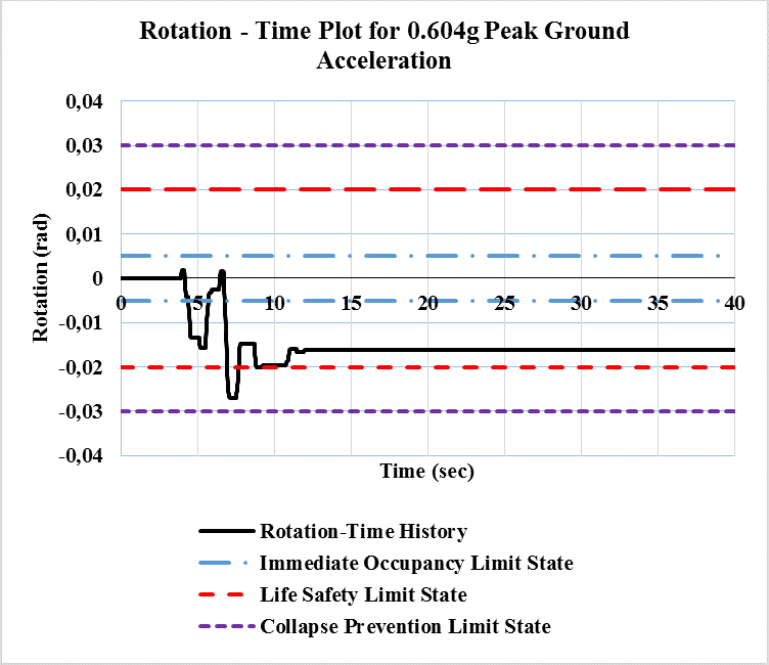

Figure 3.5. Plastic Rotation-Time Plot for pga=0.604g.

The results above indicates that columns are generally behaves in elastic range,

whereas behavior of beams shifts to immediate occupancy range at even very small acceleration values. Since beams are damaged before columns, the general behavior of the building can be assessed using the beam performance, which is controlling event and generally preferred case in order to examine the damage level of the building without collapse.

Table 3.5 shows the performance of the building, where tick mark indicates the building can meet the performance criteria of corresponding limit state and behave at this limit state.

Table 3.5. The Performance of the Building.

Accelaration Value (g)	Elastic Range	Immediate Occopancy Range	Life Safety Range	Collapse Prevention Range
0.013	√	√	√	√
0.101	X	X	√	√
0.201	X	X	√	√
0.301	X	X	√	√
0.401	X	X	√	√
0.493	X	X	√	√
0.604	X	X	X	√
0.753	X	X	X	√
0.828	X	X	X	√
0.897	X	X	X	√
1	X	X	X	√

Life Safety has been chosen as the acceptance criteria for this building, in other words, if the behavior of this building is at worse than life safety range, it is considered to fail. This table shows that up to 0.6 g, this building withstands the effects of earthquake loads and deformations. However, after 0.6 g, the performance of the building can only withstand the collapse prevention criteria.

3.4. Development of Fragility Curve

Based on the damage limit states, fragility curve has been developed considering both peak ground acceleration values and spectral acceleration values with 5% damping. Up to 0.6g, at which the behavior of the building is Life Safety range, it is considered as 0 (withstand), otherwise 1 (Fail) as shown in Table 3.6. Since the natural period of the building is almost 1.0sec, spectral accelerations at 1.0sec have also been determined from spectral acceleration plots. The graphs and values for input data motions and spectral acceleration values can be found in Appendix D.

Table 3.6. The Behavior of the Building.

Input Motion Number	PGA (g)	SA at 1.0 sec (g)	Faiy (1) / No Fail 0
1	0.013	0.01	0
2	0.101	0.13	0
3	0.201	0.14	0
4	0.301	0.5	0
5	0.401	0.16	0
6	0.493	0.22	0
7	0.604	0.61	1
8	0.753	1.13	1
9	0.828	0.77	1
10	0.897	0.4	1
11	1	0.5	1

Based on this limit states and acceleration values, the fragility curve is generated as shown in Figure 3.6. This figure shows the probability of having damage at a certain period of time at a given ground motion intensity. Blue and red lines represent the curve for life safety limit state considering peak ground acceleration and spectral acceleration at 1.0sec, respectively. For these acceleration values, the curves are approximately

overlaps onto each other.

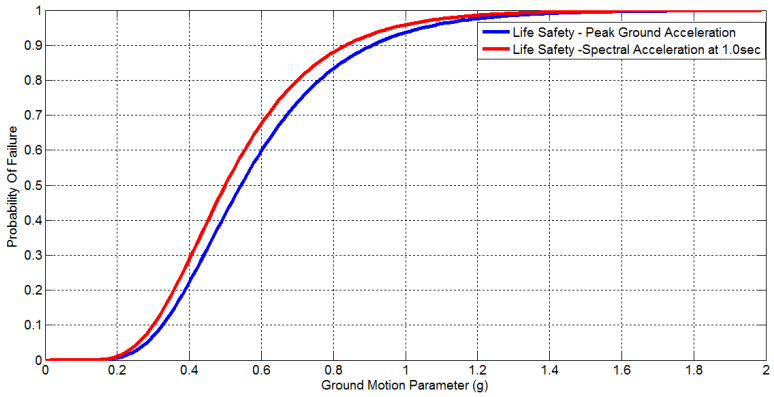

Figure 3.6. Fragility Curve of the Building for pga and Spectral Acceleration at 1.0sec Values at Life Safety Limit State.

3.5. Discussion of Results

The probability of failure for typical building located in Caddebostan, Kadikoy for different return periods and for shear wave velocities has been presented as in Table 3.7. This table can give an understanding about which acceleration value to be used for design and retrofitting purposes; and its corresponding failure probability.

Table 3.7. Probability of Failure Chart for Kadiköy District at Different Return Periods and Shear Wave Velocities.

KADIKOY				
475 years Return Period (10% Exceedance in 50 years)				
Shear Wave Velocity	Peak Ground Acceleration (g)	Probability of Failure	Spectral Acc. at 1.0sec (g)	Probability of Failure
200 m/s	0,42	26%	0,38	25%
400 m/s	0,45	32%	0,26	5%
600 m/s	0,43	28%	0,20	1%
2475 years Return Period (2% Exceedance in 50 years)				
Shear Wave Velocity	Peak Ground Acceleration (g)	Probability of Failure	Spectral Acc. at 1.0sec (g)	Probability of Failure
200 m/s	0,67	70%	0,79	87%
400 m/s	0,71	75%	0,54	58%
600 m/s	0,69	72%	0,42	33%

At each shear wave velocity, probability of failure for peak ground acceleration values gives almost same percentages, which are 30% and 70% for 475 and 2475 years return periods, respectively. However, this consistency does not reflect to the results of spectral acceleration values. There is huge difference between probabilities of failures for each shear wave velocity due to difference in spectral acceleration values. This can be assumed that the attenuation relationship, Campbell Bozorgnia 2008 (CB08), is more prone to change in shear wave velocities.

When failure probability at each shear wave velocity has been compared, except 200m/sec, there is also a huge difference due to difference in the spectral acceleration values. Since peak ground acceleration and spectral acceleration at 1.0sec are not close, it is expected to come up with such different probability failures. For instance, the most

apparent difference with more than 50% is obtained in failure probabilities of spectral acceleration values at 1.0sec at 2475 years return period.

On the other hand, the failure probabilities of spectral acceleration at 1.0sec with 400m/s and 600m/s are around 1% to 5% in 475 years return period. Actually, the behavior of the building is rigid up to 0.20g ground motion intensity. This form may be occurred due to use of only eleven ground motion input. If more input motions were used, the situation would change. Moreover, input motions are derived from the same earthquake, Northridge, California 1994. If other input motions from different earthquakes were utilized, the behavior of this curve might be different.

4. SUMMARY AND CONCLUSION

4.1. Summary

The main objective of this study is to execute a seismic loss estimation methodology for 10-story typical building in Kadiköy, İstanbul. By adding local effects, this methodology can be implemented for entire Turkey, on the part of municipalities, design and insurance companies for use in urban renewal projects, seismic design or rehabilitation works, disaster mitigation and emergency management. This methodology consists of deterministic and probabilistic approaches. Deterministic approach in this study is based on choosing the earthquake-generating sources with maximum magnitudes and the closest source-to-site distance. However, at the first glance it seems to be the "worst-case event", but without knowing the randomness associated with earthquake occurrences, it can only be defined as "reasonably large" event. It does not include the inherent uncertainty of earthquake itself. Therefore, considering the uncertainties, it is better to use "Probabilistic Seismic Hazard Analysis (PSHA)" rather than relying on deterministic earthquake scenarios.

Considering three submarine fault system underneath the Marmara Sea, F28(Off Tekirdag), F29(Mid-Marmara) and F30(Islands), peak ground acceleration and spectral acceleration at different periods, in brevity ground motion parameters, are estimated by using seismic hazard analysis. The physical properties of the submarine faults which are coordinate, seismicity, characteristic magnitude and activity rate are clearly defined in Le Pichon *et al.*, In order to compute the activities of the seismic sources, truncated characteristic exponential model is used. For attenuation relationship, the ground motion prediction equations derived by Kalkan-Gülkan (2004) and Campbell-Bozorgnia (2008) are used. In order to incorporate the site effects, the average shear wave velocity between 0 and 30-meters depth map is used. The Vs30 value changes from 200m/s to 600 m/s for İstanbul. In this study, 200m/s, 400m/s and 600m/s values are considered. Finally, the annual rate of exceedance values are computed using Poisson's Model and hereat the seismic hazard maps for different ground motion parameters are

generated. In this study, two different return periods are used, 475 and 2475 years that corresponds 10% and 2% probability of exceedance in 50 years, respectively. For the validation, the seismic hazard maps generated by OYO International Corporation for the study of İstanbul Metropolitan Municipality Earthquake Risk Management Department, and maps developed by CRISIS2007 software.

Second step is assessment of the structural performance of 10-story 4 bay moment-resisting frame building in Kadikoy, İstanbul. Two dimensional fictitious building, which complying with the Turkish Earthquake Code 2007 regulations, is assessed by using non-linear time history analysis conducted by eleven acceleration input data from Northridge Earthquake 1994 of which peak ground acceleration ranges from 0.013g to 1.000g. The damage limit states and requirements are based on the regulations of American Society of Civil Engineers, Seismic Evaluation and Retrofit of Existing Buildings. In this study, only "Life Safety" is considered as reference limit state for the building. After finding the damage states on the basis of column and beam elements, it is seen that beams are controlling elements showing the behavior of structure, therefore damage state of the whole building is determined using damage state of the beams.

Having assessed the structural performance of the building, the fragility curves are developed. These curves indicates the probability of failure for a given ground motion parameter. In this study, ground motion parameters are peak ground acceleration and spectral acceleration at 1.0 second. The reason of choosing spectral acceleration value at 1.0 second is to check the performance of the building having 0.96sec natural period for the spectral acceleration at almost same time period, 1.00sec.

Finally, fragility curves are integrated with the seismic hazard maps. For two return periods, 475 and 2475 years, the probability of exceeding defined limit state, "Life Safety", are computed for ground motion demand which has been computed in seismic hazard analysis. These results are good starting point for economical loss causality calculations.

4.2. Conclusion

Turkey is located on tectonically active fault mechanism and has witnessed dramatic earthquake events that result in physical, economic and social causalities. The occurrence of earthquake is inevitable but the precautions can reduce the effects. Past unfavorable and unforgettable experiences have proven the necessity of further studies earthquake science. This thesis refers to both deterministic and probabilistic approaches and concludes with physical loss estimation studies for different ground motion demand obtained in seismic hazard analysis for two different return periods.

Since submarine faults underneath the Marmara Sea are considered to be tectonically active, so rather than using recorded past data, the fault segments that have huge potential to rupture is preferred for the analysis. F28 (Off-Tekirdag), F29 (Mid-Marmara) and F30 (Islands) faults are chosen on purpose since they are at closer proximity to İstanbul and the the released energy from westward propagated North Anatolian Fault mechanism is considered to be transformed on these faults.

Deterministic Seismic Hazard Analysis (DSHA) with Maximum Credible Earthquake is introduced. This analysis is based on considering that fault ruptures at the closest distance to the site with its maximum, i.e., characteristic magnitude. For these three faults, deterministic seismic hazard map is developed and compared with the same study in the literature, Gülkan 2012, using the same ground motion prediction equation Kalkan-Gülkan 2004 attenuation relationship (KG04). The results are nearly same, at most 10% difference in average has occurred. Two main reasons of this difference are selection of the Vs30 value and resolution of the İstanbul map. Firstly, Vs30 map shows that the shear wave velocity is changing from 200 m/s to 600m/s for İstanbul and Gülkan uses the exact values for each district. In this study the average Vs30 value (400m/s) is considered in deterministic analysis. The second main reason of difference in grid size selection. Gülkan uses very small mesh size to divide the coordinates, 0.002^o by 0.002^o, approximately 250m by 250m. However, in this study, the grid size is selected as 0.05^o by 0.05^o, approximately 4km by 4km. This causes small differences in determining the start and end coordinates of the fault segments,

selecting the coordinates of each district, and therefore calculating distance between faults segment.

In Probabilistic Seismic Hazard Analysis, the inherent uncertainty associated with earthquake occurrences is introduced. Two different Ground Motion Prediction Equation are used for attenuation relationship; Kalkan Gülkan 2004 (KG04) and Campbell Bozorgnia 2008 (CB08). The results have been compared with the hazard maps generated by OYO International Company for the study of İstanbul Metropolitan Municipality Earthquake Risk Management Department and CRISIS2007 Software; and there exist more than 100% error.

The fictitious 2D beam-column frame located in Kadikoy-İstanbul, has been assessed using non-linear time history structural analysis. Having obtained the structural response, behavior of the building is determined based on the limit states defined in ASCE41-13. This behavior is illustrated asthe fragility curve which shows the probability of failure at different ground motion intensities. For 475 and 2475 years return periods, considering peak ground acceleration, probability of failures of the building are around 30% and 70%, respectively. For spectral acceleration at 1.0sec, the results are prone to change significantly when shear wave velocity changes.

4.3. Future Works and Recommendations

- The proposed methodology is generated for coastal cities of Marmara Sea, especially for İstanbul. By adding local effects, this can be implemented for any region in Turkey or entire Turkey.
- This study considers three faults segments that has potential to rupture underneath the Marmara Sea. This number can be increased and all the fault segments considering activity rates can be taken into consideration.
- The study considers 3 shear wave velocities (200m/s, 400m/s and 600m/s) for İstanbul region. By utilizing the Vs30 map, the exact Vs30 value of each district can be used.
- Two ground motion prediction equation has been used without verifying with

another past earthquake data. It relies on the studies in the literature. More attenuation relationships can be utilized and after verification with past earthquake data, by adding weights to attenuation relationships, the methodology can also be performed.

- In order to assess the structural performance, eleven (11) input motion data are used. This has resulted in small standard deviation value. For more reliable assessment, more earthquake data can be used.
- The mesh-grid size of the coordinates are well enough but for more local purposes, this can be increased.
- After physical loss estimation, more comprehensive studies can be conducted. A study considering all the components of seismic loss is more beneficial. This study can be developed by adding economical loss estimation, information about fatalities and injuries.
- This study is conducted on two dimensional ten story four bay fictitious reinforced concrete beam-column frame building. In practice, it can also be conducted to real structures for rehabilitation, renewal or insurance.

APPENDIX A: SEISMIC HAZARD MAPS OF MARMARA REGION

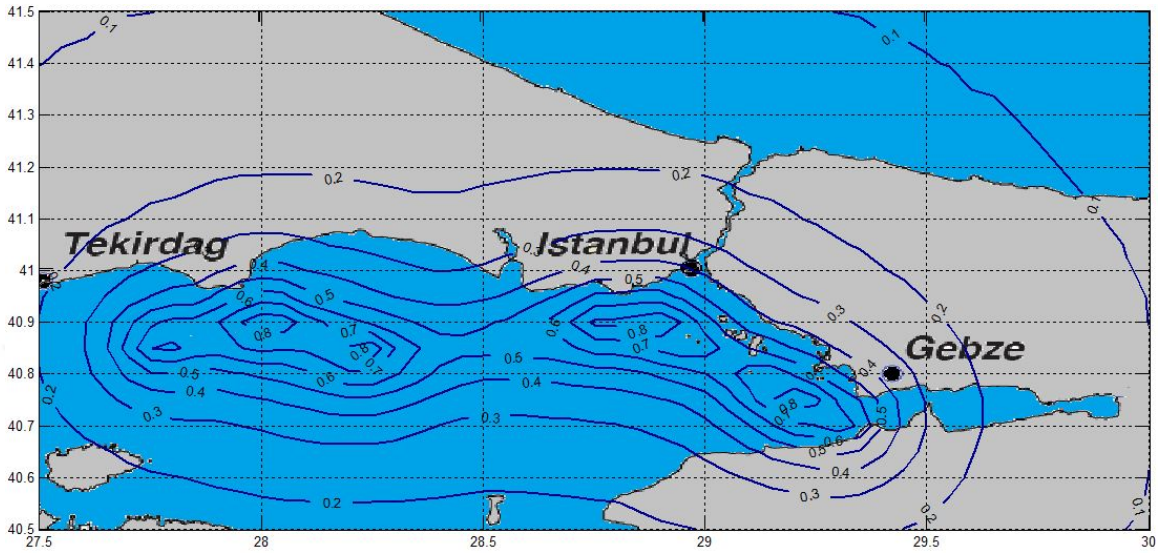

Figure A.1. Vs30 = 200m/sec and Using CB08 Attenuation Relationship PGA map with 475 Years Return Period.

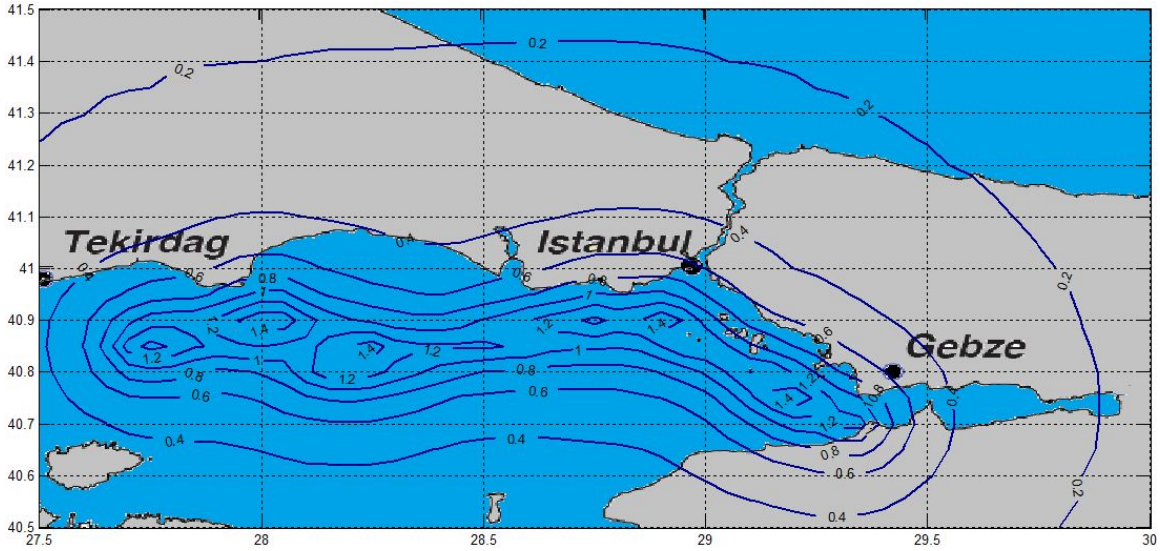

Figure A.2. Vs30 = 200m/sec and Using CB08 Attenuation Relationship PGA map with 2475 Years Return Period.

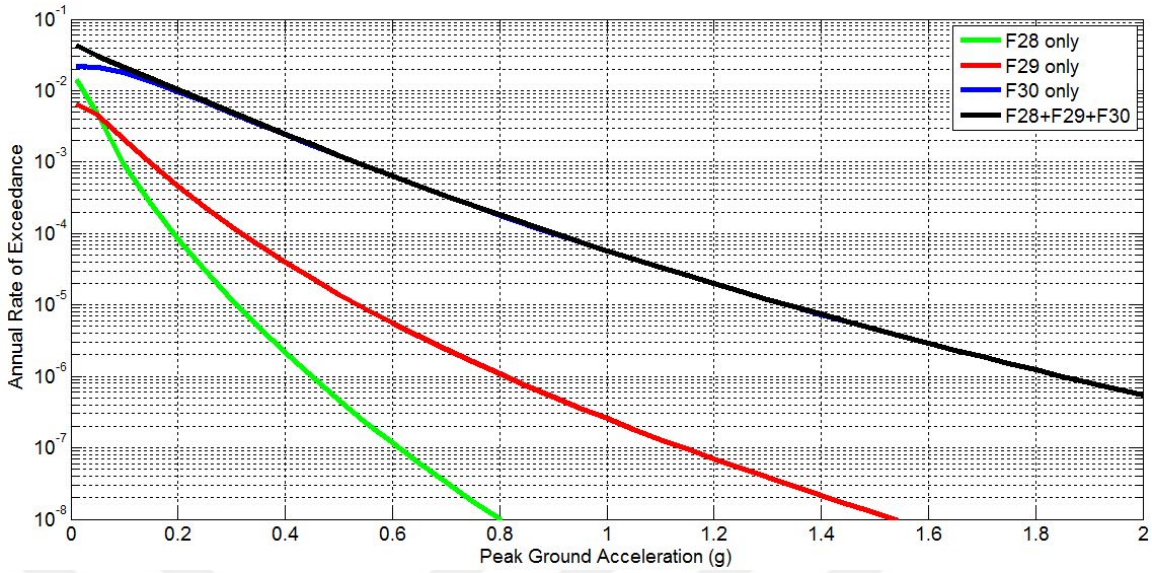

Figure A.3. Vs30 = 200m/sec and Using CB08 Attenuation Relationship Seismic Hazard Curve for PGA at Kadiköy District Considering the Fault Effects.

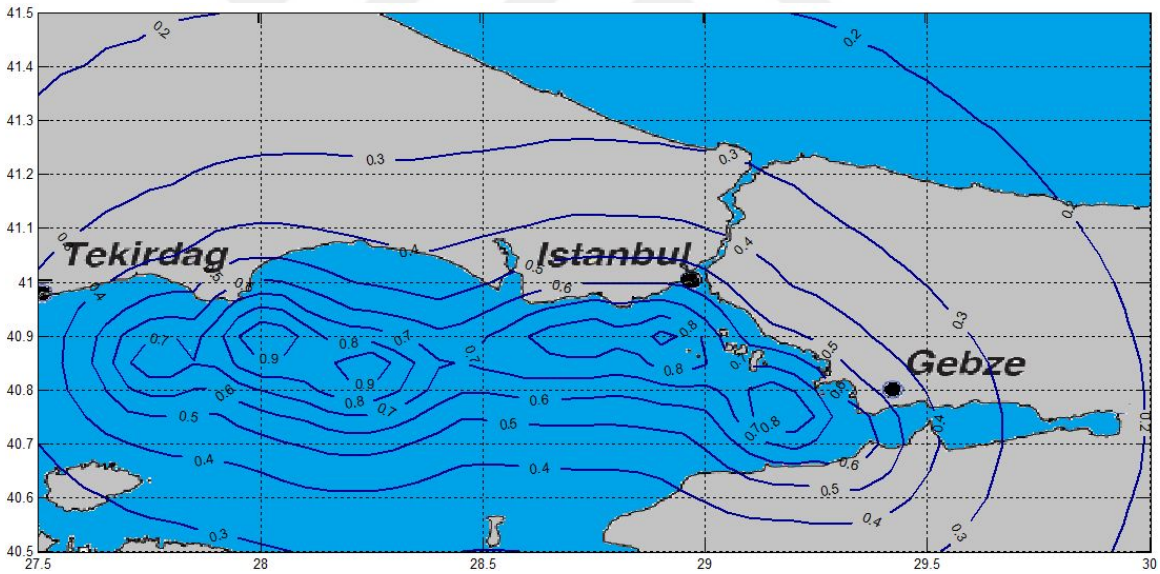

Figure A.4. Vs30 = 200m/sec and Using CB08 Attenuation Relationship SA at 0.2sec map with 475 Years Return Period.

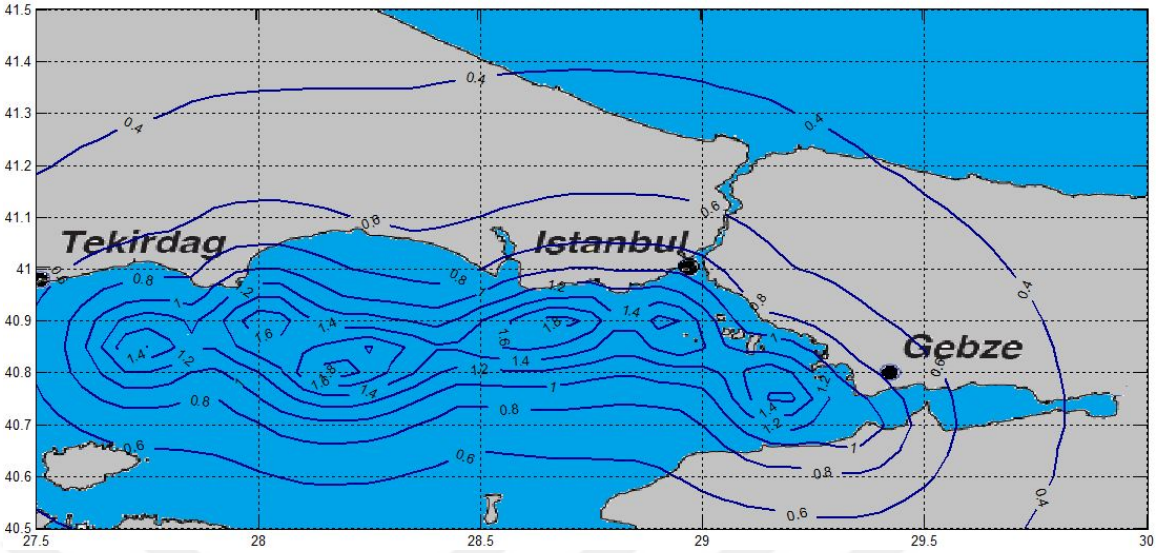

Figure A.5. Vs30 = 200m/sec and Using CB08 Attenuation Relationship SA at 0.2sec map with 2475 Years Return Period.

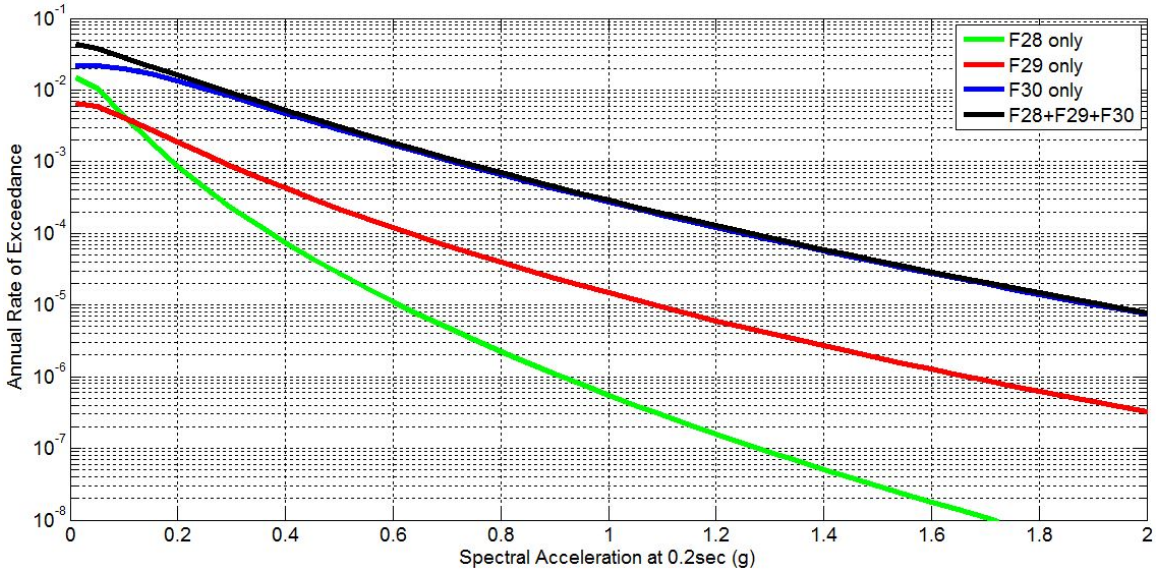

Figure A.6. Vs30 = 200m/sec and Using CB08 Attenuation Relationship Period Seismic Hazard Curve for SA at 0.2sec at Kadiköy District Considering the Fault Effects.

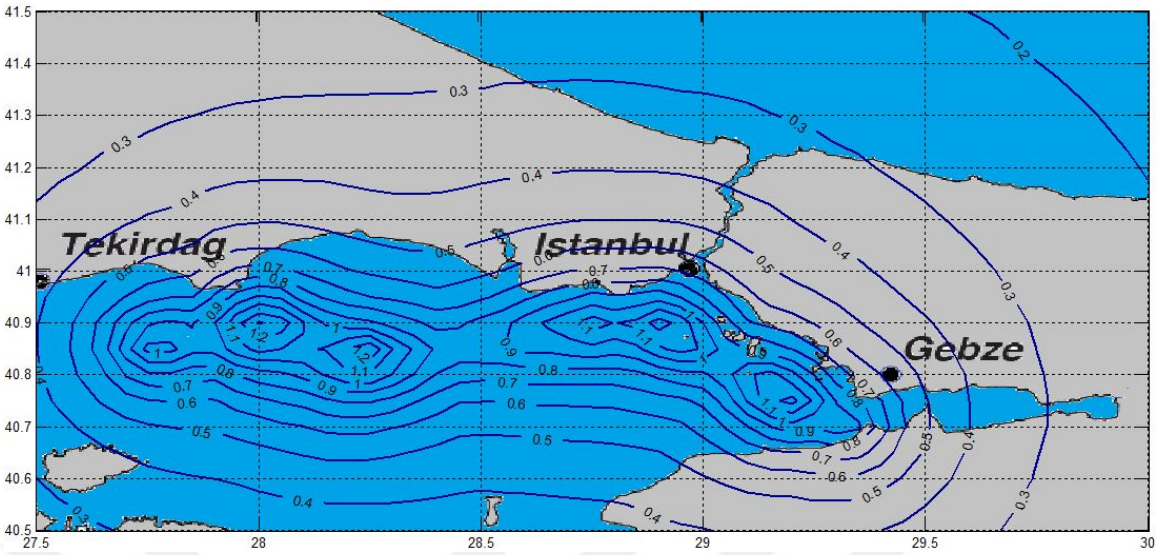

Figure A.7. Vs30 = 200m/sec and Using CB08 Attenuation Relationship SA at 0.3sec map with 475 Years Return Period.

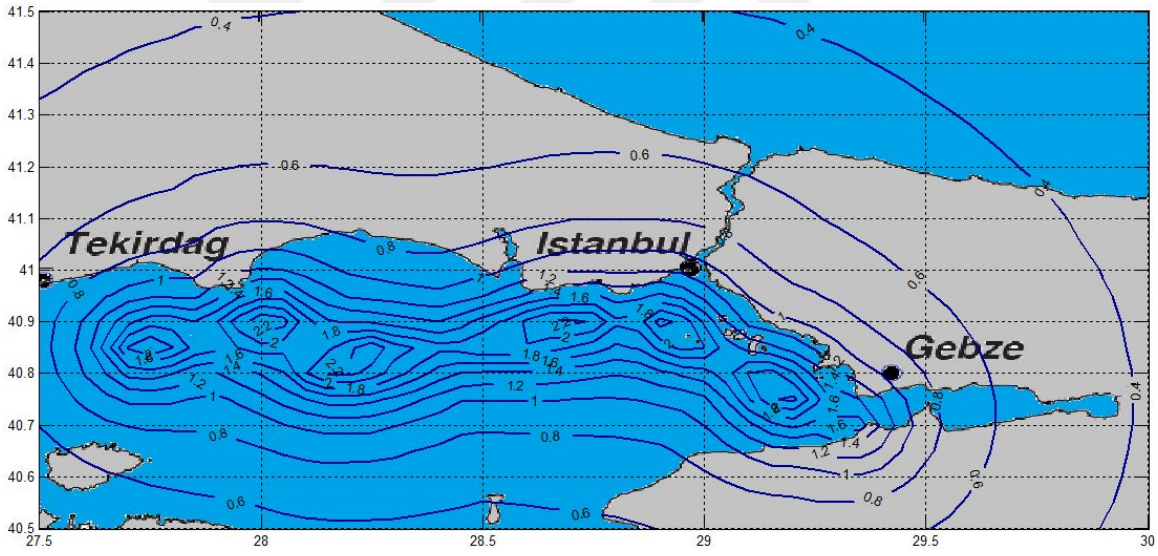

Figure A.8. Vs30 = 200m/sec and Using CB08 Attenuation Relationship SA at 0.3sec map with 2475 Years Return Period.

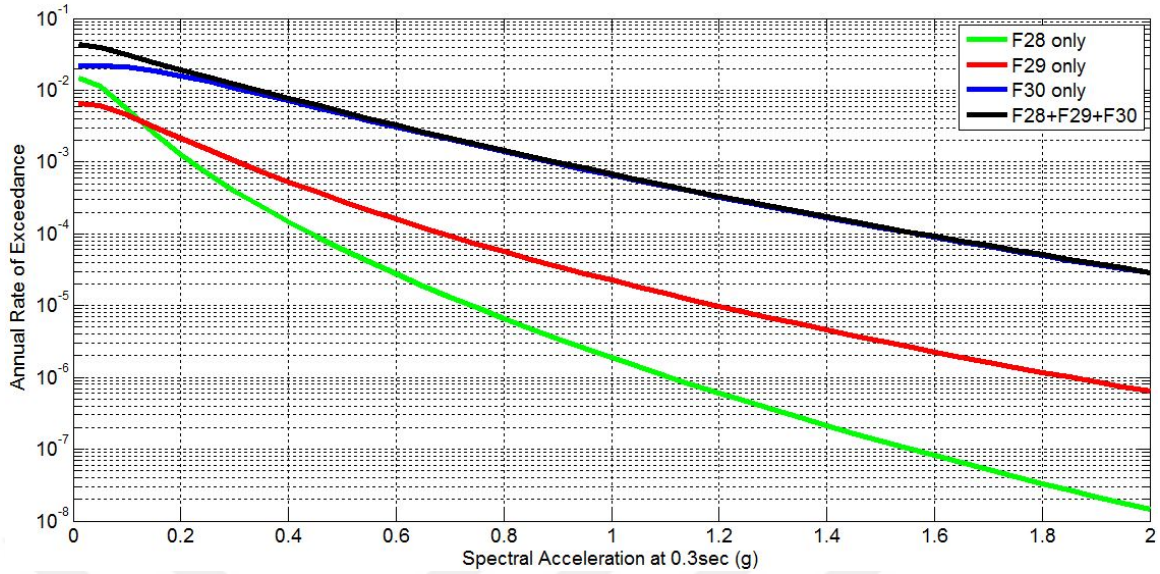

Figure A.9. Vs30 = 200m/sec and Using CB08 Attenuation Relationship Seismic Hazard Curve for SA at 0.3sec at Kadiköy District Considering the Fault Effects.

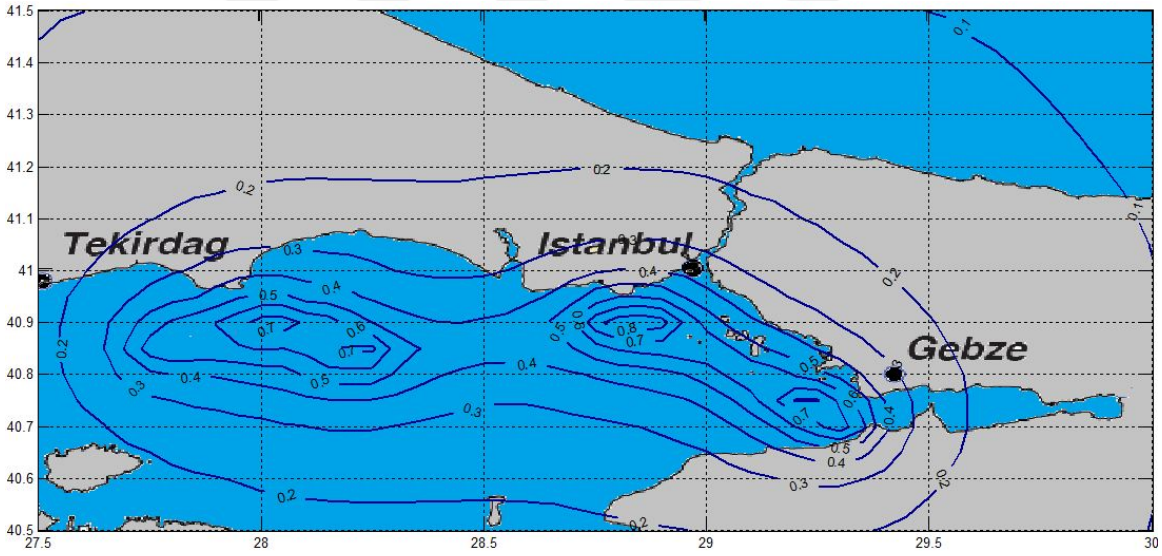

Figure A.10. Vs30 = 200m/sec and Using CB08 Attenuation Relationship SA at 1.0sec map with 475 Years Return Period.

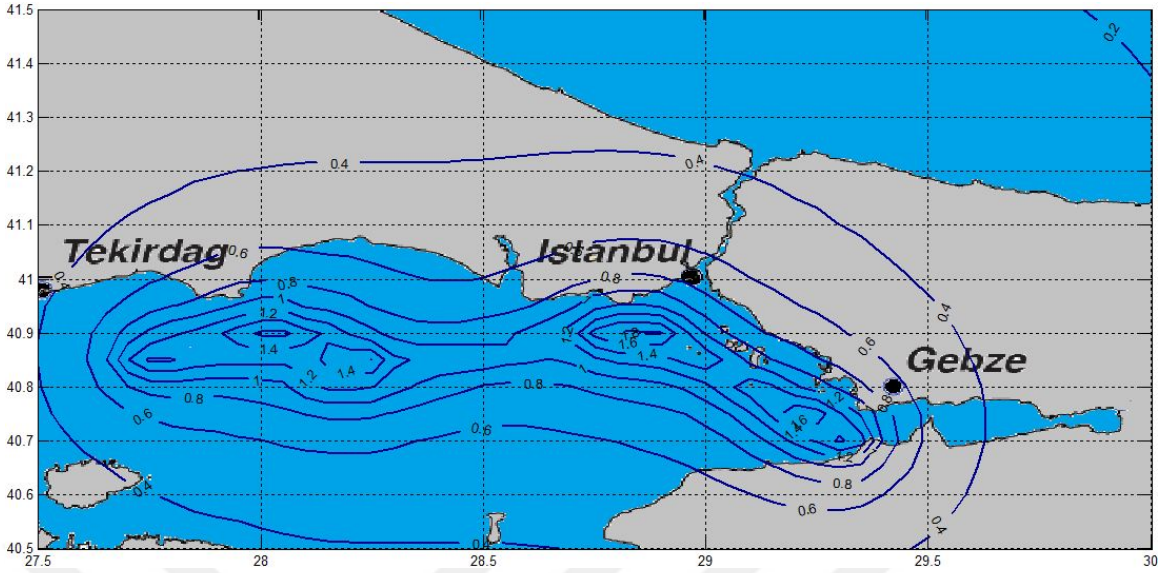

Figure A.11. Vs30 = 200m/sec and Using CB08 Attenuation Relationship SA at 1.0sec map with 2475 Years Return Period.

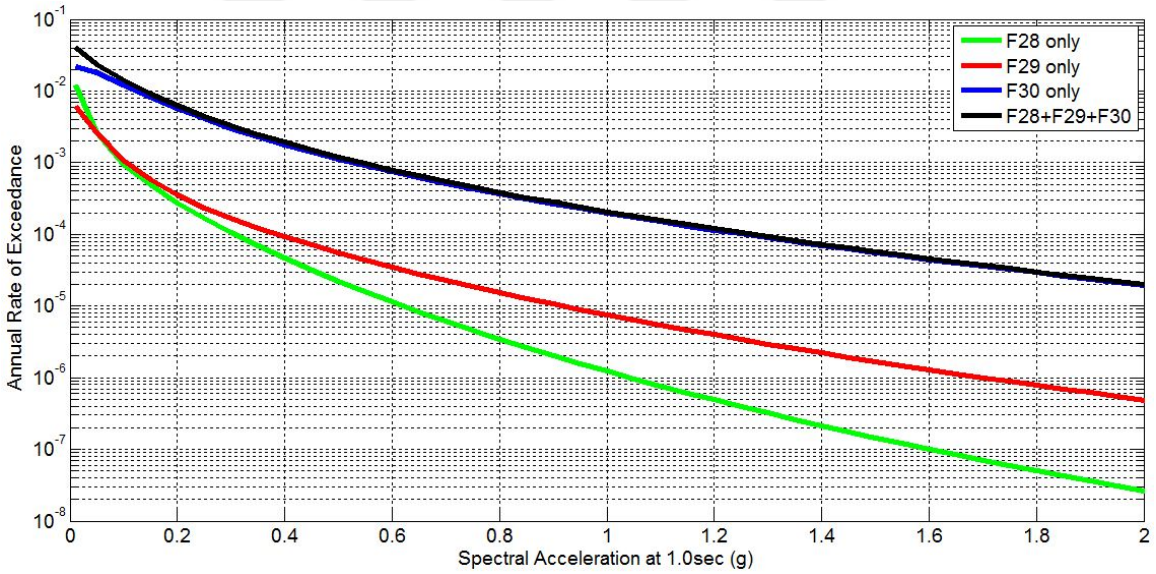

Figure A.12. Vs30 = 200m/sec and Using CB08 Attenuation Relationship Seismic Hazard Curve for SA at 1.0sec at Kadiköy District Considering the Fault Effects.

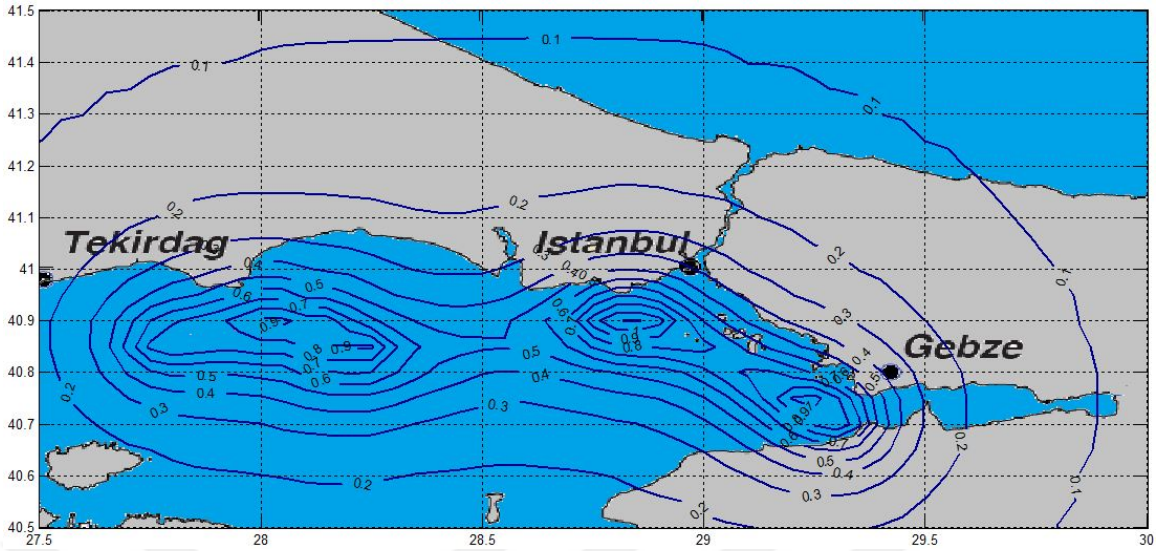

Figure A.13. Vs30 = 600m/sec and Using CB08 Attenuation Relationship PGA map with 475 Years Return Period.

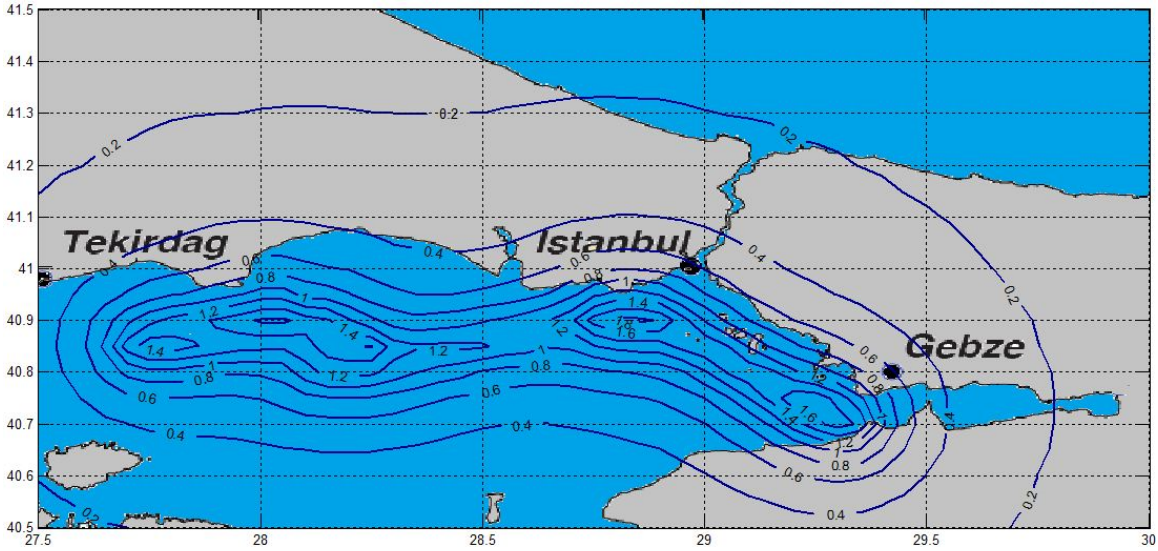

Figure A.14. Vs30 = 600m/sec and Using CB08 Attenuation Relationship PGA map with 2475 Years Return Period.

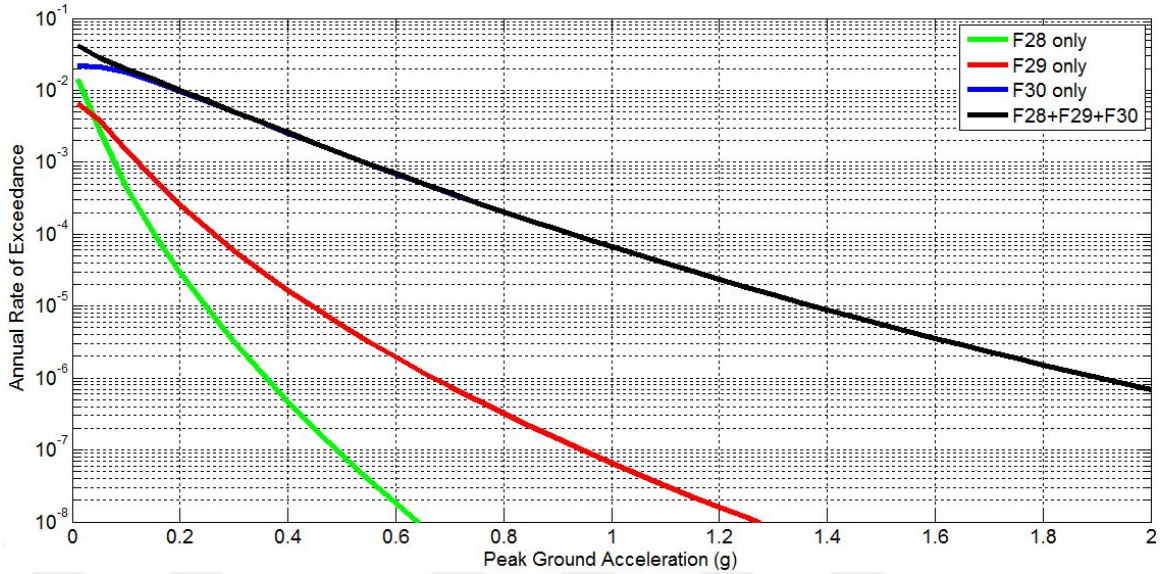

Figure A.15. Vs30 = 600m/sec and Using CB08 Attenuation Relationship Seismic Hazard Curve for PGA at Kadiköy District Considering the Fault Effects.

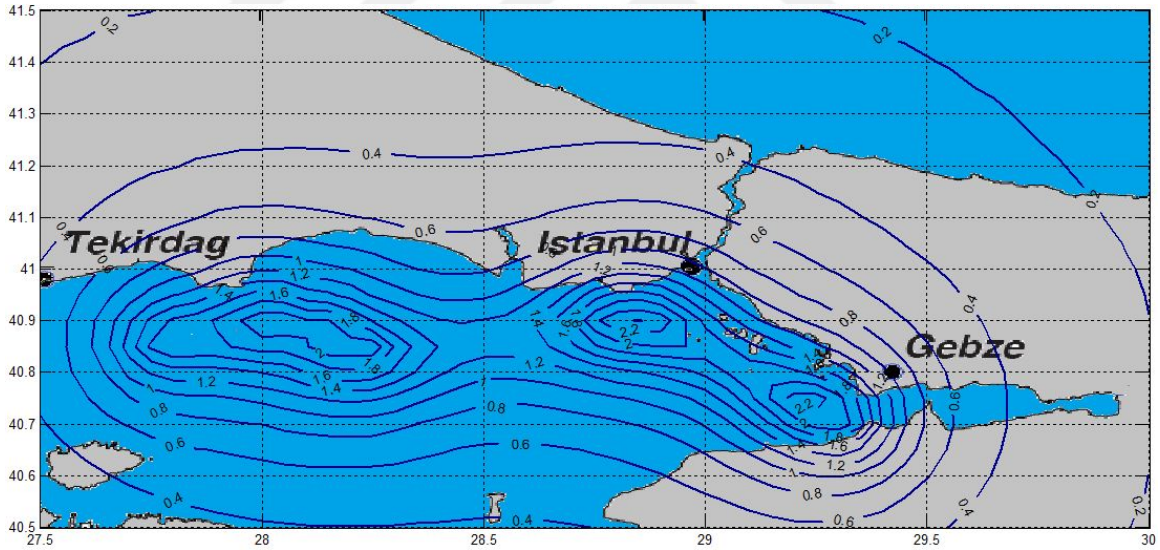

Figure A.16. Vs30 = 600m/sec and Using CB08 Attenuation Relationship SA at 0.2sec map with 475 years Return Period.

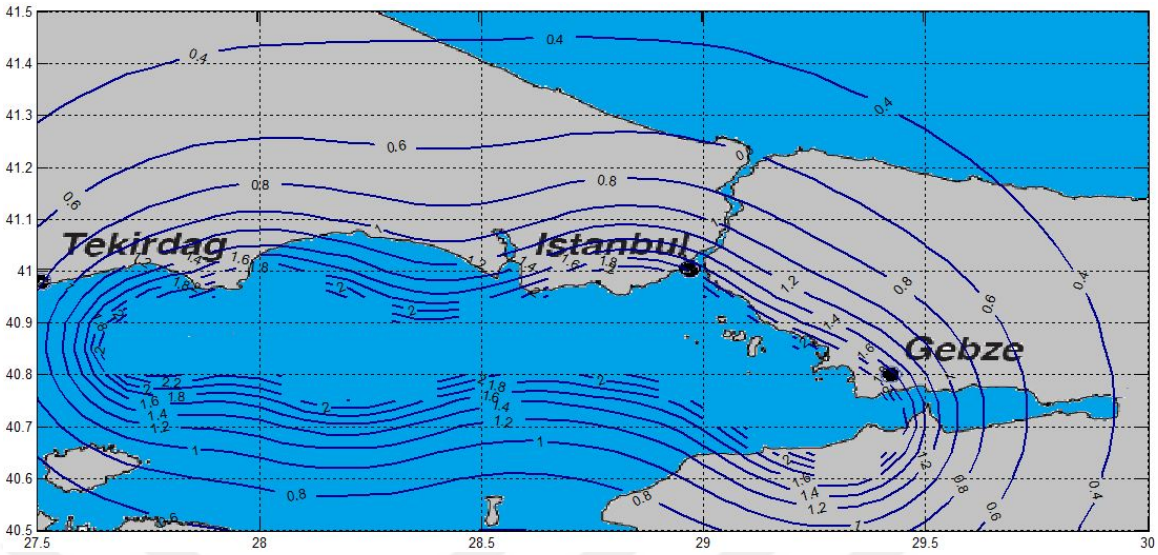

Figure A.17. Vs30 = 600m/sec and Using CB08 Attenuation Relationship SA at 0.2sec map with 2475 Years Return Period.

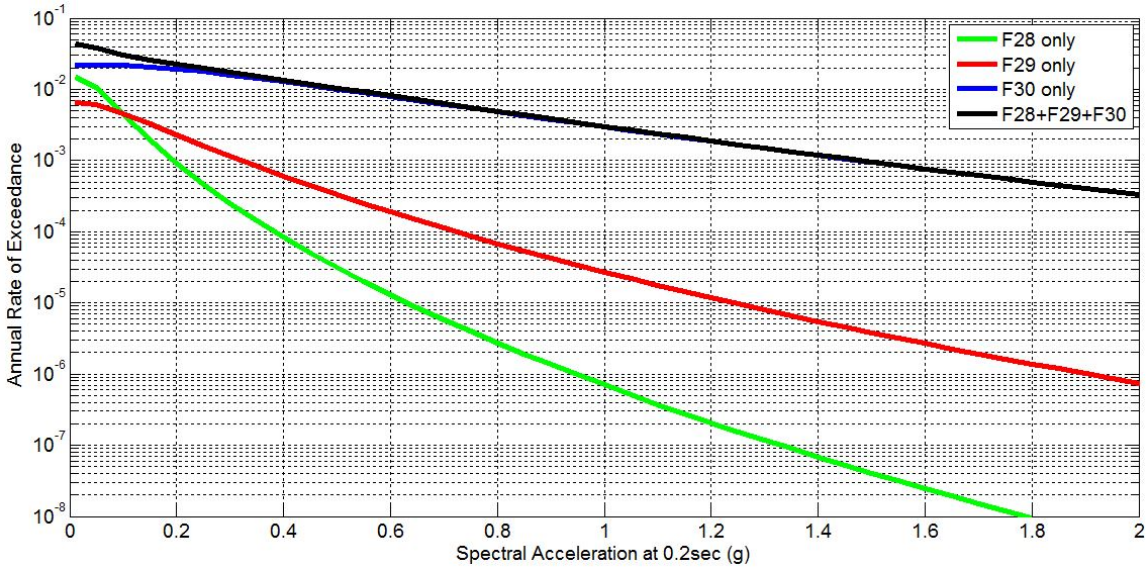

Figure A.18. Vs30 = 600m/sec and Using CB08 Attenuation Relationship Seismic Hazard Curve for SA at 0.2sec at Kadiköy District Considering the Fault Effects.

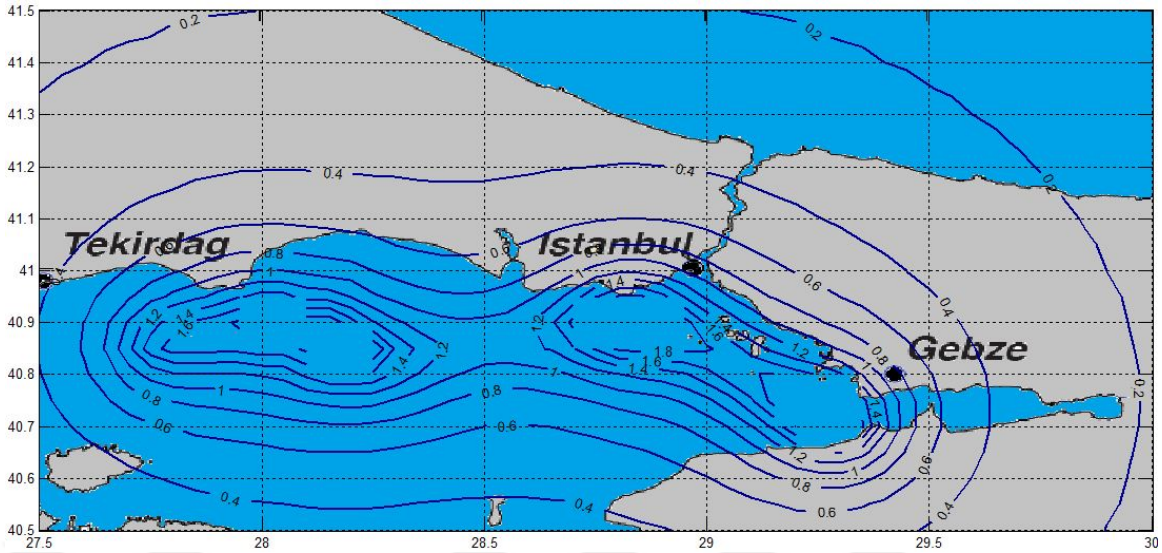

Figure A.19. Vs30 = 600m/sec and Using CB08 Attenuation Relationship SA at 0.3sec map with 475 years Return Period.

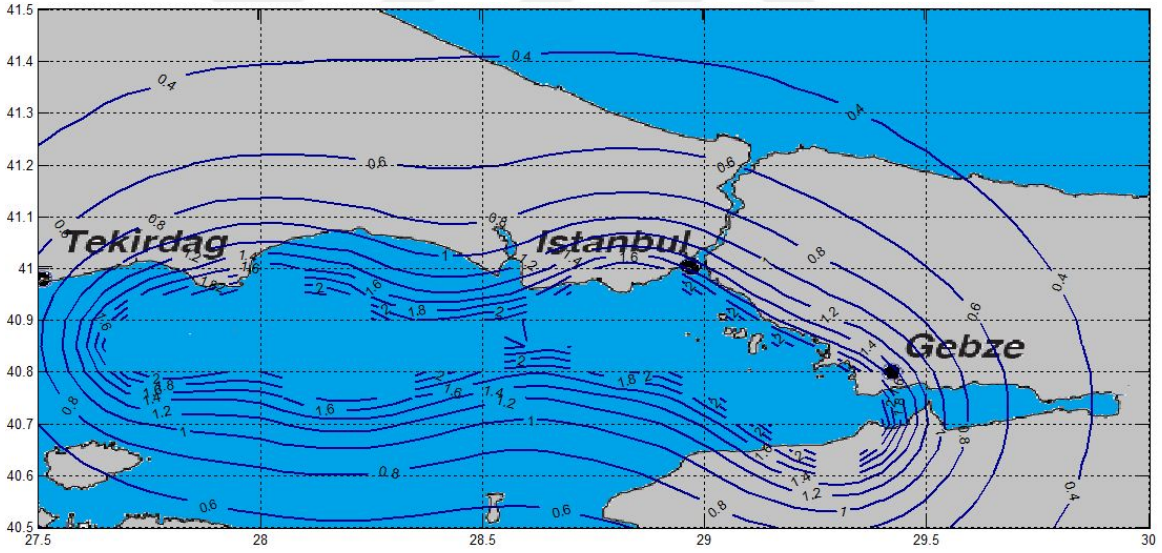

Figure A.20. Vs30 = 600m/sec and Using CB08 Attenuation Relationship SA at 0.3sec map with 2475 Years Return Period.

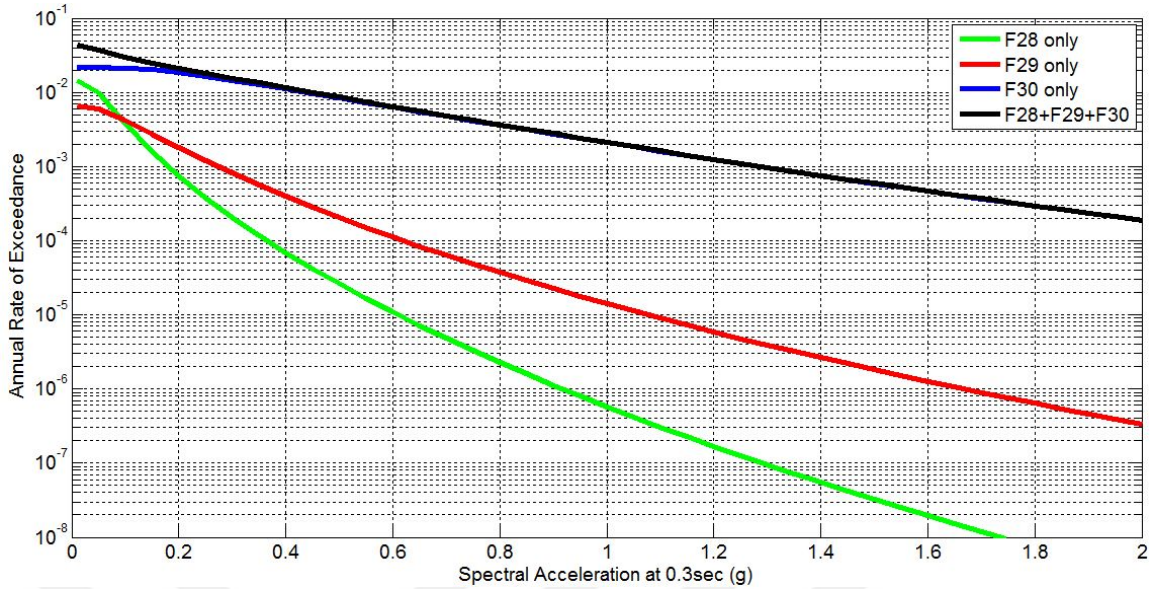

Figure A.21. Vs30 = 600m/sec and Using CB08 Attenuation Relationship Seismic Hazard Curve for SA at 0.3sec at Kadiköy District Considering the Fault Effects.

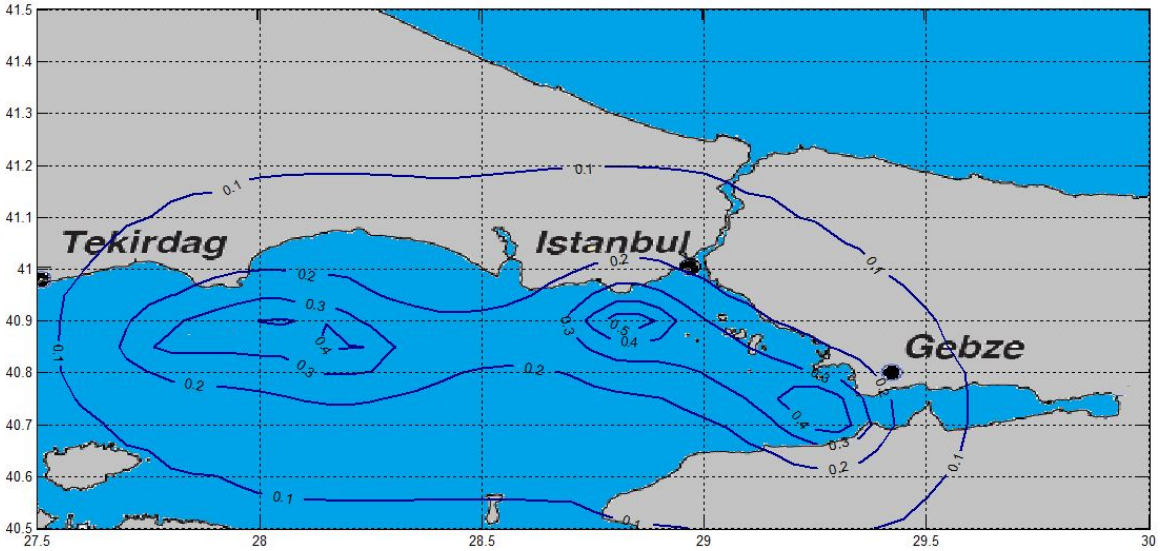

Figure A.22. Vs30 = 600m/sec and Using CB08 Attenuation Relationship SA at 1.0sec map with 475 Years Return Period.

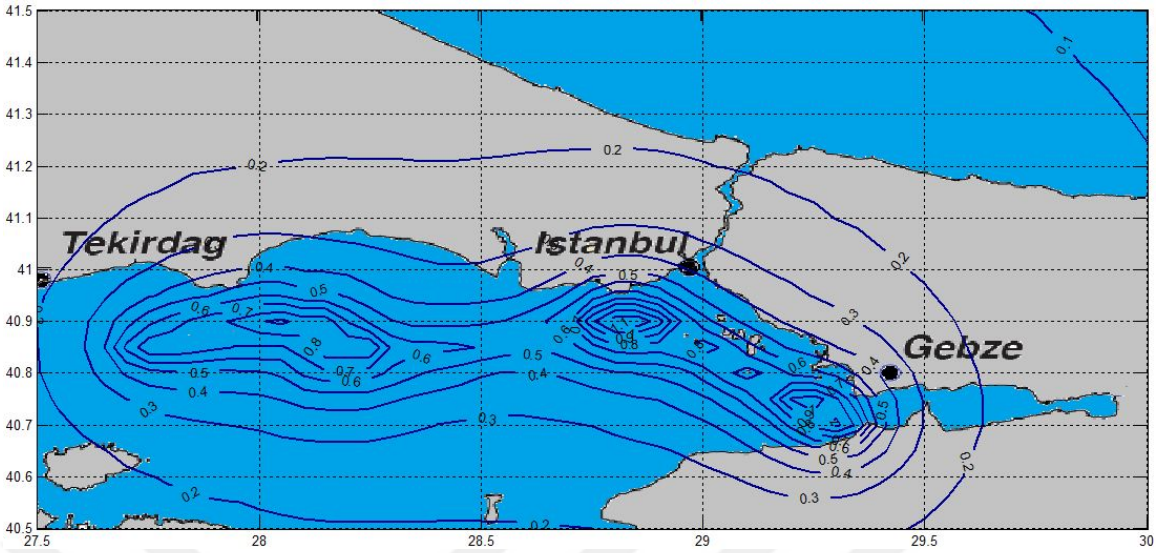

Figure A.23. Vs30 = 600m/sec and Using CB08 Attenuation Relationship SA at 1.0sec map with 2475 Years Return Period.

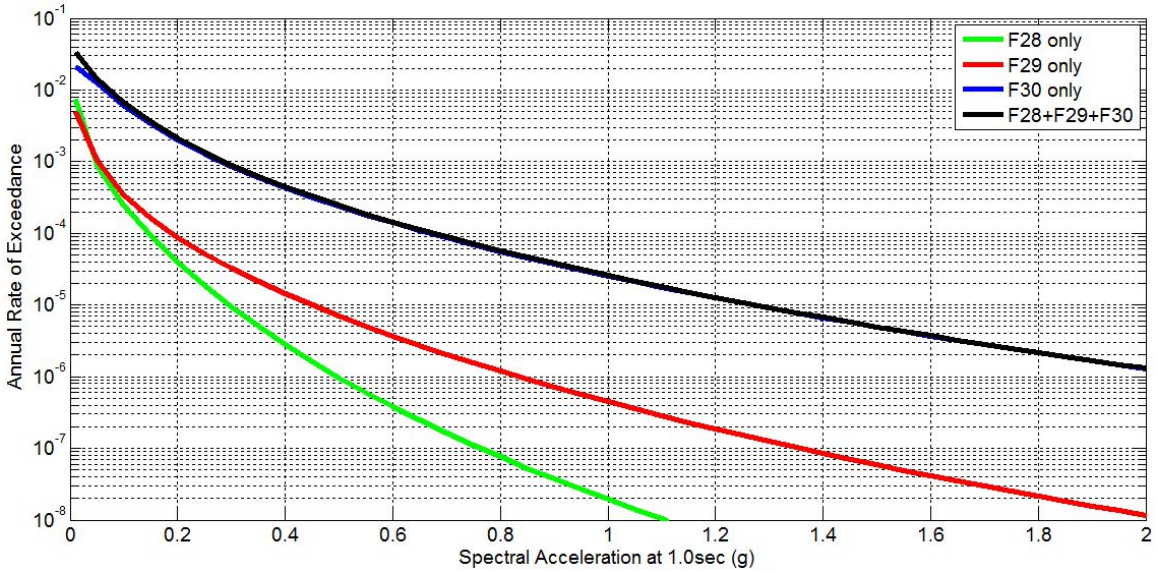

Figure A.24. Figure A.8. Vs30 = 600m/sec and Using CB08 Attenuation Relationship Seismic Hazard Curve for SA at 1.0sec at Kadiköy District Considering the Fault Effects.

APPENDIX B: COLLABORATIVE STUDY OF ISTANBUL METROPOLITAN

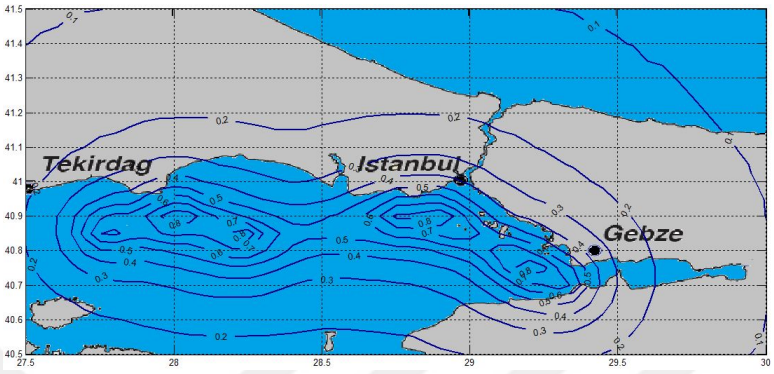

Figure B.1. PGA map for 475 Years Return Period - İstanbul Metropolitan Municipality and OYO International Company Study.

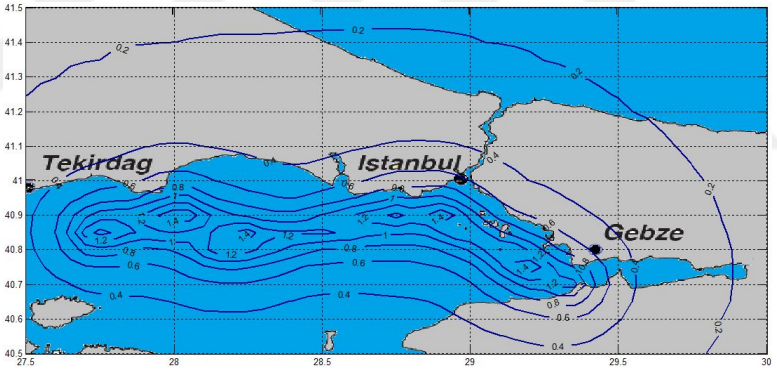

Figure B.2. PGA map for 2475 Years Return Period - İstanbul Metropolitan Municipality and OYO International Company Study.

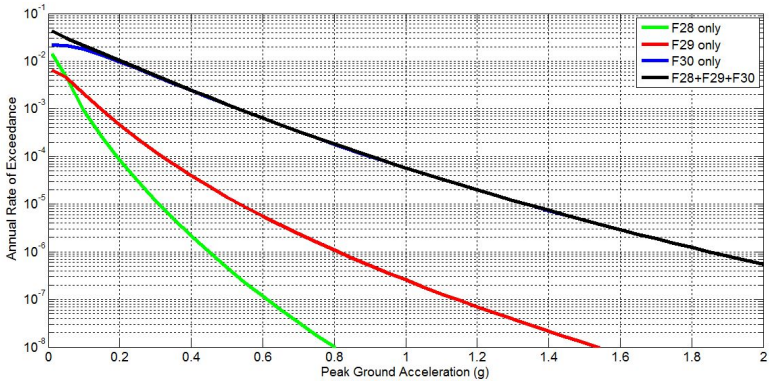

Figure B.3. Spectral Acceleration at 0.2sec map for 475 Years Return Period - İstanbul Metropolitan Municipality and OYO International Company Study.

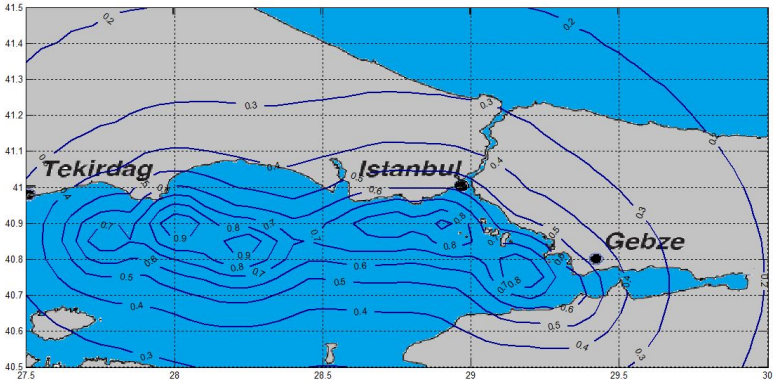

Figure B.4. Spectral Acceleration at 0.2sec map for 2475 Years Return Period - İstanbul Metropolitan Municipality and OYO International Company Study.

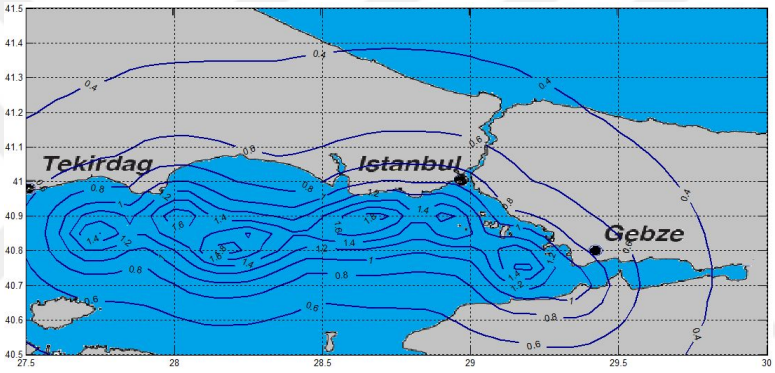

Figure B.5. Spectral Acceleration at 1.0sec map for 475 Years Return Period - İstanbul Metropolitan Municipality and OYO International Company Study.

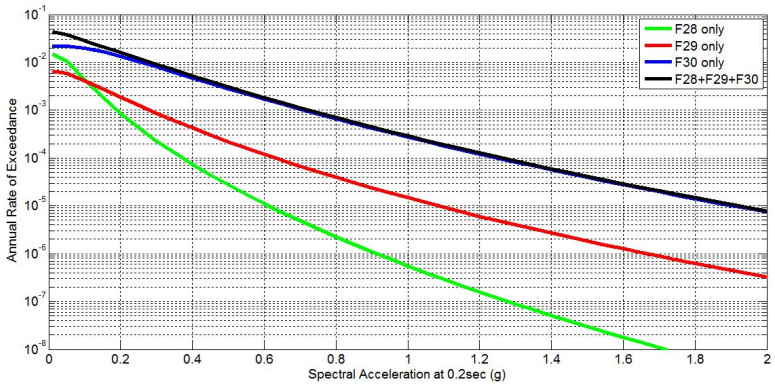

Figure B.6. Spectral Acceleration at 1.0sec map for 2475 Years Return Period - İstanbul Metropolitan Municipality and OYO International Company Study.

APPENDIX C: SEISMIC HAZARD MAPS FOR MARMARA REGION

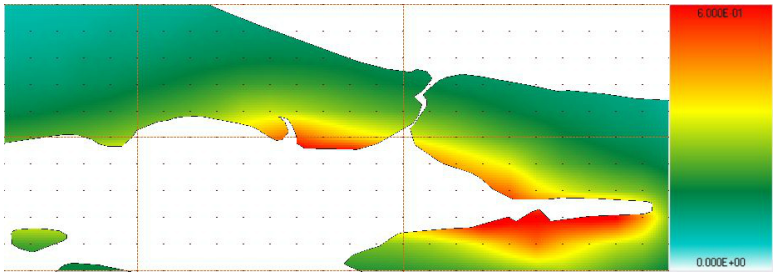

Figure C.1. PGA map for 475 Years Return Period - CRISIS2007.

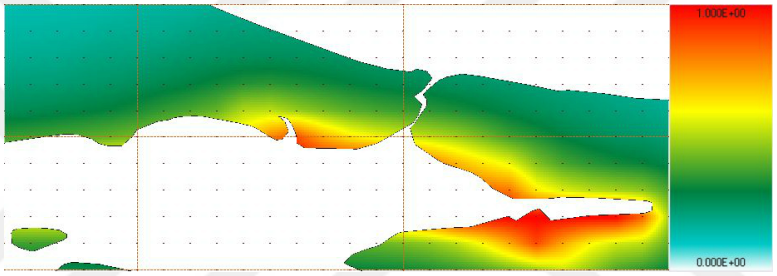

Figure C.2. PGA map for 2475 Years Return Period - CRISIS2007.

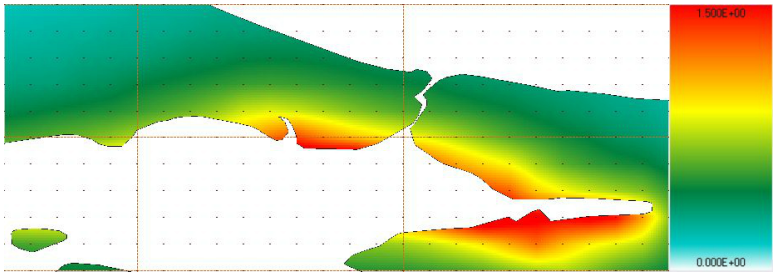

Figure C.3. Spectral Acceleration at 0.2sec map for 475 Years Return Period - CRISIS 2007.

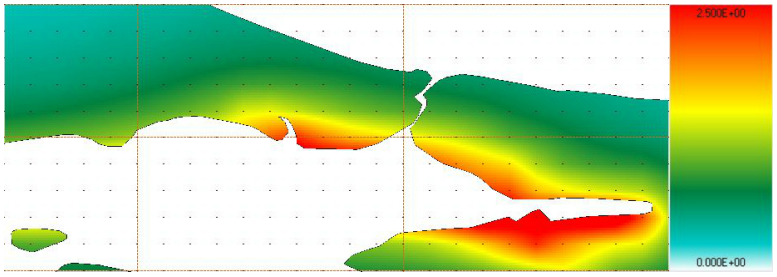

Figure C.4. Spectral Acceleration at 0.2sec map for 2475 Years Return Period - CRISIS 2007.

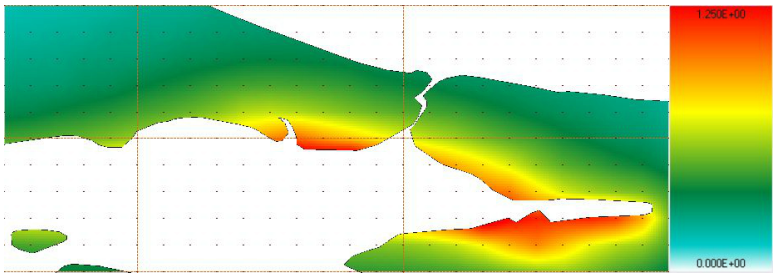

Figure C.5. Spectral Acceleration at 0.3sec map for 475 Years Return Period - CRISIS 2007.

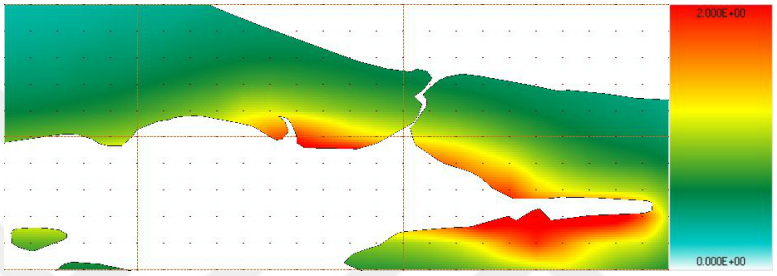

Figure C.6. Spectral Acceleration at 0.3sec map for 2475 Years Return Period - CRISIS 2007.

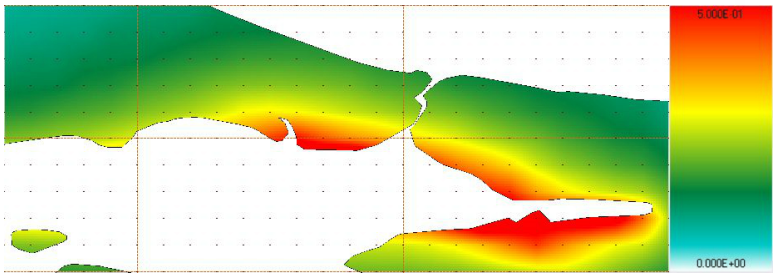

Figure C.7. Spectral Acceleration at 1.0sec map for 475 Years Return Period - CRISIS 2007.

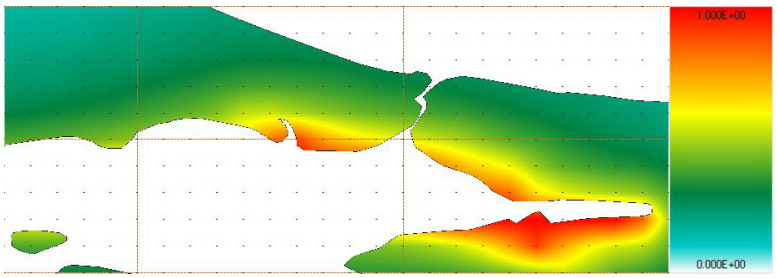

Figure C.8. Spectral Acceleration at 1.0sec map for 2475 Years Return Period - CRISIS 2007.

APPENDIX D: TIME HISTORY AND RESPONSE SPECTRUM PLOTS

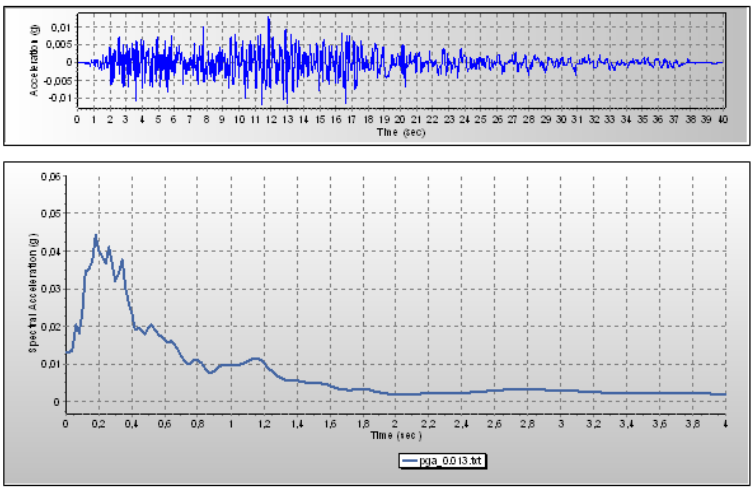

Figure D.1. PGA=0.013g (a)Acceleration-Time Graph (b)Spectral Acceleration-Time Graph.

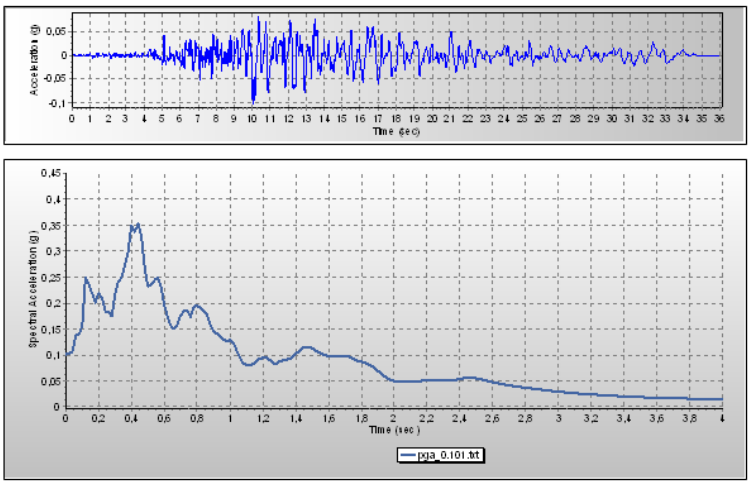

Figure D.2. PGA=0.101g (a)Acceleration-Time Graph (b)Spectral Acceleration-Time Graph.

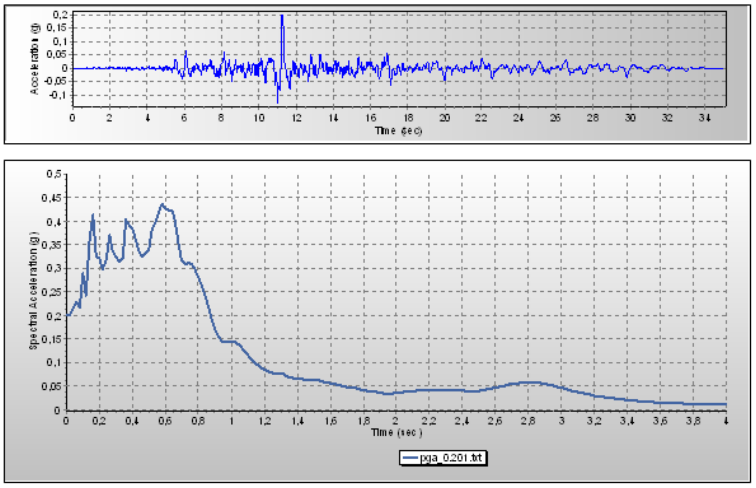

Figure D.3. PGA=0.201g (a)Acceleration-Time Graph (b)Spectral Acceleration-Time Graph.

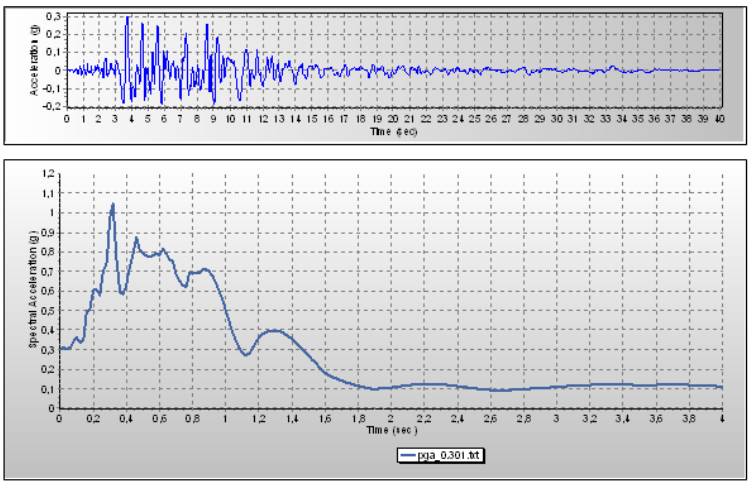

Figure D.4. PGA=0.301g (a)Acceleration-Time Graph (b)Spectral Acceleration-Time Graph.

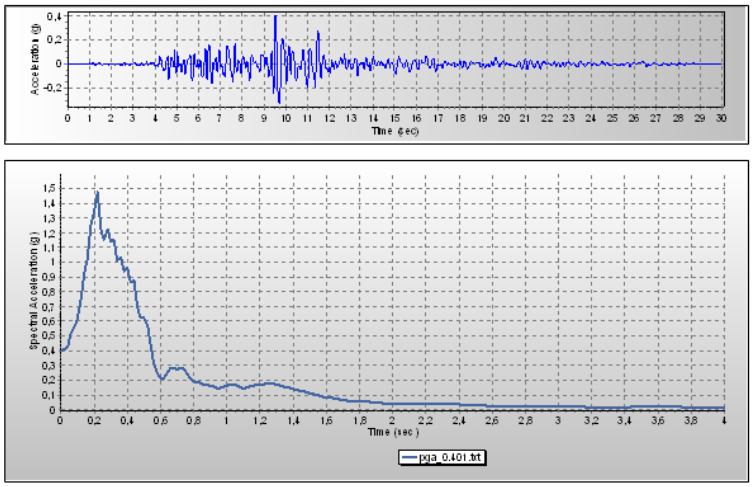

Figure D.5. PGA=0.401g (a)Acceleration-Time Graph (b)Spectral Acceleration-Time Graph.

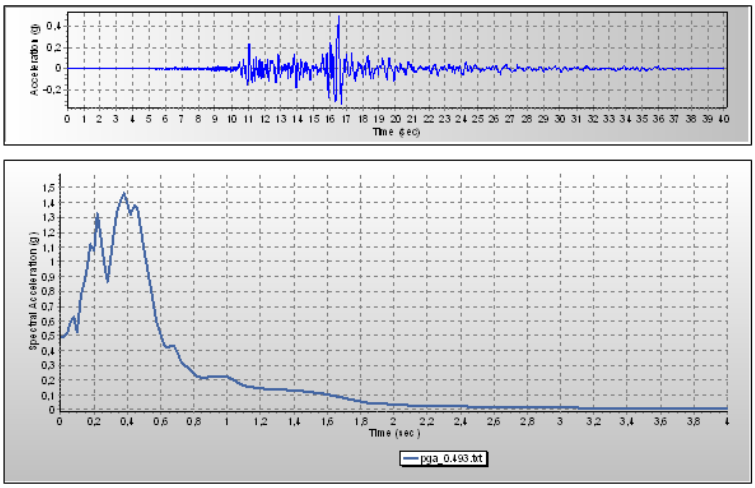

Figure D.6. PGA=0.493g (a)Acceleration-Time Graph (b)Spectral Acceleration-Time Graph.

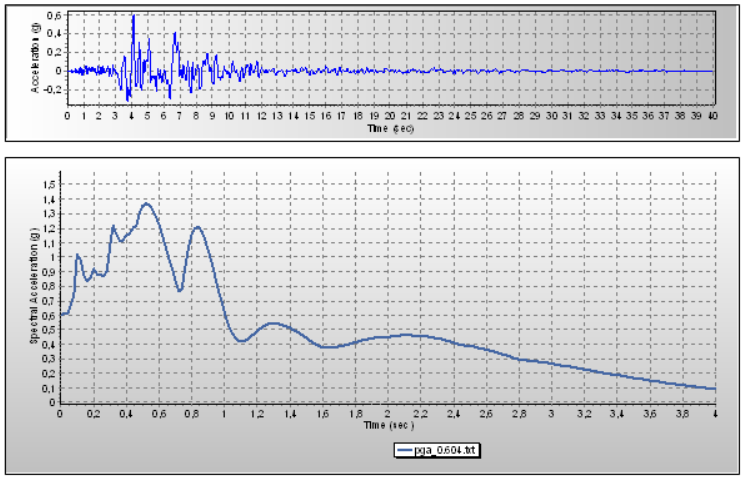

Figure D.7. PGA=0.604g (a)Acceleration-Time Graph (b)Spectral Acceleration-Time Graph.

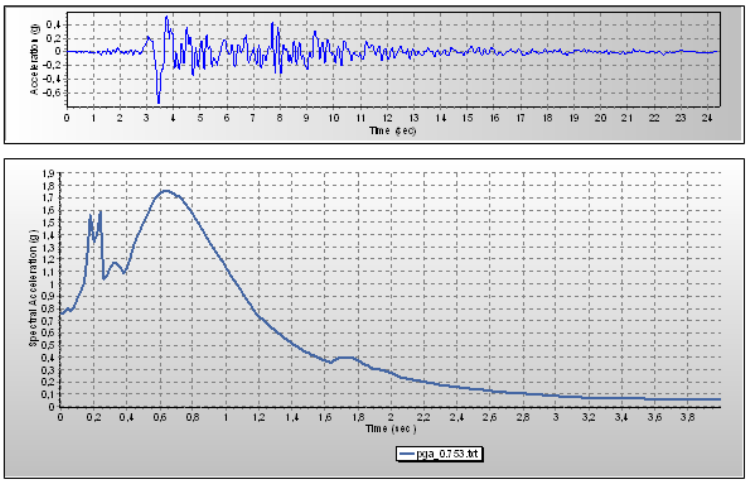

Figure D.8. PGA=0.753g (a)Acceleration-Time Graph (b)Spectral Acceleration-Time Graph.

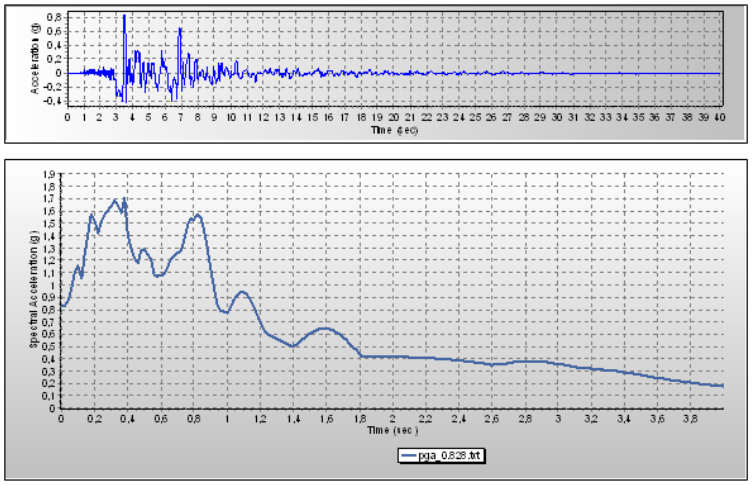

Figure D.9. PGA=0.828g (a)Acceleration-Time Graph (b)Spectral Acceleration-Time Graph.

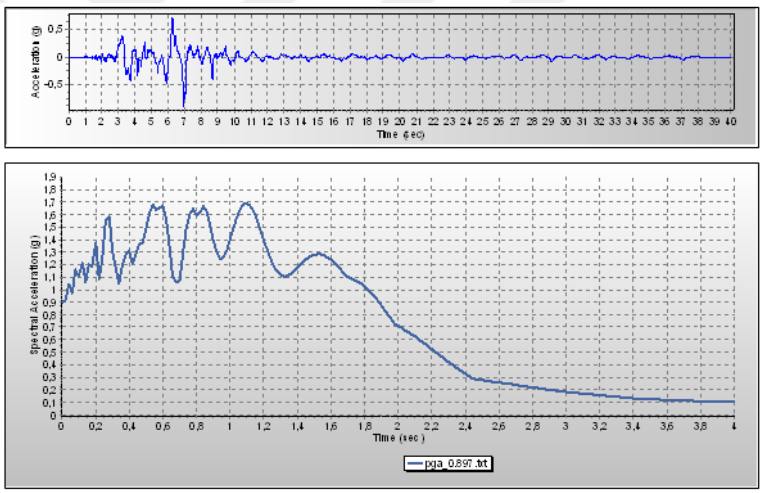

Figure D.10. PGA=0.897g (a) Acceleration-Time Graph (b)Spectral Acceleration-Time Graph.

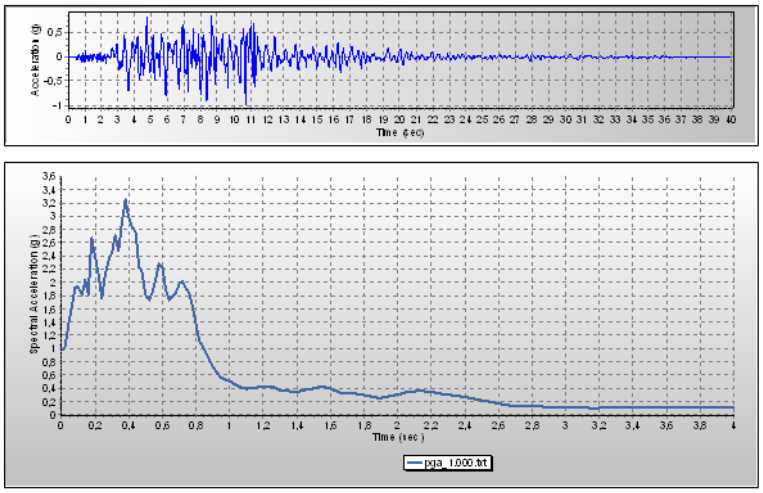

Figure D.11. PGA=1.000g (a) Acceleration-Time Graph (b)Spectral Acceleration-Time Graph.

APPENDIX E: GROUND MOTION INTENSITY OF ISTANBUL DISTRICTS

Table E.1. Ground Motion Intensities of İstanbul Districts with 475 Years Return Period.

	Return Period 2457 years (%2 Exceedance in 50 years											
	Peak Grond Accelation (g)			Spectral Acceleration 0.2 sec (g)			Spectral Acceleration 0.3 sec (g)			Spectral Acceleration 1.0 sec (g)		
	Shear Velocity			Shear Velocity			Shear Velocity			Shear Velocity		
	200 m/s	400 m/s	600 m/s	200 m/s	400 m/s	600 m/s	200 m/s	400 m/s	600 m/s	200 m/s	400 m/s	600 m/s
Adalar	0.60	0.68	0.67	0.68	1.31	1.65	0.89	1.38	1.52	0.54	0.38	0.30
Arnavutköy	0.20	0.19	0.18	0.34	0.44	0.45	0.39	0.43	0.40	0.20	0.13	0.10
Atasehir	0.31	0.31	0.30	0.45	0.71	0.80	0.55	0.69	0.70	0.29	0.20	0.15
Avcilar	0.41	0.42	0.41	0.59	0.94	1.09	0.70	0.91	0.95	0.36	0.25	0.19
Bagcilar	0.34	0.35	0.34	0.49	0.78	0.91	0.58	0.77	0.80	0.31	0.22	0.17
Bahçelievler	0.44	0.49	0.49	0.59	1.02	1.28	0.71	1.04	1.15	0.41	0.29	0.23
Bakirköy	0.44	0.48	0.47	0.60	1.02	1.23	0.72	1.02	1.09	0.40	0.28	0.22
Basaksehir	0.27	0.27	0.25	0.43	0.61	0.67	0.50	0.59	0.59	0.26	0.17	0.14
Bayrampasa	0.33	0.34	0.33	0.49	0.77	0.89	0.58	0.75	0.78	0.31	0.21	0.16
Besiktas	0.28	0.28	0.27	0.43	0.65	0.72	0.52	0.63	0.62	0.27	0.18	0.14
Beykoz	0.19	0.19	0.17	0.33	0.43	0.44	0.38	0.42	0.39	0.19	0.13	0.10
Beylikdüzü	0.38	0.38	0.36	0.57	0.87	0.98	0.67	0.83	0.84	0.34	0.23	0.18
Beyoglu	0.32	0.33	0.31	0.48	0.74	0.84	0.57	0.72	0.73	0.30	0.20	0.15
Büyükçekmece	0.27	0.26	0.24	0.43	0.61	0.65	0.51	0.58	0.56	0.26	0.17	0.14
Çatalca	0.20	0.19	0.18	0.34	0.45	0.47	0.41	0.44	0.42	0.21	0.14	0.10
Çekmeköy	0.22	0.21	0.20	0.34	0.49	0.53	0.41	0.48	0.47	0.21	0.14	0.11
Esenler	0.34	0.35	0.34	0.49	0.78	0.91	0.58	0.77	0.80	0.31	0.22	0.17
Esenyurt	0.30	0.30	0.29	0.48	0.69	0.77	0.56	0.67	0.66	0.28	0.19	0.15
Eyüp	0.22	0.22	0.20	0.37	0.50	0.53	0.43	0.49	0.47	0.22	0.14	0.11
Fatih	0.42	0.44	0.43	0.58	0.96	1.13	0.70	0.95	0.99	0.37	0.25	0.20
Gaziosmanpasa	0.33	0.34	0.33	0.49	0.77	0.89	0.58	0.75	0.78	0.31	0.21	0.16
Güngören	0.44	0.49	0.49	0.59	1.02	1.28	0.71	1.04	1.15	0.41	0.29	0.23
Kadiköy	0.42	0.45	0.43	0.58	0.98	1.15	0.71	0.96	1.00	0.38	0.26	0.20
Kagithane	0.30	0.31	0.29	0.46	0.70	0.78	0.55	0.68	0.68	0.29	0.19	0.15
Kartal	0.38	0.40	0.38	0.51	0.88	1.03	0.64	0.87	0.90	0.35	0.24	0.19
Küçükçekmece	0.43	0.47	0.46	0.60	0.99	1.20	0.72	0.99	1.06	0.39	0.27	0.21
Maltepe	0.33	0.34	0.33	0.46	0.76	0.89	0.57	0.76	0.79	0.32	0.22	0.17
Pendik	0.27	0.27	0.26	0.40	0.61	0.69	0.48	0.60	0.60	0.25	0.17	0.13
Sancaktepe	0.25	0.25	0.23	0.38	0.56	0.62	0.46	0.55	0.55	0.24	0.16	0.13
Sariyer	0.22	0.21	0.19	0.36	0.49	0.51	0.42	0.47	0.45	0.21	0.14	0.11
Silivri	0.29	0.30	0.28	0.44	0.67	0.76	0.52	0.66	0.67	0.28	0.19	0.14
Sultanbeyli	0.29	0.29	0.28	0.42	0.66	0.75	0.51	0.65	0.65	0.27	0.19	0.14
Sultangazi	0.25	0.25	0.24	0.40	0.57	0.62	0.48	0.56	0.54	0.24	0.16	0.13
Sile	0.13	0.12	0.11	0.24	0.27	0.27	0.28	0.27	0.25	0.14	0.09	0.07
Sisli	0.32	0.33	0.31	0.48	0.74	0.84	0.57	0.72	0.73	0.30	0.20	0.15
Tuzla	0.34	0.37	0.37	0.46	0.80	0.97	0.57	0.80	0.86	0.32	0.22	0.17
Ümraniye	0.31	0.31	0.30	0.45	0.71	0.80	0.55	0.69	0.70	0.29	0.20	0.15
Üsküdar	0.34	0.35	0.33	0.50	0.79	0.90	0.60	0.77	0.78	0.32	0.21	0.17
Zeytinburnu	0.44	0.48	0.47	0.60	1.02	1.23	0.72	1.02	1.09	0.40	0.28	0.22

Table E.2. Ground Motion Intensities of İstanbul Districts with 475 Years Return Period.

	Return Period 2457 years (%2 Exceedance in 50 years											
	Peak Grond Accelation (g)			Spectral Acceleration 0.2 sec (g)			Spectral Acceleration 0.3 sec (g)			Spectral Acceleration 1.0 sec (g)		
	Shear Velocity			Shear Velocity			Shear Velocity			Shear Velocity		
	200 m/s	400 m/s	600 m/s	200 m/s	400 m/s	600 m/s	200 m/s	400 m/s	600 m/s	200 m/s	400 m/s	600 m/s
Adalar	1.04	1.18	1.18	1.14	2.29	2.54	1.53	2.25	2.38	1.14	0.82	0.64
Arnavutköy	0.31	0.29	0.28	0.53	0.69	0.73	0.63	0.69	0.65	0.43	0.28	0.21
Atasehir	0.48	0.49	0.47	0.71	1.13	1.29	0.87	1.12	1.13	0.61	0.41	0.31
Avcilar	0.65	0.68	0.66	1.01	1.57	1.84	1.17	1.53	1.59	0.75	0.51	0.40
Bagcilar	0.52	0.55	0.54	0.79	1.25	1.49	0.94	1.25	1.32	0.65	0.45	0.35
Bahçelievler	0.69	0.78	0.78	0.98	1.67	2.01	1.16	1.71	1.93	0.84	0.60	0.47
Bakirköy	0.70	0.76	0.75	0.99	1.67	2.00	1.19	1.68	1.82	0.82	0.57	0.44
Basaksehir	0.42	0.42	0.40	0.68	0.98	1.09	0.80	0.96	0.96	0.54	0.36	0.28
Bayrampasa	0.52	0.54	0.52	0.79	1.24	1.45	0.94	1.23	1.28	0.64	0.44	0.34
Besiktas	0.44	0.44	0.42	0.69	1.04	1.16	0.83	1.02	1.01	0.56	0.38	0.29
Beykoz	0.30	0.29	0.27	0.51	0.68	0.71	0.61	0.67	0.64	0.42	0.27	0.21
Beylikdüzü	0.61	0.61	0.59	0.97	1.45	1.64	1.12	1.39	1.40	0.69	0.47	0.36
Beyoglu	0.50	0.52	0.49	0.77	1.20	1.37	0.92	1.18	1.20	0.62	0.42	0.32
Büyükçekmece	0.42	0.40	0.38	0.68	0.97	1.05	0.81	0.94	0.91	0.54	0.36	0.28
Çatalca	0.31	0.30	0.28	0.54	0.71	0.74	0.64	0.70	0.67	0.44	0.29	0.22
Çekmeköy	0.34	0.33	0.31	0.54	0.77	0.83	0.65	0.76	0.74	0.46	0.30	0.23
Esenler	0.52	0.55	0.54	0.79	1.25	1.49	0.94	1.25	1.32	0.65	0.45	0.35
Esenyurt	0.48	0.48	0.45	0.78	1.13	1.25	0.91	1.09	1.09	0.59	0.39	0.30
Eyüp	0.35	0.34	0.32	0.58	0.80	0.86	0.69	0.78	0.76	0.47	0.31	0.24
Fatih	0.66	0.70	0.68	0.95	1.58	1.88	1.15	1.56	1.64	0.77	0.53	0.41
Gaziosmanpasa	0.52	0.54	0.52	0.79	1.24	1.45	0.94	1.23	1.28	0.64	0.44	0.34
Güngören	0.69	0.78	0.78	0.98	1.67	1.92	1.16	1.71	1.93	0.84	0.60	0.47
Kadiköy	0.67	0.71	0.69	0.92	1.60	1.85	1.15	1.59	1.65	0.79	0.54	0.42
Kagithane	0.47	0.48	0.46	0.73	1.12	1.27	0.88	1.10	1.10	0.59	0.40	0.31
Kartal	0.59	0.62	0.60	0.82	1.41	1.67	1.02	1.41	1.47	0.72	0.49	0.38
Küçükçekmece	0.69	0.74	0.73	1.02	1.64	1.96	1.19	1.65	1.79	0.80	0.56	0.44
Maltepe	0.51	0.54	0.52	0.71	1.21	1.44	0.89	1.22	1.27	0.65	0.44	0.34
Pendik	0.41	0.42	0.40	0.63	0.97	1.10	0.77	0.97	0.97	0.54	0.36	0.28
Sancaktepe	0.38	0.38	0.36	0.59	0.89	0.98	0.72	0.88	0.87	0.51	0.34	0.26
Sariyer	0.34	0.33	0.30	0.56	0.77	0.83	0.67	0.76	0.73	0.45	0.30	0.23
Silivri	0.45	0.46	0.44	0.69	1.06	1.22	0.83	1.06	1.08	0.58	0.39	0.30
Sultanbeyli	0.44	0.45	0.43	0.66	1.05	1.19	0.81	1.04	1.05	0.57	0.39	0.30
Sultangazi	0.39	0.39	0.37	0.63	0.92	1.01	0.76	0.90	0.88	0.51	0.34	0.26
Sile	0.21	0.19	0.18	0.38	0.44	0.44	0.45	0.45	0.41	0.30	0.19	0.15
Sisli	0.50	0.52	0.49	0.77	1.20	1.37	0.92	1.18	1.20	0.62	0.42	0.32
Tuzla	0.54	0.59	0.58	0.74	1.30	1.60	0.92	1.32	1.44	0.66	0.46	0.36
Ümraniye	0.48	0.49	0.47	0.71	1.13	1.29	0.87	1.12	1.13	0.61	0.41	0.31
Üsküdar	0.53	0.55	0.52	0.79	1.27	1.46	0.96	1.25	1.27	0.65	0.44	0.34
Zeytinburnu	0.70	0.76	0.75	0.99	1.67	2.00	1.19	1.68	1.82	0.82	0.57	0.44

APPENDIX F: PLASTIC ROTATION - TIME PLOTS FOR BEAMS

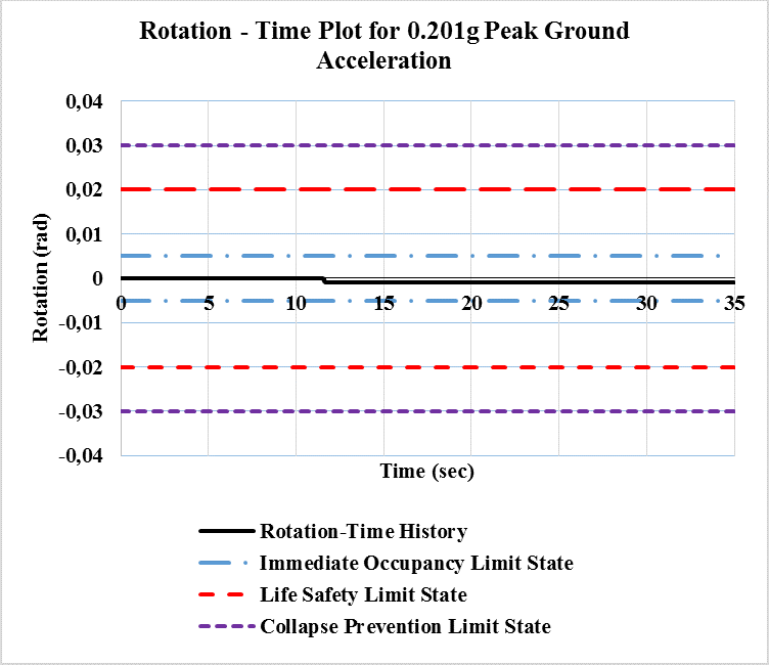

Figure F.1. Plastic Rotation-Time Plot for pga=0.201g.

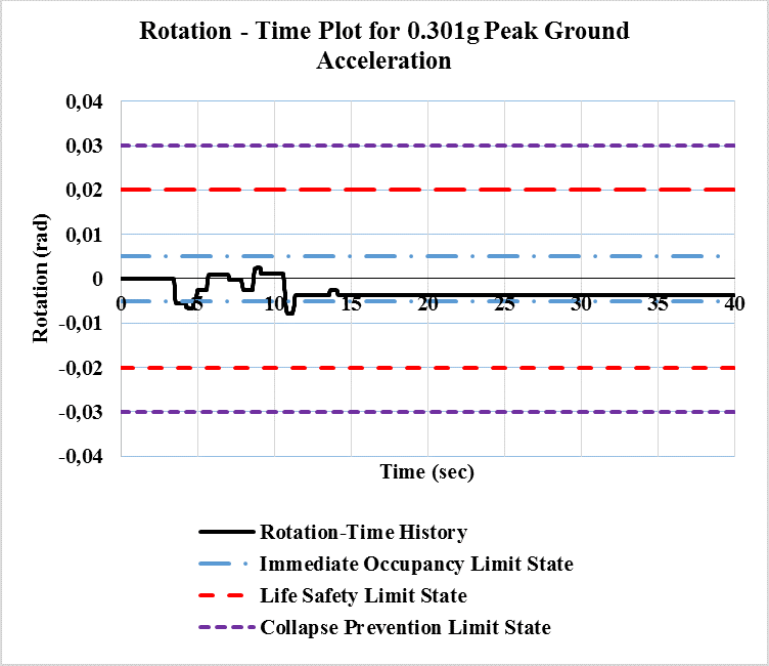

Figure F.2. Plastic Rotation-Time Plot for pga=0.301g.

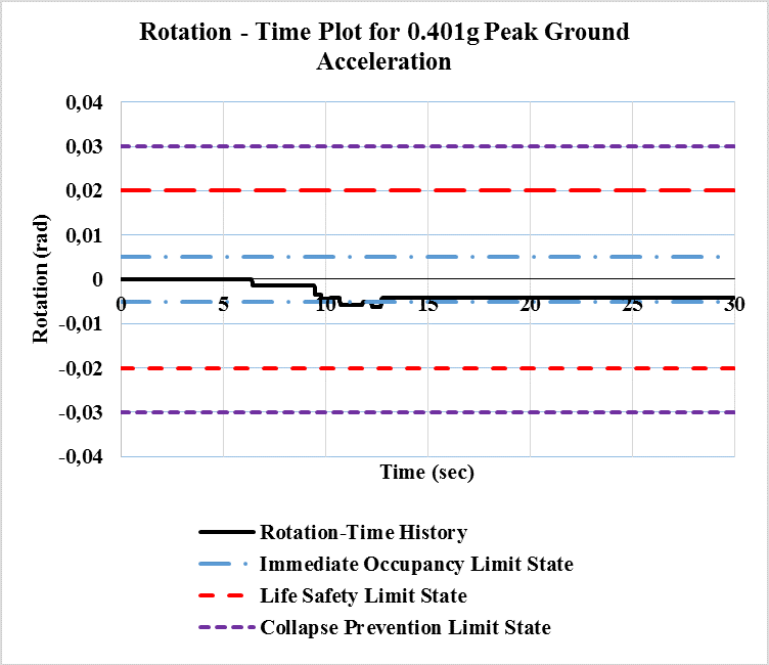

Figure F.3. Plastic Rotation-Time Plot for pga=0.401g.

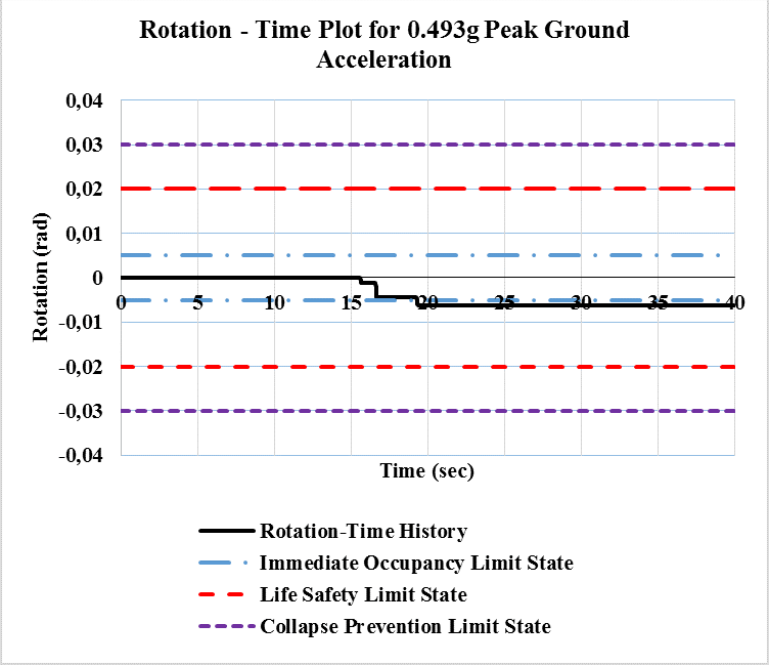

Figure F.4. Plastic Rotation-Time Plot for pga=0.493g.

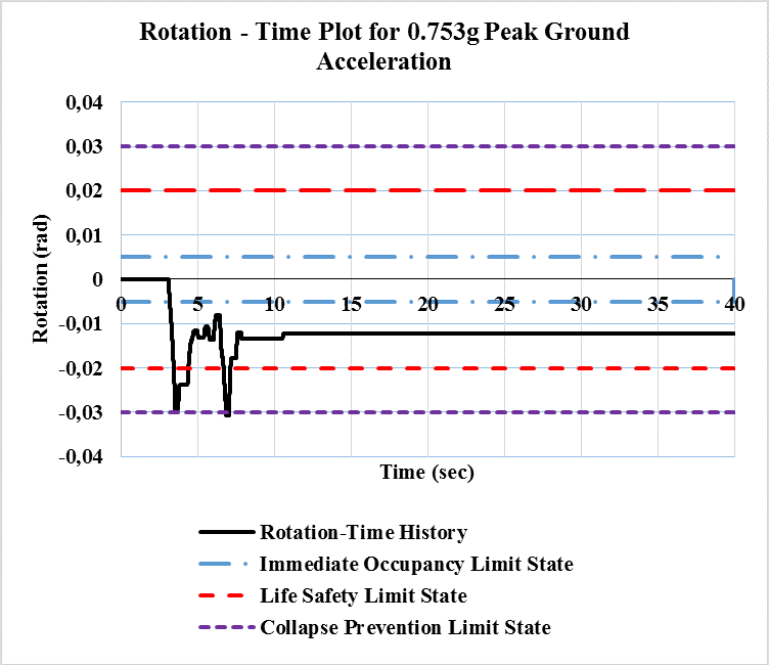

Figure F.5. Plastic Rotation-Time Plot for pga=0.753g.

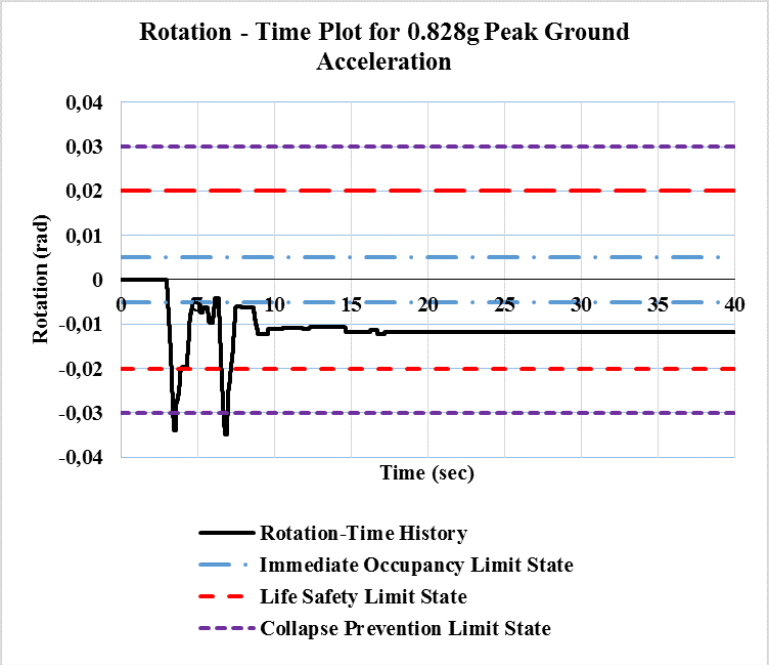

Figure F.6. Plastic Rotation-Time Plot for pga=0.828g.

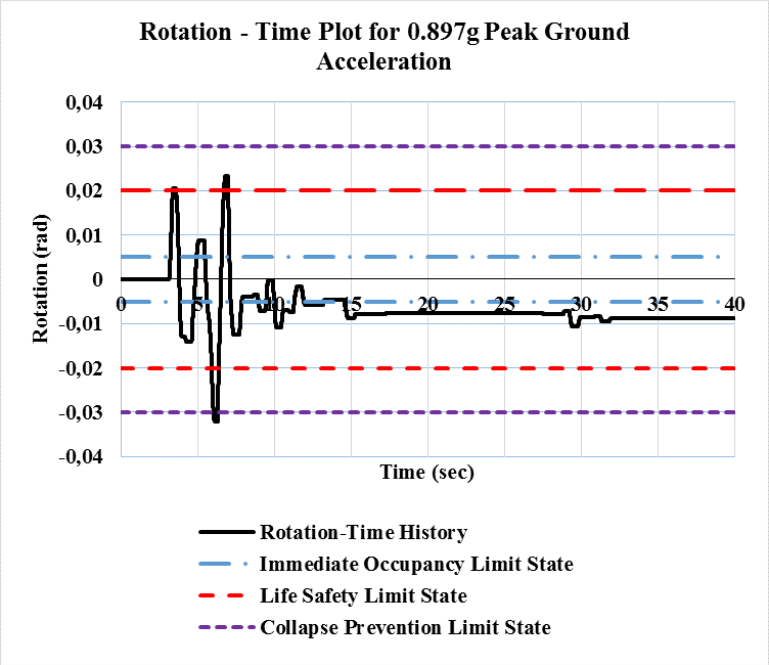

Figure F.7. Plastic Rotation-Time Plot for pga=0.897g.

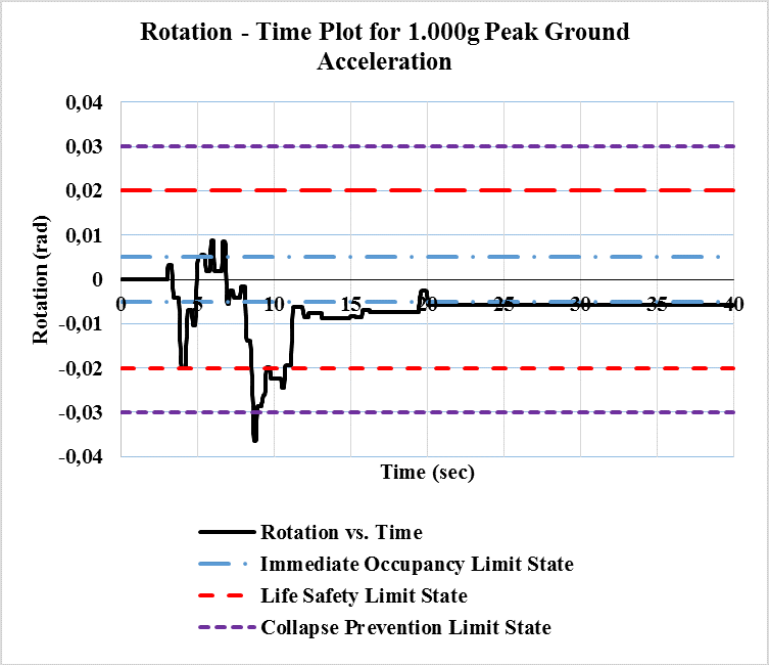

Figure F.8. Plastic Rotation-Time Plot for pga=1.000g.

REFERENCES

Abrahamson, N.A. and W.J. Silva, 2008, "Summary of the Abrahamson and Silva NGA Ground Motion Relations", *Earthquake Spectra*, Vol. 24, No 1, pp. 67-98.

Baker, J.W., 2008, "An Introduction to Probabilistic Seismic Hazard Analysis", *Probabilistic Seismic Hazard Analysis*.

Engineers, A.S. 2014, "Seismic Evaluation and Retrofit of Existing Buildings", *Virginia: American Society of Civil Engineers*.

Boore, D.M. and G. Atkinson, 2008, "Ground Motion Prediction Equations for the Average Horizontal Component of PGA, PGV, and 5%-Damped PSA at Spectral Eriods Between 0.01s and 10.0s", *Earthquake Spectra*, Vol. 24, No. 1, pp. 99-138.

Campbell, K. and Y. Bozorgnia, 2008, "NGA Ground Motion Model for the Geometric Mean Horizontal Component of PGA, PGV, PGD and 5% Damped Linear Elastic Response Spectra for Periods Ranging from 0.01to10s", *Earthquake Spectra*, Vol. 24, No. 1, pp. 139-171.

Convertito, V., A. Emolo, and A. Zollo, 1990, "Seismic-Hazard Assessment for a Characteristic Earthquake Scenario: An Integrated Probabilistic-Deterministic Method, *Napoli*.

Chiou, B. and R.Youngs, 2008, "An NGA Model for the Average Horizontal Component of Peak Ground motion and Response Spectra", *Earthquake Spectra*, Vol. 24, No. 1, pp. 173-215.

Demircioglu M. 2010, "Earthquake Hazard and Risk Assessment for Turkey", Ph.D. Thesis, Bogaziçi University.

Federal Emergency Management Agency, 2002, "Seismic Hazard Analysis", *Federal*

Emergency Management Agency, Washington, DC.

Freeman J.R., 1932, "Earthquake Damage and Earthquake Insurance: Studies of a Rational Basis for Earthquake Insurance, also Studies of Engineering Data for Earhquake-Resisting Construction", 1st Ed., *McGraw-Hill*, New York.

Gutenberg B, C.F. Richter, 1956, "Magnitude and Energy of Earthquakes", A*nnali fi Geofisica*; Vol. 9, No. 1, pp 234-238.

Gülerce, Z., and S. Ocak, 2013, "Probabilistic Seismic Hazard Assessment of Eastern", *Bull Earthquake Engineering* Vol. 11, pp. 1259-1277.

Gülkan, P., and E. Kalkan, 2010, "Ihtimallar Hesabina Dayali İstanbul ve Çevresindeki Deprem Tehlikesi", *Bilim ve Teknik*.

Gülkan, P., 2012, "Expecting the Expected: 1 g Peak Motions in the İstanbul Metropolitan Area", *World Conference of Earthquake Engineering*.

Hubert-Ferrari, A., A.A. Barka, E. Jacquess, S.S. Nalbant, B. Meyer, R. Armijo, P. Tapponier, G.C.P. King, 2000, "Seismic Hazard in the Marmara Sea Following the Izmit Earthquake", *Nature*, Vol. 404, pp. 269-272.

Kadiköy Belediyesi, 2014, "E-IMAR Interaktif Imar Durumu, Retrieved from Kadiköy Belediyesi:" $http://webgis.kadikoy.bel.tr/imardurumu/index.aspx$.

Kalkan E., P. Gülkan, 2004, "Site-Dependent Spectra Derived from Ground Motion Records in Turkey", *Earthquake Spectra*, Vol. 20, No. 4, pp. 1111-1138.

Kalkan E., P. Gülkan, N.Yilmaz and M. Çelebi, 2009, "Re-Examination of Probabilistic Seismic Hazard in the Marmara Sea Region", *Bull Seismol Socience*, Vol. 99, No. 4, pp. 2127-2146.

Kandilli 2014, "Observatory and Earthquake Research Institute", $http://www.koeri.boun.edu.tr$.

Le Pichon, X., A.M.C. Sengör, E. Demirbag, C. Rangin, C. Imren, R. Armijo, N. Görür, N. Çagatay, B. Mercier de Lepinay, B. Meyer, R. Saatcilar and B. Tok, 2001, "The Active Main Marmara Fault", *Earth and Planetary Science Letters*, Vol. 192, pp. 595-616.

Le Pichon, X., N. Chamot-Rooke, C. Rangin, and A.M.C. Sengor, 2003, "The North Anatolian Fault in the Marmara Sea", *Geophys Resistance Solid Earth Planets*, Vol. 108, pp. 2170-2179.

Lin, T., C.B. Haselton, and J.W. Baker, 2013, "Conditional-Spectrum-Based Ground Motion Selection, Part II:Intensity-Based Assessments and Evaluation of Alternative Target Spectra, *Earthquake Engineering and Structural Dynamics*.

Miranda, E., and H. Aslani, 2003, "Probabilistic Response Assessment for Building-Specific Loss Estimation". *California: Pacific Engineering Research Center*.

McGuire, R.K., 2004, "Seismic Hazard and Risk Analysis", *Colorado: Earthquake Engineering Research Institute*.

OYO International Corporation, 2007, "Avrupa Yakasi Güneyi Mikro Bölgeleme Çalismasi", İstanbul.

Parsons, T.S. Toda, R.S. Stein, A. Barka and J.H. Dieterich, 2000, "Heightened Odds Of Large Earthquake Near İstanbul: An Interaction-Based Probability Calculation", *Science*, Vol. 288, pp. 661-665.

Parsons, T., 2004, "Recalculated Probability of M $\geq$ 7 Earthquakes Beneath the Marmara Sea", *Journal Geophys Resistance*, Vol. 109, No. 304, pp. 1-21.

Schotanus M., 2005, "A Probabilistic Method for Seismic Loss Estimation", Ph.D. Thesis, Earthquake Engineering Department, Istituto Universitario.

Shinozuka M., M. Grigorlu, A.R. Ingrffea, S.L. Billington, P. Feenstra, T.T. Soong, A.M. Reinhorn, E. Maragakis, 2000, "Development of Fragility Information for

Structures and Nonstructural Components, Technical Report MCEER2000", *Multidisciplinary Center for Earthquake Engineering Research, Buffalo*, New York.

Ün, E., 2011, "An Integrated Seismic Loss Estimation Methodology: A case study in northwestern Turkey", MS Thesis, Middle East Technical University.

Youngs R.R., K.J. Coppersmith, 1985, "Implications of Fault Slip Rates and Earthquake Recurrence Models to Probabilistic Seismic Hazard Estimates", *Bulletin of the Seismological Society of America*, Vol. 75, No. 4, pp. 939-964.